Macrophage-mediated antibody dependent effector function in aggressive B cell lymphoma treatment

Inaugural-Dissertation

zur Erlangung des Doktorgrades

der Mathematisch-Naturwissenschaftlichen Fakultät

der Universität zu Köln

vorgelegt von

Verena Barbarino

aus Düsseldorf

2021

Berichterstatter: Prof. Dr. Christian P. Pallasch

Prof. Dr. Marcus Krüger

Tag der mündlichen Prüfung: 23.07.2021

For my greatest support, Bastian

Table of contents

1 Publications

V. Barbarino, S. Henschke, S. J. Blakemore, E. Izquierdo, M. Michalik, N. Nickel, I. Möllenkotte, D. Vorholt, L. Müller, R. Brinker, O. Fedorchenko, N. Mikhael, T. Seeger-Nukpezah, M. Hallek, and C. P. Pallasch, "Macrophage-mediated antibody dependent effector function in aggressive B-cell lymphoma treatment is enhanced by ibrutinib *via* inhibition of JAK2," *Cancers (Basel).*, vol. 12, no. 8, pp. 1–25, 2020, doi: 10.3390/cancers12082303.

E. Izquierdo, D. Vorholt, B. Sackey, J. L. Nolte, S. J. Blakemore, J. Schmitz, V. Barbarino, N. Nickel, D. Bachurski, L. Lobastova, M. Nikolic, M. Michalik, R. Brinker, O. Merkel, R. Neuhaus, M. Koch, G. Knittel, L. Frenzel, H. C. Reinhardt, M. Peifer, R. Rebollido-Rios, H. Bruns, M. Krüger, M. Hallek, and C. P. Pallasch, "Loss of TP53 mediates suppression of Macrophage Effector Function *via* Extracellular Vesicles and PDL1 towards Resistance against Chemoimmunotherapy in B-cell malignancies," *bioRxiv*, 2020, doi: 10.1101/2020.06.11.145268.

A. Meyer, S. Yan, V. Golumba-Nagy, R. L. Esser, V. Barbarino, S. J. Blakemore, L. Rusyn, A. Nikiforov, T. Seeger-Nukpezah, H. Grüll, C. P. Pallasch, and D. M. Kofler, "G-protein signaling modulator 2 deficiency leads to impaired regulatory T cell migration in rheumatoid arthritis," *Annals of the Rheumatic Diseases* (submitted February 2021, in review)

D. Hirani, C. M. Alvira, S. Danopoulos, C. Milla, M. Donato, L. Tian, J. Mohr, K. Dinger, C. Vohlen, J. Selle, S. v. Koningsbruggen-Rietschel, V. Barbarino, C. Pallasch, S. Rose-John, M. Odenthal, G. S. Pryhuber, S. Mansour, R. Savai, W. Seeger, P. Khatri, D. Al Alam, J. Dötsch, M. A. Alejandre Alcazar, "Macrophage-derived IL-6 trans-signaling as a novel target in the pathogenesis of bronchopulmonary dysplasia," *European Respiratory Journal* (submitted April 2021, in review)

2 Zusammenfassung

Bruton's Tyrosin Kinase (BTK)-Inhibitoren und monoklonale Antikörper sind ein wichtiger Bestandteil der Behandlung von chronisch lymphatischer Leukämie (CLL), Morbus Waldenström, Mantelzell-Lymphom und diffuses großzelliges B-Zell-Lymphom (DLBCL). Klinische Studien beschäftigten sich bereits mit der Kombination solcher niedermolekularer Inhibitoren und monoklonalen Antikörpern. Aufbauend darauf befasst sich diese Arbeit mit dem Verständnis der Synergie beider Therapien auf zellulärer und molekularer Ebene. Hier konnte gezeigt werden, dass der BTK-Inhibitor Ibrutinib zusammen mit monoklonalen Antikörpern die Makrophagen-vermittelte Phagocytose von malignen B-Zellen erhöht. BTK-Inhibitoren der zweiten Generation führten hier jedoch zu keiner erhöhten Phagocytoserate, woraufhin mit Hilfe von Kinaseaktivitätsprofilen die Januskinase (JAK) 2 als Off-Target von Ibrutinib hervorgehoben werden konnte. Die direkte Inhibition von JAK *in vitro*, sowie *JAK2* knock out (KO) *in vivo* in Kombination mit monoklonalen Antikörpern zeigte dabei eine erhöhte Phagocytoserate und längeres Überleben. Des Weiteren konnte gezeigt werden, dass der Phänotyp von Makrophagen durch die Inhibition von JAK beeinflusst wird und *JAK2* KO Lymphom-Zellen weniger programmed cell death ligand (PD-L1) exprimieren. Beide Effekte können dabei den Mechanismus hinter der gesteigerten Phagocytosrate erklären. Zusammenfassend deutet diese Arbeit darauf hin, dass die Synergie von ibrutinib mit monoklonalen Antikörpern unabhängig von der Inhibition von BTK agiert, dafür jedoch über die Inhibition des Januskinase/ signal transducers and activators of transcription (JAK/STAT) Signalwegs. Aus diesem Grund stellen Inhibitoren des JAK/STAT Signalwegs in Kombination mit monoklonalen Antikörpern eine wichtige Therapiemöglichkeit von B-Zell-Lymphomen dar.

Unabhängig von dieser Arbeit konnte unser Labor der Arbeitsgruppe Pallasch zeigen, dass eine Mutation von *TP53* in B-Zell-Lymphomen die Makrophagen-vermittelte Phagocytose von Chemoimmunotherapie (CIT) blockiert. Diese Resistenz gegen CIT wurde durch erhöhte PD-L1 Expression sowie vermehrte Ausschüttung von extrazellulären Vesikeln (EV) verursacht. Darauf aufbauend beweist diese Arbeit, dass die Blockade von EVs der B-Zell-Lymphome mit mutiertem *TP53 in vivo* zu einer erhöhten Überlebensrate und Resonanz auf CIT führte. Des Weiteren konnte gezeigt werden, dass die Behandlung von B-Zell-Lymphomen mit mutiertem *TP53* mit anti-PD1 Antikörpern oder einem zusätzlichen KO in *PD-L1* das Überleben sowie die Reaktion auf CIT verbessert. Zusammenfassend belegt diese Arbeit, dass die Blockade von

Immuncheckpoints und EVs in B-Zell-Lymphomen mit mutiertem *TP53* eine wichtige Rolle in der Aktivierung von Makrophagen-vermittelte Phagocytose durch CIT spielt.

3 Abstract

Inhibition of the Bruton's Tyrosine Kinase (BTK) *via* ibrutinib and tumour surface antigen targeting monoclonal antibodies have become an important treatment strategy in chronic lymphocytic leukaemia (CLL), Waldenström's macroglobulinemia, Mantle cell lymphoma, and non-GCB diffuse large B cell lymphoma (DLBCL). Clinical trials have already considered the combination of such small molecule inhibitors with monoclonal antibodies, without prior assessment of the biological understanding between their potential synergistic interactions. Therefore, the work of this thesis has evaluated the synergistic interaction of BTK-inhibitors and monoclonal antibody therapy *via* macrophage mediated antibody dependent cellular phagocytosis (ADCP). Whilst the first generation BTK-inhibitor ibrutinib exhibited an increased ADCP, second generation BTK-inhibitors failed to synergistically interact with monoclonal antibody treatment. To understand the differential effect of first and second generation BTK-inhibitors, kinase activity profiling was undertaken and identified significant inhibition of janus kinase (JAK) 2 only under ibrutinib treatment. Validating this potential off-target effect *via* JAK inhibition *in vitro* as well as with *JAK2* knock out (KO) experiments *in vivo*, increased ADCP and prolonged survival was shown, respectively. Moreover, JAK inhibition led to a change of macrophage polarisation and additionally *JAK2* KO lymphoma cells showed a decreased expression of programmed cell death ligand 1 (PD-L1). Both effects could explain the mechanism of action behind the increase in ADCP under JAK inhibition. Taken together, this data supports the synergistic interaction of ibrutinib and monoclonal antibodies being independent of the inhibition of BTK, but rather of the inhibition of the janus kinase/ signal transducers and activators of transcription (JAK/STAT) signalling pathway. For this reason, JAK/STAT signalling inhibitors in combination with monoclonal antibodies display new potential treatment strategies in B cell malignancies activating macrophage immune responses.

Independently, the AG Pallasch laboratory demonstrated that PD-L1 upregulation and increased release of extracellular vesicles (EVs) mediates resistance of B cell lymphoma with a loss of *TP53* to chemoimmunotherapy (CIT) by suppressing macrophage phagocytosis. Here, the work of this thesis has validated *in vivo* that blocking the release of EVs derived from *TP53* deficient B cell lymphoma cells improved survival and response to CIT. Moreover, using anti-PD-1 antibodies or B cell lymphoma cells with a KO in *PD-L1* improved the survival and response to CIT of B cell lymphoma cells with a loss of *TP53*. In summary, immune checkpoint

inhibition and EVs in B cell lymphoma with a loss in *TP53* display important targets in re-activating macrophage phagocytosis induced by CIT.

4 Introduction

Cancer is one of the main public health challenges of the 21st century with around 18 million cases in the world in 2018 [1]. In general, cancer is defined as cells that start to proliferate and differentiate in an uncontrolled manner. Six characteristics were described that are important for the development of cancer: (1) sustained signalling that promotes proliferation, (2) circumvent growth suppressors, (3) resist cell death, (4) facilitate replicative immortality, (5) induce angiogenesis, and (6) enable invasion and metastasis [2]. Tumour cells can recruit healthy cells to achieve the named characteristics by creating a tumour microenvironment (TME).

Mostly, cancer is caused by mutations of genes involved in the regulation of cell growth or apoptosis. Mutations can occur by age because of deoxyribonucleic acid (DNA) damage and due to carcinogenic substances or viruses. Cancer can appear in all cell types of the body. With its growing global burden the investigation of new strategies and therapeutical approaches becomes more and more important [3].

4.1 Leukaemia and lymphoma

Tumours are classified in three major groups: first the epithelial tumours, second the non-epithelial tumours and, third the MIXED multilineage tumours. Here, leukaemia and lymphoma belong to the group of non-epithelial tumours deriving from the haematopoietic lineage that gives rise to blood cells [3]. Leukaemia and lymphoma are often grouped together since they share a lot of similarities, nevertheless there are differences to distinguish between both groups. In leukaemic cancers, the bone marrow produces excessive malignant white blood cells (leukocytes) that freely circulate in the blood system [3], [4]. Under healthy conditions, these leukocytes serve as immune defence [5] whereas in leukaemia the multiplied malfunctioning leukocytes spill over in the blood system and keep red blood cells from oxygen supply [6]. Leukaemia can be categorised into four major types: Acute myeloid leukaemia (AML), chronic myeloid leukaemia (CML), acute lymphocytic leukaemia (ALL), and chronic lymphocytic leukaemia (CLL) [3]. Patients suffering from acute leukaemia require treatment whereas patients with chronic leukaemia are mostly indolent in the beginning and treatment is required after tumour progression over several years [7], [8]. Moreover, myeloid derived tumours derive from the bone marrow and cells that are not attributed to the lymphatic system [9].

Different to leukaemia affecting the blood circulation and bone marrow, lymphoma tend to affect the lymph nodes forming solid tumours through malignant lymphocytes [3]. Lymphocytes represents a sub group of leukocytes containing B-lymphocytes (B cells) and T-lymphocytes (T-cells) [10]. There are two groups of lymphoma: Hodgkin lymphoma and Non-Hodgkin lymphoma [11]. The former is represented by Reed-Sternberg cells, that are giant, multinucleated cells usually derived from B cells. These cells fail to express most B cell specific genes, including immunoglobulin genes [12]. The second group, the Non-Hodgkin lymphomas represent all other lymphomas like Burkitt lymphoma or diffuse large B cell lymphoma (DLBCL) [13]. Likewise, CLL is listed under Non-Hodgkin lymphoma. However, CLL fulfils the criteria of lymphoma being lymphocytic-derived but starting tumour progression in the bone marrow which is a criteria for leukaemia [14], [15].

4.1.1 *MYC*/*BCL-2* "double hit" lymphoma

"Double hit" lymphomas belong to the group of Non-Hodgkin lymphoma and are defined as a high-grade B cell lymphoma (HGBCL) [16], [17]. In detail, according to the World Health Organisation (WHO) these lymphomas are classified as a subgroup of mature B cell lymphoma classified with their characteristics between DLBCL and Burkitt lymphoma [18]. The "double hit" lymphoma is defined to have a chromosomal breakpoint affecting two oncogenes – the *MYC* oncogene and an additional breakpoint such as the *B cell lymphoma gene 2* (*BCL-2*) or *BCL-6*. In most cases, a combination of the *MYC*/*BCL-2* "double hit" occurs [16], [19].

MYC represents one of the most frequently activated oncogenes in human cancers [20]. *MYC* is located on chromosome 8 and *via* copy number alterations or chromosomal translocation with chromosomes like 2, 14 or 22 affecting the regulatory or promoter region it is oncogenically activated [16], [19], [21], [22]. The overexpression of *MYC* leads to the dimerization of the protein MYC with MAX, whereby this MYC-MAX complex binds DNA and leads to the transcription of genes activating proliferation [3], [23], [24]. This growth stimulatory effects *via* the overexpression of *MYC* is limited by its MYC-induced apoptosis through inactivation by the retinoblastoma protein (pRB) [3], [23].

The oncogenic version of *BCL-2* is formed through reciprocal chromosomal translocation pointing the exchange of the chromosome arms 14 and 18. This exchange leads to the placement of the reading frame of the *BCL-2* gene under control of a promoter that increases transcription. The overexpression of *BCL-2* leads to a prolonged survival of lymphocytes [3]. To be more precise, the BCL-2 protein acts in the outer membrane of the mitochondrion. Here, it causes the

blockade of channels that release cytochrome c, which normally functions to transfer electrons as part of the oxidative phosphorylation. Once cytochrome c leaves the mitochondrion through respective channels, it activates a signalling cascade in the cytosol which subsequently initiates apoptosis. Therefore, the overexpression of *BCL-2* blocks apoptosis [3], [25]. Lymphocytes with a mutation only in *BCL-2* are not actively proliferating which explains that mice carrying only a *Bcl-2* transgene do not bear a haematopoietic tumour [26].

The combinatorial activation of the *MYC* and *BCL-2* oncogenes leads to a very aggressive type of lymphoma. Thus, *MYC* drives the proliferation of malignant cells and *BCL-2* neutralises the MYC-induced apoptotic actions [3]. Patients suffering from "double hit" lymphoma have a generally poor outcome with a median survival of 6 months [27]. Additionally, they show poor response to the standard treatment of chemotherapy [28] demonstrating the necessity to develop new therapeutic strategies (see chapter 4.5).

4.1.2 Chronic lymphocytic leukaemia (CLL)

CLL represents the most common type of leukaemia in the western world. The median age of prognosis is about 72 years mainly affecting the male population [29]–[32]. It is likely that due to demographic changes in society and increased ageing the susceptibility and mortality for CLL will increase in the next decades [14].

Disease progression of CLL is associated with the clonal proliferation of mature B cells that circulate in the blood between bone marrow, lymph nodes and spleen [15]. The exact causes of this uncontrolled B cell proliferation are still unclear. Nevertheless, it is assumed that genetic changes acquired during life are responsible for the disease [33]. However, malignant B cells can be distinguished from healthy B cells *via* flow cytometry of the cell surface markers cluster of differentiation (CD) 5, CD19, CD20 and CD23 [34]. Additional genomic alterations can aggravate CLL disease progression and occurs in about 80 % of all patients [35]. Here, one example is the deletion of the short arm of chromosome 17p13 that affects the tumour suppressor gene *TP53* (see chapter 4.3). In general, mutations in *TP53* occurs in 4-37 % of CLL patients and predicts poor prognosis [36], [37]. Moreover, whole exome sequencing identified 44 more mutated genes in CLL including genes like *NOTCH1*, *MYD88*, *ATM* and *PTPN1* [38]–[40]. These genes collectively affect MYC activity, mitogen-activated protein kinase (MAPK) signalling and the DNA damage response (DDR) as central pathways involved in CLL [38], [41].

The survival and proliferation of CLL cells is supported by the interaction with cells of the TME like macrophages, T cells or dendritic cells [42]–[44]. Consequently, the TME interacts with CLL cells through different proteins like chemokines, cytokines, and angiogenic factors that can bind to cell surface receptors like the B cell receptor (BCR, see chapter 4.2) or receptors of the janus kinase/ signal transducer and activator of transcription (JAK/STAT) signalling pathway (see chapter 4.4.1.3) [43], [45]–[48]. The role of the TME in B cell malignancies will be further discussed in chapter 4.4.

One major factor to prognose CLL is the number of $\geq 5,000$ B lymphocytes/µl in the peripheral blood for at least three months. Moreover, the clonality of B cells is confirmed by flow cytometry measuring the above mentioned surface markers [14]. In order to identify the progression status of CLL two staging systems exist: Rai [49] and Binet [50]. In both systems the progression status is classified into three major groups with discrete clinical outcome. Nevertheless, due to many genetic alterations and additional mutations that influence treatment response independent on clinical stage this classification has become insufficient [14], [51]. Therefore, the CLL International Prognostic Index (CLL-IPI) displays the most relevant prognostic scoring system combining clinical, biological and genetic factors [52]. The CLL-IPI uses five independent prognostic factors: *TP53* deletion or mutation, Ig heavy chain variable region (IGHV) mutation, serum β_2-microglobulin, clinical stage and age [14], [52]. The current therapeutic approaches to CLL will be discussed in chapter 4.5.

4.2 B cell receptor (BCR) pathway

The BCR signalling pathway plays a key role in the proliferation and survival of normal and malignant B cells [48], [53]. Therefore, therapeutic targeting of the BCR is a common strategy in B cell malignancy like CLL (see chapter 4.5) [54].

Activation of the BCR is mediated *via* antigen binding and leads to the formation of a complex signalosome and kinase cascade signalling (Figure 1). The BCR is a transmembrane complex formed by immunoglobulin heavy and light chains [48]. Antigen binding to the immunoglobulin light chain of the BCR causes phosphorylation of the immunoreceptor tyrosine-based activation motifs (ITAMs) of CD79A and CD79B that are located in the c-terminal tail of the receptor [55]. This phosphorylation is supported by protein tyrosine kinase LYN [48]. The phosphorylated ITAMs further activate spleen tyrosine kinase (SYK) that recruits B cell linker protein (BLNK), phospholipase gamma 2 (PLCγ2), and Bruton's tyrosine kinase (BTK) [56]. Though, BLNK allows SYK to phosphorylate BTK [57]. Nevertheless,

BTK can be also directly phosphorylated by LYN. Further downstream signalling leads to the mobilisation of Ca^{2+} and activation of protein kinase C (PKC). Next, PKC activates the extracellular signal-regulated kinase and mitogen-activated protein kinase (ERK/MAPK) signalling and nuclear factor kappa-light-chain-enhancer of activated B cells (NFκB) [56].
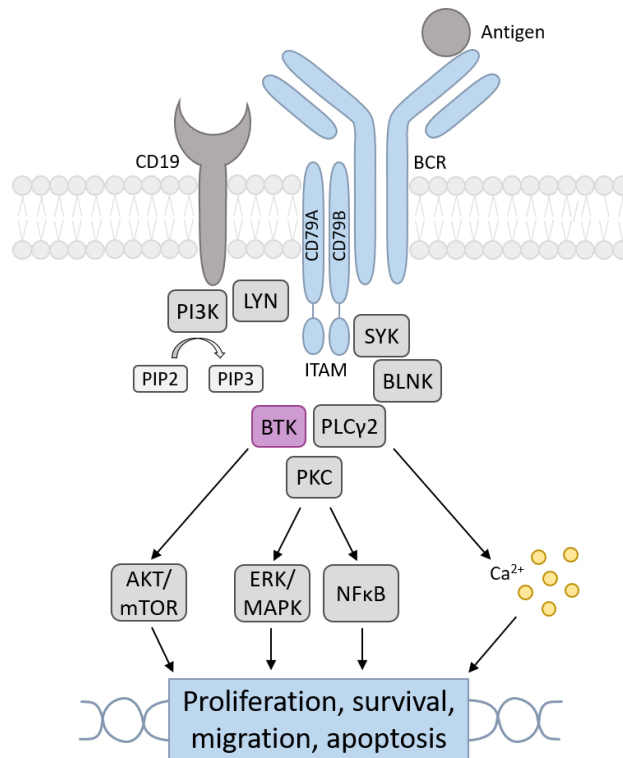
Figure 1 BCR signalling
Antigen binding to the BCR induce phosphorylation of the ITAMs CD79A and CD79B. With the support of LYN downstream signalling including SYK, BLNK, PLCγ2, BTK, and PKC leads to Ca^{2+} mobilisation and activation of the pathways ERK/MAPK and NFκB. Moreover, activation of the CD19 receptor by LYN induce activation of PI3K and phosphorylation of PIP2 to PIP3. Lastly, PIP3 activates BTK and PLCγ2 inducing the AKT/mTOR pathway. Finally, activation of the BCR and downstream pathways regulates proliferation, survival, migration, and apoptosis of B cells.

Moreover, the activation of the BCR co-receptor CD19 by LYN contributes to the BCR signalling over the activation of phosphatidylinositol-3-kinase (PI3K). In the next step PI3K phosphorylates phosphatidylinositol-4,5-bisphosphate (PIP2) to phosphate-idylinositol-3,4,5-triphosphate (PIP3). Consequently, PIP3 activates BTK and PLCγ2. Moreover, PIP3 contributes to Ca^{2+} mobilisation and activates the protein kinase B/ mechanistic target of rapamycin (AKT/mTOR) pathway, that is also activated by BTK [56]. The activation of the BCR and downstream ERK-MAPK, NFκB, and Akt/mTOR signalling leads to the transcription of genes involved in proliferation, survival, migration, and apoptosis of B cells [48], [53].

Prognostic markers in CLL can influence the BCR signalling and therefore the clinical outcome of patients. One prognostic factor is the mutational status of the IGHV of the BCR. Here,

unmutated IGHV (U-CLL) correlates with faster disease progression and shorter survival as mutated IGHV (M-CLL) mediated by higher response to BCR stimulation and faster B cell proliferation [58]–[60]. Another prognostic factor is the expression of zeta-chain-associated protein kinase 70 (ZAP-70) in more than 20 % of CLL cells [61]. ZAP-70 was initially identified in T cells and is structurally similar to the protein SYK [58]. Therefore, the expression of ZAP-70 in CLL is linked to increased BCR signalling [62].

4.3   *TP53* and its role in the DNA damage response (DDR)

The DDR is a highly complex system, that detects and repairs DNA damage [63]. DNA damage can be induced by wrong replication or alkylation and environmental influences such as UV light or chemical agents [3]. Moreover, DDR regulates apoptosis and stimulates immune responses [64], [65]. This function is used by therapeutic agents like cyclophosphamide that cause DNA damage and kill tumour cells by inducing apoptosis and activating the immune response *via* upregulation of inflammatory cytokines [66], [67].

TP53 is one of the most studied genes in the DDR signalling. DNA double strand breaks activate serine protein kinase ATM and checkpoint kinase 2 (CHK2) that regulates TP53 and induce apoptosis, senescence, and cell cycle arrest [68]. Besides its apoptotic functions, TP53 can also induce DNA repair [69].

In healthy tissues TP53 act as a tumour suppressor and is mainly synthesised in proliferating cells whereas resting cells show only low levels of TP53. TP53 is negatively regulated by mouse double minute protein 2 (MDM2) through the ubiquitin-proteasome pathway [66], [70]. In many types of cancer, *TP53* is mutated leading to increased cell proliferation and survival. Moreover, mutations in *TP53* mediate genomic instability and resistance to chemotherapy [66], [71].

4.4   **Tumour microenvironment (TME)**

The communication of different cell types within an organism is very important for tissue organisation and to maintain homoeostasis. Cancer cells can manipulate this communication and the surrounding microenvironment according to its needs. Consequently, tumour cells create their own niche called the TME. The TME is a very complex system regulating tumour growth and survival. Understanding the interactions between tumour cells and the microenvironment plays a fundamental role in investigating new therapeutic strategies to treat

different types of cancer (see chapter 4.5). Thereby, the TME consists of different cell types that can be divided into three major groups: Angiogenic vascular cells, cancer-associated fibroblasts (CAFs), and immune cells (Table 1) [72]–[74].

Table 1 Cell types of the TME and their function in supporting tumours [72]–[74]

Cell type	Sub-Type	Tumour supportive function
Angiogenic vascular cells	Endothelial cells	- Angiogenesis - Support of tumour invasion and metastasis - Suppression of tumour fighting immune system - Reduce apoptosis
	Pericytes	
Cancer-associated fibroblasts		- Support angiogenesis - Support tumour progression - Support metastasis - Reduce apoptosis - Supply tumour with energy
Immune cells	T cells, T_{reg} cells	- Support angiogenesis - Support tumour progression - Reduce apoptosis - Support of tumour invasion and metastasis growth - Suppression of antigen presentation - Suppression of tumour fighting immune system
	NK cells	
	MDSCs	
	Dendritic cells	
	Macrophages	

The first group of angiogenic vascular cells persist mainly of endothelial cells and pericytes, which arrange tube formation and compromise the angiogenic vasculature, respectively [75]. In general, angiogenic vascular cells support the tumour with oxygen and nutrients by forming new blood vessels [74]. Moreover, the generation of lymphatic vessels are important for the tumour to spread and invade other tissue compartments [76]. The formation of vessels is introduced *via* pro-angiogenic factors like vascular endothelial growth factor (VEGF) that are released by cells such as tumour associated macrophages (TAMs) or CAFs into the TME [77], [78]. Another tumour supportive role of angiogenic vascular cells is their limited ability to transit anti-tumour acting immune cells like natural killer (NK) cells or T cells to the tumour region. Furthermore, angiogenesis leads to a reduced apoptosis signalling which additionally supports tumour growth [73].

The second group includes CAFs. Fibroblasts play a role in the connective tissue by supporting wound healing and tissue repair [73], [74]. In many tumours CAFs are recruited in high numbers and once activated secrete growth factors like VEGF that support angiogenesis, tumorigenesis and metastasis [74], [79]–[82]. Moreover, CAFs limit cell apoptosis through secretion of survival factors such as insulin-like growth factor (IGF) 1 and 2 [80]. Another tumour supportive action is supplying energy in form of lactate and pyruvate to cancer cells, whilst reactive oxygen species released by cancer cells support aerobic glycolysis in CAFs [73], [83].

The third category represents immune cells derived from haematopoietic stem cells (HSCs) such as T cells, NK cells, myeloid-derived suppressor cells (MDSCs), dendritic cells, and macrophages [73], [74]. Normally, immune cells act anti-tumoral. However, immune cells can be also recruited from tumours to support the growth and progression of cancer cells [84]. In line with this, MDSCs or TAMs can be stimulated by cancer cells to secrete cytokines like VEGF that assist in angiogenesis [73], [74], [85]. Moreover, immune cells of the TME provide proliferative signalling to cancer cells through epidermal growth factors (EGFs), transforming growth factor-β (TGF-β), tumour necrose factor-α (TNF-α), fibroblast growth factors (FGFs), interleukins (ILs), chemokines, histamines and heparins [73], [86]. Immune cells further reduce apoptosis through *e.g.* TAMs and the PI3K/AKT signalling pathway [87]. Once recruited, immune cells support tumour invasion and metastasis through remodelling the extracellular matrix (ECM) by TAMs [73], [88], [89]. It was also shown in a mouse model that depletion of MDSCs reduced metastasis [90]. Another tumour supporting mechanism is the suppression of antigen presentation to T cells by *e.g.* loss of major histocompatibility complex (MHC) II expression on malignant cells [91], [92]. Additionally, tumours recruit regulatory T cells (T_{reg}) to make use of their immune suppressive function [93].

Although the progression of "double hit" lymphoma of *MYC* and *BCL-2* is less dependent on the TME due to strong autonomous pro-survival signalling by *MYC* [19], [72], considering the TME regarding instrumentalization for new therapeutic strategies is important. Also in consideration of the absolute monocyte cell count that correlates with prognosis in DLBCL as well as in CLL [94], [95]. In CLL the progression of cancer is highly dependent on the TME being protected from apoptosis, promoting homing by secretion of cytokines and chemokines such as C-X-C motif chemokine (CXCL) 12 and 13, and getting pro-survival signals like A proliferation-inducing ligand (APRIL) and B cell activating factor (BAFF) [72].

Giving an insight about the wide spectrum of cells in the TME and their ability to help in the tumour development, Pallasch *et al.* demonstrated that treatment of leukaemia bearing mice

with anti-CD52 antibody alemtuzumab induce tumour cell clearance through activation of macrophage effector cell function and induction of phagocytosis [96]. Therefore, this thesis is focused on the interaction of malignant B cells with macrophages as described in more detail in the next chapters.

4.4.1 Macrophages

In the bone marrow the myeloid lineage of HSCs can differentiate into monocytes. Monocytes circulate in the blood and can be recruited into several tissues where they differentiate into phagocytes like macrophages. As part of the innate immune system, they play a role in remaining tissue homeostasis by phagocyting pathogens or removing dead cells and cell debris. Moreover, they secrete a wide range of inflammatory factors leading to the activation of the immune system. As part of the adaptive immune system they show the ability to present antigens to T cells and consequently triggering immune response [97], [98].

The phenotype and hence the function of macrophages differ according to the signals of their surrounding microenvironment [99]. For example, the spleen accommodate macrophages such as marginal-zone, metallophilic, red pulp, and white pulp macrophages [100], [101]. However, the bone marrow harbours resident bone marrow and red pulp macrophages being responsible for the recycling of iron due to erythrophagocytosis and maintaining of HSCs and their circadian release into the blood stream [102]–[105]. The stimuli leading to polarisation into the different phenotypes of macrophages is explained in more detail in the next chapter 4.4.1.1.

4.4.1.1 M1 and M2 macrophage polarisation

Macrophages can switch their functional role and phenotypes according to stimuli from the microenvironment. The "classical" M1 and "alternative" M2 macrophage polarisation state represents the two phenotypic extremes of this multidimensional system. An imbalance of macrophage polarisation is often caused by diseases or inflammatory processes [106]–[108].

M1 and M2 macrophages differ in many aspects such as their function, stimulation, and secretion profiles (Figure 2). M1 macrophages are more involved in inflammatory processes and show potentially increased antigen presentation to promote killing of pathogens [106], whereas M2 macrophages act more immunosuppressively showing potentially a resting phenotype [107]. Moreover, M2 macrophages maintain tissue homeostasis, wound healing and promote angiogenesis [106], [108], [109].
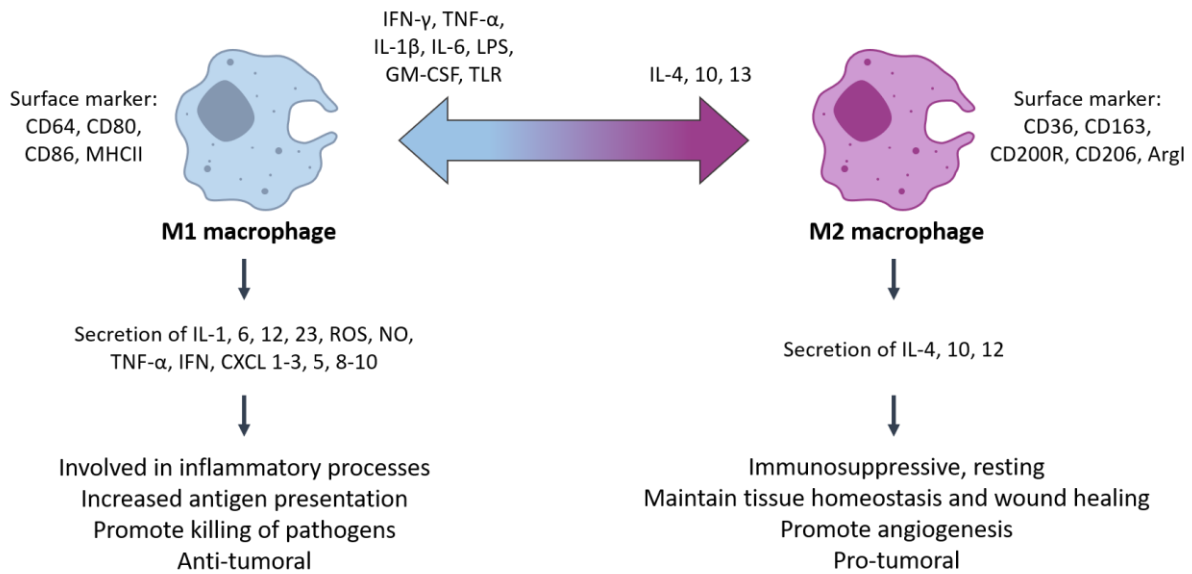
Figure 2 M1 and M2 macrophage polarisation
Macrophages can gradually polarise in M1 or M2-like phenotypes. Polarisation is induced *via* several cytokines. M1 and M2 macrophage phenotypes differ in surface marker expression and cytokine release. In general, M1 polarised macrophages act pro-inflammatory and anti-tumoral, whereas M2 polarised macrophages act anti-inflammatory and pro-tumoral.

Macrophages can be stimulated to switch their phenotype into M1 or M2 direction. Stimulators activating the M1 like phenotype are interferon (IFN)-γ, TNF-α, IL-1β, IL-6, lipopolysaccharide (LPS), granulocyte-macrophage colony-stimulating factor (GM-CSF), and toll-like receptor (TLR). These M1 activators can be produced by NK cells, T cells, antigen-presenting cells , or pathogens [106], [107], [109], [110]. Switching macrophages to an M2-like phenotype is caused by IL-4, IL-10, and IL-13 produced by Th2 cells, eosinophils, and basophils [106], [107], [110], [111]. These activators pushing macrophages into an M1 or M2-like phenotype essentially react through the JAK/STAT signalling pathway that will be further discussed in chapter 4.4.1.3.

Once activated, M1 macrophages release pro-inflammatory cytokines such as IL-1, 6, 12, and 23, TNF-α, IFN, CXCL 1-3, 5, and 8-10, reactive oxygen species (ROS), and nitric oxide (NO) [109], [112]. Cytokines are defined as proteins involved in cell signalling regulating proliferation and differentiation of cells. There are five main groups of cytokines: Chemokines, interferons, interleukins, lymphokines, and tumour necrosis factors being produced by a wide spectrum of cells including immune cells like macrophages, B cells, T cells, and mast cells, as well as endothelial cells, fibroblasts, and various stromal cells [113], [114]. M2 polarised macrophages mainly release anti-inflammatory cytokines like IL-4, IL-10, and IL-12 [106], [115].

Macrophages that switch their phenotypes also change their expression profile of surface markers. M1-like macrophages express more CD64, CD80, CD86, and MHCII, whereas M2-like macrophages express more CD36, D163, CD200R, CD206, and arginase 1 (ArgI, only in mice) [106], [108], [116]–[119].

The phenotype of macrophages can influence their role in tumour progression. Hence, M1-like macrophages are associated with hindering tumour growth whereas M2-like macrophages support tumour growth [106], [120] as described in more detail in the next chapter 4.4.1.2.

4.4.1.2 Tumour associated macrophages (TAMs)

In the development of cancer an inflammatory microenvironment contributes to tumour progression [121], [122]. Since TAMs regulate inflammatory pathways, they play a key role in the TME and tumour progression [123], [124].

Tumours recruit TAMs from monocytes or monocyte-related myeloid-derived suppressor cells (M-MDSCs) that circulate in the blood and from tissue resident macrophages [121], [125]–[127]. This recruitment to the tumour side are initiated by cytokines like CCL2, CCL5, VEGF, and colony stimulating factor-1 (CSF-1) that also drives TAM polarisation towards an immunosuppressive, tumour promoting, M2-like phenotype [85], [120], [121], [125], [128], [129]. Respective cytokine signalling can be mediated through tumour cells, T cells, B cells, and stromal cells [121].

The phenotype of TAMs can differ according to the type and developmental status of tumours [121], [130]. Hence, in early tumour development M1-like macrophages can contribute to chronic inflammation and tumour mutation *via* production of ROS and NO [131]. Later on these macrophages switch into an M2-like phenotype [120], [121], [132]. TAMs play a role in diverse tumour supporting factors such as stimulating tumour growth and survival through the secretion of EGFs [133] (Figure 3). They support tumour invasion and metastasis by producing proteolytic enzymes that digest the ECM and they produce factors like IL-1 that helps cancer cells to accumulate [121]. Additionally, TAMs stimulate angiogenesis by VEGF and promote the mutation of cancer cells as mentioned earlier [120], [131]. One major function of TAMs is to suppress immune responses *via* the release of immunosuppressive cytokines such as IL-10 or TGF-β [121], [134]. IL-10 leads to the activation of STAT3 in the JAK/STAT signalling pathway which will be further discussed in detail in chapter 4.4.1.3 [135], [136]. The suppression of the immune response includes low antigen presentation, suppression of T helper (T_h) cells, and the activation of T regulatory (T_{reg}) cells [119], [137], [138]. Another very important immunosuppressive action of TAMs is the overexpression of immune checkpoints

like CD47 or programmed cell death protein 1 (PD-1) and PD-L1. Both immune checkpoints are defined as "don't eat me" signals that keep cancer cells from phagocytosis by macrophages [139], [140].
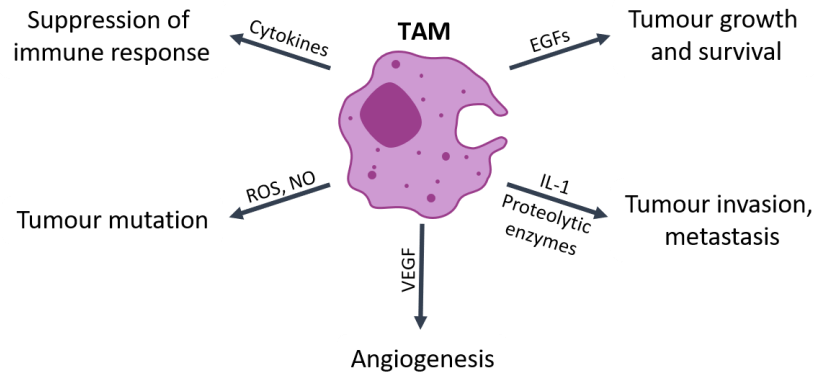
Figure 3 Functions of TAMs
TAMs can support tumour growth, survival, invasion, metastasis, angiogenesis, and mutation. Moreover, TAMs supress the immune system and create a microenvironmental niche. This tumour supportive role is mediated *via* growth factors, cytokines, proteolytic enzymes, ROS, and NO.

The high infiltration of TAMs to tumour sites are mostly associated with poor prognosis. Nevertheless, TAMs can be targeted with therapeutic substances in order to inhibit their tumour supportive function or to make use of their anti-tumour, M1-like phenotype [121], [125]. One possible therapeutic strategy is to inhibit chemokines that are responsible for the recruitment of TAMs and consequently to stop their contribution to tumour growth and survival [121]. Another strategy is to overcome the ability of TAMs to suppress the immune response. Thus, TAMs can be reprogrammed by cytokines, antibodies, or small molecule inhibitors to a pro-inflammatory, M1-like phenotype [123]. Moreover, angiogenesis can be blocked by anti-VEGF antibodies [141], [142]. Newer strategies block the above mentioned immune checkpoints *via* antibodies or mark those cancer cells with antibodies to guide macrophages and induce phagocytosis [121], [140], [143]–[145]. Targeting specific expression markers of cancer cells with antibodies and guiding macrophages to phagocyte those target cancer cells is called antibody-dependent cellular phagocytosis (ADCP, see chapter 4.4.1.4). Furthermore, the use of therapeutic antibodies can lead to antibody-dependent cell-mediated cytotoxicity (ADCC) where macrophages bind to the antibody coated target cell and release cytotoxic proteins [146].

4.4.1.3   Janus kinase/ signal transducer and activator of transcription (JAK/STAT) signalling pathway

Macrophage polarisation is regulated *via* several pathways such as the Notch-, c-Jun N-terminal kinase (JNK)-, TGF-β-, PI3K/AKT-, and TLR/NFκB-pathway. One of the most important pathways regulating macrophage polarisation is the JAK/STAT signalling pathway (Figure 4) [147], [148].
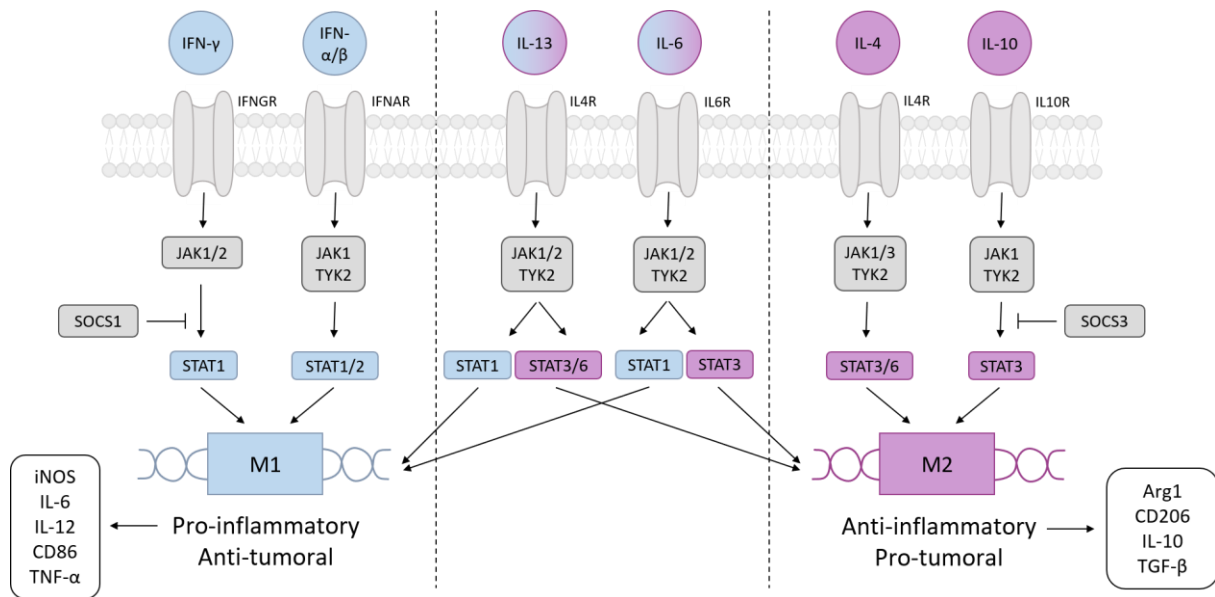
Figure 4 JAK/STAT signalling pathway
The JAK/STAT signalling pathway plays a role in macrophage polarisation and transcription of pro- and anti-inflammatory genes. Pathway activation is mediated by cytokines activating JAKs and downstream STATs that migrate into the nucleus and induce gene transcription. SOCS1 and SOCS3 serve as negative feedback inhibitors, regulating downstream transcription.

The JAK/STAT pathway is induced by cytokines like IFN-γ, IFN-α/β, IL-13, IL-6, IL-4, and IL-10 that stimulate cytokine receptors and activate downstream JAKs and STATs [47], [136], [147]. There are four different types of JAKs, namely, JAK1, JAK2, JAK3, and tyrosine kinase (TYK2) and seven types of STATs, STAT1-4, STAT5A, STAT5B, and STAT6 [147], [149]. As soon as STATs are phosphorylated by JAKs they enter the nucleus and act as transcription factor of anti- and pro-inflammatory genes leading to the polarisation of macrophages into an M1-, or M2-like phenotype [47], [136], [147].

Stimulation of the JAK/STAT signalling pathway by IFN-γ and IFN-α/β induce transcription of pro-inflammatory genes that polarise macrophages towards M1 [136], [150], [151]. Binding of IFN-γ to the interferon-gamma receptor (IFNGR) induces phosphorylation of JAK1/2 and downstream activation of STAT1 [136], [152], [153]. The binding of IFN-α/β to the interferon-α/β receptor (IFNAR) activates JAK1, Tyk2 and downstream STAT1/2 [151], [154]. Hence,

STAT1 and 2 enter the nucleus and drive transcription of pro-inflammatory factors such as cytokine-inducible nitric oxide synthases (iNOS), IL-6, IL-12, CD86, and TNF-α resulting in an antitumour response [47], [136], [147].

Stimulation of the JAK/STAT signalling pathway *via* IL-4 and IL-10 drives transcription of anti-inflammatory genes leading to an M2 polarisation of macrophages [136], [155]. IL-4 binds to the IL-4 receptor (IL4R), phosphorylates JAK1/3 and Tyk2, and activates STAT3/6 [136], [147], [156]–[158]. IL-10 binds to the IL-10 receptor (IL10R), activates JAK1 and Tyk2, and phosphorylates STAT3. Hence, STAT3 and 6 enter the nucleus and drive transcription of anti-inflammatory factors like arginase 1 (Arg1), CD206, IL-10, and TGF-β resulting in a tumour supportive response. Moreover, the activation of IL-10 leads to the repression of pro-inflammatory factors such as TNF-α, IFN-γ, IL-1β, IL-6, and IL-12 [136], [147], [155].

IL-13 and IL-6 can stimulate the JAK/STAT pathway leading to the transcription of pro- and anti-inflammatory genes. IL-13 binds to the IL4R and phosphorylates JAK1/2 and Tyk2 that activates STAT1 or STAT3/6 targeting pro- or anti-inflammatory gene expression [158]. IL-6 binds to the IL-6 receptor (IL6R) and phosphorylates JAK1/2 and Tyk2 that activates either STAT1 leading to pro-inflammatory gene expression or activating STAT3 leading to anti-inflammatory gene expression [159]–[161].

The JAK/STAT pathway is regulated by negative feedback inhibition *via* suppressor of cytokine signalling (SOCS) proteins, where SOCS1 regulates the transcription of pro-inflammatory genes and SOCS3 of anti-inflammatory gene expression, respectively [147], [162].

4.4.1.4   Antibody-dependent cellular phagocytosis (ADCP)

ADCP plays a major role in the treatment of cancer with immunotherapeutics [144], [163], [164]. Therapeutic IgG antibodies, like anti-CD20 rituximab binds with its antigen-binding fragment (Fab) to the cancer target cell. Likewise, the crystallisable fragment (Fc) part of the therapeutic antibody binds to Fc receptors (FcR) that are expressed on effector cells leading to internalisation and destruction of opsonised target cells [165]–[167].

The majority of macrophage-mediated ADCP occurs *via* FcγR signalling [166], [168]. As a consequence of antibody FcγR binding, ITAMs become phosphorylated with the help of SRC tyrosine family kinases [169]–[171]. The exact molecular process of kinase activation remains to be clarified. Nevertheless, it is known that phosphorylated ITAM activates SYK and downstream kinases that redistribute to actin-rich phagocytic cups [172]. Importantly, particle internalisation requires reorganisation of actin cytoskeleton and membrane fusion events. These

membrane fusion events depend on the formation of N-ethylmaleimide-sensitive-factor attachment receptor (SNARE) complexes [170], [173]. Once a particle has entered the cell as a phagosome, it fuses with lysosomes that contain enzymes destructing the internalised particle [174]. Understanding the mechanism of ADCP of tumour cells is necessary to improve and develop therapeutic drugs and possible combination treatments.

4.4.2 Extracellular vesicles (EVs)

EVs play a role in the short and long distance communications between different cells and their microenvironment as well as in the TME [175], [176]. They are lipid bilayer-delimited particles that are released by cells [177] and carry a variety of proteins, nucleic acids, metabolites, lipids, and immune related ligands such as PD-L1 [177], [178].

EVs differ in size and function and can be grouped in exosomes and ectosomes. Exosomes are membrane bound EVs that are produced in the endosomal compartment of most cells. Moreover, they are surrounded by a multivesicular body that fuses with the plasma membrane *via* exocytosis. In contrast, ectosomes or microvesicles origin from the plasma membrane and are directly released from it [175], [179].

In the diagnosis and treatment of cancer, EVs represent a promising target. It is known that tumour cells release EVs in a high amount mediating a pro-survival TME. Hence, treatment strategies suggest to impair EV release by cancer cells or to use biologically engineered EVs to disrupt and manipulate communication with the TME [176], [178].

4.5   Therapy of B cell malignancies

Therapy options for B cell malignancies include a variety of treatments that directly affect malignant B cells or target the TME, with treatment strategies being initiated according to the biological and genetic disease status, patient age and fitness [14], [180].

Patients with a "double hit" lymphoma show poor survival after frontline therapy with rituximab, cyclophosphamide, hydroxydaunorubicin, vincristine, and prednisone (R-CHOP). It was shown that therapeutics such as vincristine or doxorubicin promote aneuploidy and polyploidy in *MYC/BCL2* "double hit" lymphoma leading to re-entering of lymphoma cells into the cell cycle during off-therapy periods [181]. Therefore, new treatment strategies are required such as small molecule inhibitors focusing on the disease biology.

For the patients suffering from CLL a broad spectrum of therapeutic options has been tested in clinical trials. However, therapy is only applied to CLL patients with progressed Rai and Binet stages or symptomatic course [14]. Moreover, the CLL-IPI categorise four groups of patients from low-risk to very high-risk defining the potential clinical consequences [34]. As treatment options following strategies were tested: Cytostatic agents, monoclonal antibodies, signalling inhibitors, checkpoint inhibitors, and chimeric antigen receptor T (CART) cell therapy. In addition, clinical trials investigate the synergistic or additive effects of combining respective treatment options with each other [14].

For several decades cytostatic therapy with chlorambucil was given as the standard treatment for CLL [182]. Furthermore, fludarabine, pentostatin, cladribine, cyclophosphamide, and bendamustin belong to the group of cytostatic agents [14], [183]–[186].

Treatment strategies with monoclonal antibodies mainly address anti-CD20 antibodies such as rituximab, ofatumumab, and obinutuzumab [187]–[190]. CD20 is expressed by mature B cells as well as by most malignant B cells [191] and was reported to play a role in the activation of the BCR signalling [191]. Subsequently, treatment with rituximab was shown to inhibit BCR signalling [192]. Moreover, rituximab is efficiently used in combination with chemotherapeutics such as the triple combination of fludarabine, cyclophosphamide, and rituximab (FCR) for young and fit CLL patients [193], [194]. However, patients with mutations in *TP53* and/or 17p deletion show resistance to the combination of chemo- and immunotherapy [195], [196]. Another monoclonal antibody is the anti-CD52 antibody alemtuzumab [197]–[199]. CD52 (Campath1-antigen) is a surface protein on mature lymphocytes [200]. Alemtuzumab treatment is highly effective in patients with a mutation in *TP53* [201], [202]. Moreover, it was tested in combinations with fludarabine [203] or fludarabine and cyclophosphamide [204]. Nevertheless, due to strategic decisions of Sanofi, the license for the CLL therapy was withdrawn in 2012. However, alemtuzumab is still available through an international compassionate use program [14].

Molecular signalling inhibitors like ibrutinib became a prominent treatment approach in B cell malignancies. Inhibition of the BCR signalling pathway plays an important role as it controls proliferation and survival of B cells (see chapter 4.2) [48], [53]. BTK is one major target of the BCR pathway and can be inhibited *via* ibrutinib. Ibrutinib covalently binds to the cysteine 481 residue of BTK and can be taken orally in a daily dose of 420 mg [205]–[207]. Discontinued therapy or mutations in BTK can lead to a resistance to ibrutinib therapy [208], [209]. Ibrutinib treatment can also affect the TME as BTK is not only expressed in B cells but also in macrophages [210]. Combination treatment of ibrutinib and rituximab showed a benefit in

survival compared to FCR therapy [211]. However, another study could not prove the benefit of ibrutinib and rituximab combination compared to ibrutinib mono therapy [212]. Other trials combined ibrutinib with bendamustin and rituximab [213] or ofatumumab [214]. BTK inhibition using second generation inhibitor acalabrutinib, that is more specific for BTK, needs to be further tested [14], [215]. The BCR pathway can be also inhibited using amongst others the PI3K-inhibitor idelalisib [216]. Moreover, BCL-2-inhibitor venetoclax and lenalidomide that inactivates the function of casein kinase 1α are used for CLL therapy [217]–[219]. Here, venetoclax serves as a new treatment strategy for patients with relapsed or refractory *TP53* mutation [14]. Venetoclax has been also tested in two clincal trials in combination with ibrutinib with first promising results [220], [221].

Another very important therapeutic strategy is the inhibition of immune checkpoints such as PD-1 and PD-L1. Pembrolizumab is an anti-PD-1 antibody that blocks the binding of PD-1 to PD-L1 activating T cells or macrophages helping in tumour cell clearance. Both immune checkpoints can be overexpressed in B cell malignancies and the TME [139], [140], [222].

Moreover, CART cell therapy with specificity to CD19, CD137, and CD3-zeta was investigated in CLL treatment but needs further investigation [223], [224].

In general, the combinatorial benefit of respective treatment strategies and their influence on B cell malignancies and the TME needs to be further investigated and understood on a molecular level.

5   Aim of the research

In B cell malignancies inhibition of the BCR signalling pathway using BTK-inhibitors like ibrutinib has become a very important therapeutic strategy [56]. Additional combination of small molecule inhibitors with monoclonal antibodies have been used in clinical trials with the molecular understanding of their synergistic interaction lagging behind [211]–[214]. The mechanisms of beneficial treatment combination need to be addressed not only on the tumour cell side but also in context of the TME. Here, phagocytosis of antibody-opsonized tumour cells by macrophages play a major role in the treatment of cancer with immunotherapeutics [144], [163], [164]. Accordingly, Pallasch *et al.* demonstrated that treatment of leukaemia bearing mice with anti-CD52 antibody alemtuzumab induce tumour cell clearance through activation of macrophage effector cell function and induction of phagocytosis [96].

Therefore, the work of this thesis hypothesised that combination therapy with small molecule inhibitors and monoclonal antibodies influence the ability of macrophages to induce phagocytosis of tumour cells. In particular, the following points were addressed:

1. Determining the role of ibrutinib and alemtuzumab combination therapy in the TME of malignant B cells and non-transformed macrophages *in vitro* and *in vivo*
2. Dissecting kinase signalling pathways in the interplay of lymphoma cells and macrophages
3. Defining synergistic mechanisms of enhancing antibody-mediated phagocytosis

6   Material and methods

If not explicitly stated in the text materials are listed alphabetically in Table 2 and Table 3. Parts of the materials and methods chapter are published in Barbarino *et al.*, 2020 [225].

6.1   Lists of materials

Table 2 Chemicals, substances and kits

Chemical / substance	Supplier/ Ingredients
10 X Towbin buffer	0.25 M Tris, 1.92 Glycine, H_2O to 1 L
10 X transfer buffer	200 ml Methanol, 100 ml 10 x Towbin buffer, H_2O to 1 L
10 X Tris buffered saline (TBS)	0.2 M Tris, 1.83 M NaCl, HCl (pH 7.6), H_2O to 1 L
2 X HEPES buffered saline (HBS)	Alfa Aesar, Haverhill, USA
5 X sample buffer	10 % Sodium dodecyl sulphate (SDS), 50 % glycerol, 0.08 % Bromphenolblau, 125 mM Tris HCl pH 6.8, 200 mM DTT
7-Aminoactinomycin D (7AAD)	Invitrogen, Carlsbad, USA, #2255903
Acalabrutinib	Selleckchem, München, Germany
Alemtuzumab	Genzyme, Cambridge, USA
Ammonium-chloride-potassium (ACK) lysis buffer	Thermo Fisher Scientific, Waltham, USA
Ampicillin	Carl Roth, Karlsruhe, Germany
Anti-PD1, GS-696882	Gilead, Foster City, USA
Bovine serum albumin (BSA)	PAA, Pasching, Austria
Calcium Chloride Dihydrate ($CaCl_2$)	Sigma, St. Louis, USA
CD293 media	Thermo Fisher Scientific, Waltham, USA
Chloroquine Diphosphate Salt	Sigma, St. Louis, USA
CHMFL-BMX-078	MyBioSource, San Diego, USA
Cyclophosphamide monohydrate (CTX)	Sigma, St. Louis, USA
Dulbecco's Modified Eagle Medium (DMEM)	Thermo Fisher Scientific, Waltham, USA

ELISA MAX™ Standard Set human and mouse IL-6, IL-10, TNF-α	BioLegend, San Diego, USA
Entospletinib	Gilead Sciences, Foster City, USA
Erlotinib	Selleckchem, München, Germany
F480 allophycocyanin (APC) antibody	BioLegend, San Diego, USA, #123116
Fetal bovine serum (FBS)	Biochrom GmbH, Berlin, Germany
GlutaMAX	Thermo Fisher Scientific, Waltham, USA
Halt Phosphatase Inhibitor Cocktail (100x)	Thermo Fisher Scientific, Waltham, USA, #78428
Halt Protease Inhibitor Cocktail, ethylenediaminetetraacetic acid (EDTA) free (100x)	Thermo Fisher Scientific, Waltham, USA, #78437
Human CD19 fluorescein isothiocyanate (FITC) antibody	BioLegend, San Diego, USA, #363008
Ibrutinib	Bertin, M.-le-Bretonneux, France
Iscove's Modified Dulbecco's Medium (IMDM)	Thermo Fisher Scientific, Waltham, USA
LPS	Sigma, St. Louis, USA
Mini protean pre-cast gel	BioRad, Hercules, USA
Mouse Fc-receptor blocking reagent	Miltenyi Biotec, Berg. Gladbach, Germany, #130092575
M-PER lysis buffer (Mammalian Extraction buffer)	Thermo Fisher Scientific, Waltham, USA, #78503, #78420, #87785
Nitrocellulose membrane	GE Healthcare, Freiburg, Germany
Obinutuzumab (GA101)	Roche, Basel, Switzerland
Odyssey Blocking buffer (PBS or TBS)	LI-COR Biotech., Bad Homburg, Germany
PageRuler Plus Prestained Protein Ladder	Thermo Fisher Scientific, Waltham, USA
Penicillin/Streptomycin (P/S)	Thermo Fisher Scientific, Waltham, USA
Phosphate buffered saline (PBS)	Thermo Fisher Scientific, Waltham, USA
Pierce BCA Protein Assay	Thermo Fisher Scientific, Waltham, USA, #23225
PMD2.G	Addgene, Watertown, USA, #12259
Polybrene	Sigma, St. Louis, USA

Polyethylenglykol (PEG) 400	Roth, Karlsruhe, Germany
Propylene glycol	Sigma, St. Louis, USA
PsPax2	Addgene, Watertown, USA, #12260
Puromycin	Invivo Gen, San Diego, USA
Radioimmunoprecipitation assay (RIPA) buffer	Cell Signaling, Danvers, USA
rh IFN-γ	ImmunoTools GmbH, Friesoythe, Germany
Rituximab	Roche, Basel, Switzerland
Roswell Park Memorial Institute (RPMI)	Thermo Fisher Scientific, Waltham, USA
Running buffer for SDS polyacrylamide gel electrophoresis (SDS-Page)	100 ml 10 X Towbin buffer, 0.1 % SDS, H_2O to 1 L
Ruxolitinib	AdipoGen Life Sciences, Liestal, Switzerland
Sodium butyrate	Sigma, St. Louis, USA
SP600125	Selleckchem, München, Germany
Thioglycolate	BD, Franklin Lakes, USA
Tirabrutinib (GS4059)	Gilead, Foster City, USA
Tofacitinib	Selleckchem, München, Germany
Total exosome isolation reagent	LifeTechnologies, Carlsbad, USA
Tris buffered saline with Tween-20 (TBS-T)	100 ml 10 X TBS, 0.1 % Tween-20, H_2O to 1 L
Tween 80	Sigma-Aldrich, St. Louis, USA
Zombie NIR^{M}Fixable Viability Staining	BioLegend, San Diego, USA
β-Mercaptoethanol	Thermo Fisher Scientific, Waltham, USA

Table 3 Devices

Device	Supplier
BD FACSCanto flow cytometer	BD, Franklin Lakes, USA
CASY Cell Counter Model TTC	Roche, Basel, Switzerland
Centrifuge 5810R	Eppendorf, Hamburg, Germany
FluoStar Optima	BMG Labtech, Ortenberg, Germany
Incubator	Labotect, Göttingen, Germany
LI-COR Odyssey infrared imaging system	LI-COR Biosciences, Lincoln, USA

MACSQuant VYB and X flow cytometer	Miltenyi Biotec, Berg. Gladbach, Germany
Mini Protean Tetra Cell apparatus	BioRad, Hercules, USA
Multitron Pro incubator shaker	Infors ht, Einsbach, Germany
Nanodrop 1000 Spectrophotometer	Thermo Scientific, Dubuque, USA
Optima Max-XP ultracentrifuge	Beckman Coulter, Brea, USA
Thermomixer Compact	Eppendorf, Hamburg, Germany

Table 4 Cell lines

Cell line	Background
Amphotropic phoenix cell line (HEK293T derivate)	Embryonic kidney derived packaging cell line, (AlleleBiotech, San Diego, USA, ABP-RVC-10001)
Humanised *MYC/BCL2* cell line (hMB) (strain 102)	Humanised model of *MYC/BCL2* driven "double hit" B cell lymphoma, green fluorescent protein (GFP)$^{+}$, [226]
J774A.1	Murine macrophages derived from ascites, ATCC, Manassas, USA
Murine primary peritoneal macrophages wt and *BTK*$^{-/-}$	Macrophages were obtained *via* peritoneal lavage from C57BL/6 mice (Charles River, Wilmington, USA and Jackson Laboratory, Bar Harbor, USA)
Primary CLL patient cells	CLL-Biobank, Cologne, Germany

6.2   Cell culture and cell lines

All cell lines (Table 4) were cultivated at 37 °C in a humidified incubator with 5 % CO_2. At a density/confluency of 80-90 % cells on the plate, cells were sub-cultured in a ratio of 1:10 or 1:20 (media containing cells : fresh media). For the experiments, cells were counted with the CASY cell counting technology.

The human-*MYC/BCL2* (hMB) "double hit" lymphoma cell line (strain 102) was generated by Leskov *et al.* [226] and sub-cultured in B cell culture medium (BCM). The BCM consisted of a 1:1 ratio of IMDM and DMEM, supplemented with 10% FBS, 1 % P/S, 1 % GlutaMAX and 1% β-Mercaptoethanol.

Murine J774A.1 macrophages and primary peritoneal macrophages were sub-cultured in DMEM supplemented with 10 % FBS and 1 % P/S. To isolate murine primary peritoneal macrophages, 8 to 24 weeks old wt and $BTK^{-/-}$ C57BL/6 mice were injected intra peritoneal (*i.p.*) with 1 ml prewarmed thioglycolate. After four days macrophages were obtained *via* peritoneal lavage. To achieve this, 20 ml DMEM was initially injected into the peritoneal cavity and after one minute incubation extracted with a venous catheter. Afterwards, the cell suspension was centrifuged for 10 min at 1500 rpm. Then 3-5 ml ACK lysis buffer was added to the cell pellet and incubated for 3 min at room temperature (RT). After incubation, the cell suspension was filled up to a volume of 50 ml with PBS and again centrifuged for 10 min at 1500 rpm. Next the pellet was resuspended into 10 ml DMEM and cells were plated out for 24 h prior starting the experiment. Primary peritoneal macrophages were used for up to one week post peritoneal lavage. C57BL/6 mice were generated by $BTK^{-/-}$ mice backcrossed to C57BL/6J background [227], [228].

Primary CLL patient cells were isolated from peripheral blood as previously described [229] and experiments were performed in RPMI with 1 % P/S and 10 % FBS. Experiments were approved by the ethical commission of the medical faculty of the University of Cologne (reference no. 13-091) and an informed written consent was obtained from all patients.

6.3 ADCP assays

To measure the antibody-mediated phagocytosis of lymphoma cells by macrophages, ADCP assays were performed. To set this up, J774A.1 macrophages were plated out at a density of 1 x 10^4 cells/well on a 96 well plate. After 4-24 h incubation at 37 °C macrophages attached to the bottom of the plate and 1.5 x 10^5 GFP$^+$ hMB lymphoma cells/well were added. Respective co-culture was treated for 16-17 h with different concentrations of tyrosine kinase inhibitors and monoclonal antibodies (alemtuzumab 10 µg/ml, rituximab 20 µg/ml, obinutuzumab 1 µg/ml) in combination or as mono therapy (Figure 5). Each condition was performed with five technical replicates. For the determination of ADCP GFP$^+$ hMB lymphoma cells were measured *via* the MACSQuant VYB flow cytometer. The percentage of ADCP was calculated as follows:

$$100 - \left(100 * \left(\frac{\frac{cells}{\mu l}\ treated}{\frac{cells}{\mu l}\ untreated} \right)\right)$$
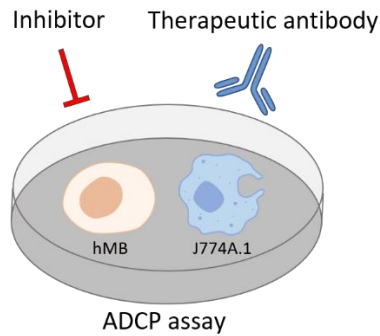
Figure 5 ADCP set-up
Co-culture of macrophages and hMB "double hit" lymphoma cells treated with therapeutic antibody and tyrosine kinase (TK) inhibitor.

6.3.1 ADCP assays with murine primary peritoneal macrophages

Murine primary peritoneal macrophages from C57BL/6J mice were harvested and cultivated as described in chapter 6.2. For the ADCP assays primary peritoneal macrophages were plated out at a density of 5 x 10^4 and co-cultured with hMB lymphoma cells and treated as described above (6.3).

6.3.2 ADCP assay with primary CLL patient cells

For the ADCP assays with primary CLL patient samples, CLL cells were thawed 2-4 h prior to the experiment and pre-treated for 24 h with different concentrations of ibrutinib. Afterwards, 5 x 10^5 CLL cells/well were co-cultured with J774A.1 macrophages as described in chapter 6.3. Here, the co-culture was treated with alemtuzumab for 2 h and then CLL cells were stained with CD19 FITC fluorescent antibody for 15 min at 4 °C before measurement by flow cytometry. Since the CLL patient cells show a low proliferation rate *ex vivo* and to better determine the additional effect of alemtuzumab antibody treatment the ADCP was calculated as follows:

$$100 - \left(100 * \left(\frac{\frac{cells}{\mu l} \ treated \ with \ alemtuzumab}{\frac{cells}{\mu l} \ without \ alemtuzumab \ treatment}\right)\right)$$

Here, the remaining cells/µl of the co-culture treated with alemtuzumab are normalised against without alemtuzumab treatment. In contrast, the calculation in chapter 6.3 normalise the remaining cells/µl of the co-culture with treatment against without any treatment.

6.3.3 Pre-treatment of hMB and J774A.1 macrophages for the ADCP assays

For the pre-treatment ADCP assays, 1 x 10^5 J774A.1 macrophages/ml and 2.25 x 10^6 hMB lymphoma cells/ml were pre-treated with different concentrations of respective tyrosine kinase inhibitors for 24 h. Afterwards the cells were scraped off and washed twice with 3 ml media by centrifuging at 300 g for 5 min. Then cells were counted and plated out for ADCP assay as described above (6.3).

6.3.4 Generation of conditioned media for the ADCP assays

For the generation of conditioned media 1.5 x 10^6 hMB cells/ml were incubated with different concentrations of respective tyrosine kinase inhibitors in 10 ml media for 24 h. Afterwards, the inhibitor was washed off in two centrifugation steps with 3 ml media at 300 g for 5 min and the pellet was resuspended in 10 ml fresh media for another 24 h. After 24 h, the supernatant was passed through a 0.45 µm filter. The ADCP assay was performed according to 6.3. To generate conditioned media of hMB *JAK2* knock out (KO) cells, respective cells were incubated in fresh media for 24 h and the supernatant was directly taken and filtered as described above.

6.3.5 Isolation of extracellular vesicles (EVs) for the ADCP assays

To isolate EVs for the ADCP assays, 5 x 10^8 hMB lymphoma cells were plated out in 30 ml CD293 media on a 15 cm cell culture dish and incubated for 24 h at 37 °C. Next, the cells were centrifuged for 5 min at 300 g. In the following steps the supernatant was taken and centrifuged again, first for 10 min at 2,900 rpm and then again for 20 min at 3500 rpm. The supernatant of the last centrifugation was then filtered through a 0.2 µm filter. Afterwards, total exosome isolation reagent (Table 2) was added to the supernatant in a 1:2 ratio and incubated at 4 °C for 24 h. Then the solution was centrifuged for 60 min at 10,000 g at 4 °C. After centrifugation, the dry pellet was resuspended into 1,200 µl PBS and ultracentrifuged for 110 min at 110,000 g at 4 °C. The respective pellet was resuspended again in 500 µl PBS and EVs were stored prior to use at -80 °C.
The ADCP assay was performed as described above (6.3) and EVs were added with 5 µl of the isolated sample per well.

6.3.6 Phagocytosis F480 staining

In order to calculate the amount of lymphoma cells phagocyted by macrophages, J774A.1 macrophages were plated out at a density of 1×10^5 cells in 1 ml media. After 4 h incubation at 37 °C 1.5×10^6 hMB cells in 1 ml media were added. Additionally, 250 µl alemtuzumab (10 µg/ml), and 250 µl of different ibrutinib concentrations were added. After 16 h incubation at 37 °C all cells were blocked with 10 µl Fc-receptor blocking agent for 10 min and afterwards macrophages were stained with F480 APC antibody for 15 min at 4 °C. GFP$^+$ and F480$^+$ double positive cells were measured on BD FACSCanto.

6.4 Toxicity staining

To analyse the influence of tyrosine kinase inhibitors on macrophages, 1×10^6 J774A.1 macrophages were cultivated in 2 ml media with different concentrations of respective tyrosine kinase inhibitors. After 24 h incubation at 37 °C, macrophages were stained with 100 µl Zombie NIR^{M}Fixable viability staining diluted 1:100 in PBS and incubated for 15 min at RT in the dark. The Zombie viability staining was measured with the BD FACSCanto.

To analyse the influence of tyrosine kinase inhibitors on lymphoma cells, 1.2×10^5 hMB cells were cultivated in a 96 well plate in 200 µl BCM with different concentrations of respective tyrosine kinase inhibitors. After 24 h incubation, hMB cells were either stained with 7AAD diluted 1:100 in PBS for 15 min at 4 °C or the GFP$^+$ hMB cells were directly measured *via* MACSQuant flow cytometer.

All toxicity stainings included a positive control with 10 or 20 % dimethyl sulfoxide (DMSO) and a negative control considering the influence of the DMSO concentration used as dilution for the highest tyrosine kinase inhibitor concentration. Moreover, all stainings included three biological replicates.

6.5 Immunophenotyping

To detect changes in the expression of cell surface markers on macrophages or lymphoma cells multi-colour fluorescence flow cytometry was used. Thereby, the number of positive fluorescently labelled cells were calculated as follows:

(Sample stained with fluorescently labelled antibody) − (sample stained with isotype control)

The median fluorescence intensity (MFI) shows the median surface marker expression profile across all cells. All stainings were repeated with at least three biological replicates.

6.5.1 Macrophage polarisation marker

In order to measure the influence of tyrosine kinase inhibitors on macrophage polarisation, 2 x 10^5 J774A.1 macrophages were cultivated in 1 ml media and treated with respective concentrations of tyrosine kinase inhibitors. After 4 h incubation at 37 °C, 100 ng/ml LPS was added and incubated for another 20 h. Next, the supernatant was removed, cells were scraped off, and resuspended in 100 µl PBS with 100 µl Fc-receptor blocking reagent diluted 1:10 in PBS. After 10 min incubation at 4 °C, M1 and M2 macrophage polarisation markers were stained with fluorescently labelled antibodies (Table 5) according to the manufacturer's instructions and with the recommended isotype for another 10 min at 4 °C. Antibodies that did not bind to respective markers were washed off at 300 g for 5 min with 1 ml PBS. The pellet was resuspended in 100 µl PBS and measured with either the MACSQuant X flow cytometer or the BD FACS Canto.

Table 5 Macrophage polarisation marker FACS-antibodies

Antibody	Colour	Marker	Supplier
Mouse Arg1	PE	M2	BioLegend, San Diego, USA, #IC5868
Mouse CD206	PE-Cy7	M2	BioLegend, San Diego, USA, #141719
Mouse CD64	PE	M1	BioLegend, San Diego, USA, #139304
Mouse CD80	APC	M1	BioLegend, San Diego, USA, #104714
Mouse CD86	Phycoerythrin (PE)	M1	Milteny Biotech, B. Gladbach, Germany, #130-102-604
Mouse MHCII	FITC	M1	BioLegend, San Diego, USA, #107605

6.5.2 Cell surface marker expression of lymphoma cells

To identify the influence of tyrosine kinase inhibition on cell surface markers of lymphoma cells, 1.5 x 10^5 hMB cells were cultured in 100 µl BCM and incubated for 17 h at 37 °C with respective tyrosine kinase inhibitor concentrations. Afterwards, cells were stained with fluorescently labelled antibodies (Table 6) according to the manufacturer's instructions and

with the recommended isotype for 20 min at 4 °C. Antibodies that did not bind to respective markers were washed off at 300 g for 5 min with 1 ml PBS. The pellet was resuspended in 100 µl PBS and measured with MACSQuant X flow cytometer.

Table 6 Cell surface marker FACS-antibodies

Antibody	Colour	Supplier
Human CD20	PE	Milteny Biotech, B. Gladbach, Germany, #130-098-084
Human CD47	PE	BioLegend, San Diego, USA, #323109
Human CD52	APC	BioLegend, San Diego, USA, #316008
Human PD-L1 (CD274)	Brilliant violet (BV)	BioLegend, San Diego, USA, #329713

6.6   Enzyme-linked immunosorbent assay (ELISA)

In order to measure the influence of tyrosine kinase inhibition on the expression of IL-6, IL-10 and TNF-α in macrophages and lymphoma cells, ELISA's were performed. Therefore, 2×10^5 J774A.1 macrophages and 1.5×10^6 hMB cells were cultivated in 1 ml of respective media and treated with tyrosine kinase inhibitors for 24 h. Additionally, J774A.1 macrophages were treated after 4 h with 100 ng/ml LPS. After incubation, the supernatant was centrifuged at 300 g for 5 min and ELISA assay from BioLegend was performed according to the manufacturer's instructions. The absorbance was measured with the microplate reader FluoStar Optima.

6.7   Generation of CRISPR-mediated knock-out in hMB cells

To generate hMB lymphoma cells with a KO in *BTK* and *JAK2* the CRISPR/Cas9 system was used. Therefore, hMB cells expressing Cas9 were generated using an mCherry/Cas9 guide ribonucleic acid (RNA, #99154, Addgene, Watertown, USA) gifted from Agata Smogorzewska. Afterwards, the mCherry Cas9 expressing hMB cells were transfected with guide RNAs inducing a KO in *BTK* (#7707 1-4) or *JAK2* (#7572 6-7) and a non-target (#80248) guide RNA (Addgene, Watertown, USA), all gifted from John Doench and David Root [230].

6.7.1 Preparation and generation of plasmid guide RNA

Guide RNAs from Addgene were sent in DH5α bacteria as agar stab with resistance to ampicillin. Therefore, respective bacteria were plated out on a LB-medium plate containing ampicillin. After incubation over night at 37 °C colonies were picked and resuspended into 150 ml LB-media containing 100 ng/ml ampicillin and incubated in a shaking incubator for another 12-16 h at 37 °C. Next, the plasmid DNA was extracted using the Qiagen Plasmid Plus kit (Qiagen, Hilden, Germany). The purification and amount of DNA was measured by Nanodrop.

6.7.2 Transduction of virus producing phoenix cells with plasmid DNA

To produce guide RNA containing virus, amphotrophic phoenix cells were transduced with respective plasmid DNA using the calcium phosphate method. Phoenix cells were normally kept in DMEM plus 10 % FBS and 1 % P/S. At a density of 80 % cells on the plate the media was changed to DMEM$^{-/-}$ plus 2.5 % FBS and 25 µM chloroquine. Then a mixture was prepared containing 18.5 µg of respective plasmid DNA, 3 µg PMD2.G, 5 µg PsPax2, 99 µl 2M CaCl$_2$ and filled up with sterile H$_2$O to a total volume of 790 µl. While producing bubbles in this mixture 790 µl 2xHBS was added dropwise. Afterwards, the whole mixture was given dropwise to the phoenix cells and incubated for 4 h at 37 °C. Next, the transfection media was aspirated from the cells and fresh DMEM with 10 % FBS and 1 % P/S was added. After 24 h at 37 °C 80 µl sodium butyrate was added to the cells and incubated for another 24 h. Then, the supernatant was taken and filtered through a 0.45 µm filter. The virus containing media was stored at -80 °C. To the remaining phoenix cells fresh media with sodium butyrate was added and incubated for another 24 h. Then, supernatant was harvested and filtered again.

6.7.3 Transfection of hMB lymphoma cells with guide RNA containing virus and single cell sorting

To transfect the hMB lymphoma cells with the guide RNA containing virus, 3 x 10^6 hMB cells/well in 3 ml BCM were plated out on a 12 well plate together with 3 ml of virus containing media and 4 µg/ml polybrene. After spin infection for 2 h at 800 g and 32 °C the cells were incubated for 48 h at 37 °C. After incubation, the media was changed to BCM and cultured for 4-5 days so that the cells could rest from the spin infection. To select the successfully transfected cells from the non-transfected cells 5 µg/ml puromycin was added to the BCM and cultured for 2 weeks.

To collect single cell clones, selected hMB lymphoma cells were diluted in serial dilution steps to a concentration of 1×10^2 cells in 100 ml DMEM plus 20 % FBS and plated out with 200 µl/well on five 96 well plates. Expanded clones were sub-cultured in a 24 well plate prior to protein cell lysis. To validate if the guide RNA knocked out its respective target, western blot analysis was performed as described in chapter 6.8. For the detection of BTK and JAK2 primary antibodies from Cell Signaling were used (BTK: D3H5 rabbit mAB #8547; JAK2: D2E12 XP® rabbit mAB #3230) and afterwards stained with secondary fluorescent dye-labelled antibodies (LI-COR Biotech., Bad Homburg, Germany). Protein bands were detected at 700 or 800 nm using the LI-COR Odyssey infrared imaging system. Protein loading was normalised against glyceraldehyde 3-phosphate dehydrogenase (GAPDH). Densitometry was performed with Image Studio Lite Ver 5.2 software (LI-COR Biosciences, Lincoln, USA).

6.8 Western blot analysis

In order to detect proteins of cell lysates or validate KO's of cell lines western blot analysis was performed.

6.8.1 Preparation of cell lysates

To perform western blot analysis, 8×10^6 hMB lymphoma cells were lysed with RIPA buffer containing Halt phosphatase inhibitor and protease inhibitor cocktail, EDTA free diluted 1:100 with RIPA buffer. After 30 min incubation on ice, cells were centrifuged at 13,200 rpm at 4 °C for 15 min. The supernatant was transferred to a fresh tube and protein concentration was determined using Pierce BCA Protein Assay from Thermo Fisher and measured with microplate reader FluoStar Optima.

To analyse phosphorylated proteins by western blot, hMB cells were treated with respective concentration of tyrosine kinase inhibitors for 1 h and then stimulated with 100 ng/ml rh IFN-γ for another 1 ½ h. Afterwards, cells were lysed without adding halt phosphatase inhibitor cocktail.

6.8.2 SDS polyacrylamide gel electrophoresis (SDS-Page)

For the separation of proteins 10-50 µg of total protein of each sample was separated on pre-casted gradient gels from BioRad. Prior to loading the samples on the gels, lysates were mixed with 5 X sample buffer and heated for 5 min at 95 °C. Additionally to the samples, 5 µl of a

pre-stained protein marker (page ruler) was loaded onto the gel. Protein separation was carried out in 1 X running buffer on a Mini Protean Tetra Cell apparatus from BioRad for 60-90 min at 160 V.

6.8.3   Western blotting

To detect proteins and validate hMB KO's, the separated proteins on the gel were transferred onto a nitrocellulose membrane in 1 X transfer buffer for 90 min at 100 V and 4 °C using a wet tank blotting system from BioRad. After protein transfer, the membrane was blocked with 5 % BSA in TBS for 1 h at RT. Immunoblotting was performed incubating the blocked membrane with the corresponding primary antibodies (Table 7) diluted in 5 % BSA and TBS-T according to the manufacturer's instructions over night at 4 °C. After washing the membrane three times with TBS-T for 5 min, secondary fluorescent dye-labelled antibodies diluted in Odyssey blocking buffer (PBS or TBS for pSTAT3 and STAT3) were applied for 1 h at RT in the dark. Following washing the membrane again, protein bands were detected at 700 or 800 nm *via* LI-COR Odyssey infrared imaging system. For the detection of BTK and JAK2, protein loading was normalised against GAPDH using Image Studio Lite Ver 5.2 software (LI-COR, Lincoln, USA).

Table 7 Antibodies for the western blotting

Antibody	Supplier
BTK D3H5 rabbit mAb	Cell Signaling, Danvers, USA, #8547
GAPDH (anti human)	Cell Signaling, Danvers, USA, #649202
IRDye goat anti-mouse 680RD/800CW	LI-COR Biotech., Bad Homburg, Germany
IRDye goat anti-rabbit 680RD/800CW	LI-COR Biotech., Bad Homburg, Germany
JAK2 D2E12 XP® rabbit mAb	Cell Signaling, Danvers, USA, #3230
pSTAT3 mouse mAb	Cell Signaling, Danvers, USA, #4113
STAT3 rabbit mAb	Cell Signaling, Danvers, USA, #12640

6.9   Kinase activity profiling by PamChip peptide microarrays

In order to elucidate kinase activity profiles of treated cell lysates PamChip peptide microarrays from PamGene (International B. V., Netherlands https://www.pamgene.com/en/pamchip.htm) were used.

6.9.1 Cell lysate preparation and protein quantification

For the lysate preparation 5×10^6 hMB, J774A.1 macrophages, or CLL patient cells were treated for 6 h with either 1 μM ibrutinib, acalabrutinib or tirabrutinib. Afterwards cells were washed with PBS and centrifuged for 5 min at 300 g. Next, 100 μl M-PER lysis buffer with 1 μl Halt Phosphatase Inhibitor Cocktail and 1 μl Halt Protease Inhibitor Cocktail, EDTA free was given to the cell pellet and incubated for 15 min on ice. Then the cell pellets were centrifuged for 15 min at 16,000 g at 4 °C. The supernatant containing the proteins was transferred into a fresh tube and frozen at -80 °C in 10 μl aliquots. Protein concentration was determined using Pierce BCA Protein Assay from Thermo Fisher and measured with the microplate reader FluoStar Optima.

6.9.2 Kinase activity profiling by PamChip peptide microarray

The kinase activity profile of respective lysates was measured *via* PamChip peptide microarrays on a Pam Station 12 (PamGene International B. V., 's-Hertogenbosch, Netherlands https://www.pamgene.com/en/pamchip.htm). PamChip microarrays contain distinct peptides with 12-15 amino acids representing different proteins. These peptides get phosphorylated depending on the kinase activity in the lysates. Phosphorylated peptides are recognised by phospho-specific PY20 FITC-conjugated antibodies and then detected with a charge-coupled device (CCD) camera (Figure 6).

For the kinase activity profiling, Protein-Tyrosine kinase (PTK) and Serine/Threonine (STK) Chips containing 196 and 140 peptides targeting the main kinase families were used. For the PTK activity profiling 5 μg of total protein concentration was loaded on the chip and dissolved in 4 μl 10x PK buffer, 0.4 μl 100x BSA, 4 mM ATP, 0.6 μl FITC conjugated antibody, 10 mM DTT, 4 μl PTK additive and filled up with distilled water to 40 μl total volume (basic mix). All reagents were supplied by PamGene International B.V. ('s-Hertogenbosch, Netherlands). For the STK 1 μg of total protein concentration was loaded on the chip and dissolved in 4 μl 10x PK buffer, 0.4 μl 100x BSA, 4 mM ATP, 0.5 μl STK primary Antibody mix and filled up with distilled water to a total volume of 35 μl (basic mix). Moreover, 0.4 μl FITC conjugated antibodies dissolved in 3 μl 10x AB buffer and 26.6 μl water were added after an initial incubation time (detection mix). Prior to sample loading a blocking step was performed loading 30 μl of 2% BSA. To determine the kinase activity kinetics, the samples were pumped several times (cycles) through the microarray and imaged at certain cycle passages. For all experiments,

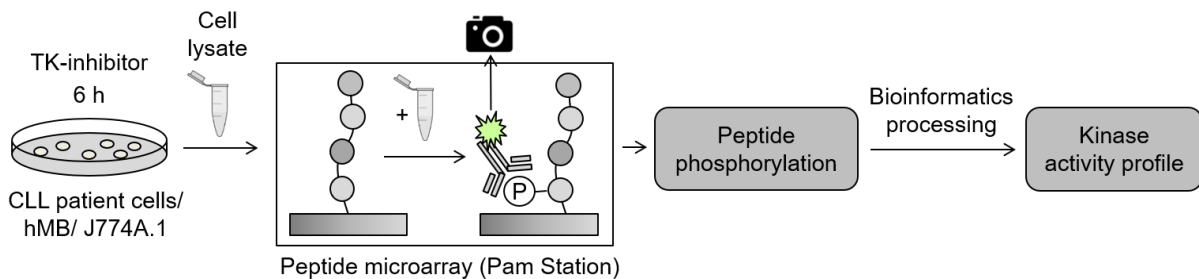three biological replicates were performed. CLL patient samples were measured in technical replicates.

Figure 6 Kinase activity profiling by PamChip peptide microarray
Target cells were treated with tyrosine kinase (TK) inhibitors for 6 h and the kinase activity of respective cell lysate was measured *via* PamChip peptide microarrays on a Pam Station 12 (PamGene International B. V., 's-Hertogenbosch, Netherlands https://www.pamgene.com/en/pamchip.htm). PamChip microarrays contain distinct peptides representing different proteins. These peptides get phosphorylated depending on the kinase activity in the lysates. Thereby, phosphorylated peptides were recognised by fluorescently labelled antibodies and then detected with a CCD camera. Finally, the peptide phosphorylation outcome was transformed *via* bioinformatics processing to a kinase activity profile.

6.10 Animal experiments

Animal experiments were conducted with permission of the Landesamt für Natur, Umwelt und Verbraucherschutz Nordrhein-Westfalen under the file numbers 84-02.04.2016.A119 and Uniklinik Köln_Anzeige §4.16.009. For *in vivo* experiments, NOD.Cg-Prkdc^{scid} II2rg^{tm1Wjl}/SzJ (NSG, Jackson Laboratory, Bar Harbor, Hancock, USA) immunodeficient mice were used. This mouse model allows to grow human lymphoma by circumventing the problem of species incompatibility. Furthermore, they accept and tolerate therapy with human specific antibodies. Mice had *ad libitum* access to sterile autoclaved normal chowed diet and 2 % H_2SO_4 acidified water.

For the experiments, 8–14 weeks old male NSG mice were injected intravenous (*i.v.*) with 1 x 10^6 hMB lymphoma cells diluted in 100 µL PBS [226] (Figure 7). Ten days after injection mice were treated *i.p.* on three consecutive days with ibrutinib (30 mg/kg), alemtuzumab (day 1, 1 mg/kg; day 2 and day 3, 5 mg/kg), tirabrutinib (30 mg/kg), CTX (day 1 and 3 100 µl PBS; day 2, 1 mg/kg), anti-PD1 antibody (day 1,3, and 5, 10 mg/kg) or 100 µl PBS as control. Agents were dissolved in PBS, except for ibrutinib that was dissolved in 30 % PEG 400, 0.5 % Tween 80 and 5 % Propylene glycol. After treatment, the health status of the mice were monitored

according to the German animal experiment committees (Tierversuchsantrag, TVA) score sheet. Under achievement of humane endpoints, mice were sacrificed by cervical dislocation.
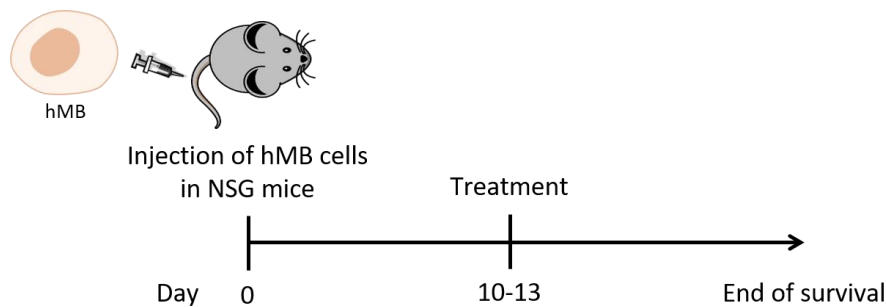

Figure 7 *In vivo* **set-up**
Male 8–14 weeks old NSG mice were injected *i.v.* with hMB lymphoma cells and treated ten days after injection. Upon reaching humane endpoints according to the German animal experiment committees (Tierversuchsantrag, TVA), mice were sacrificed by cervical dislocation.

Since B cells home to the lymph nodes and spleen [72], the spleen and bone marrow were harvested after cervical dislocation and analysed for the number of GFP$^+$ hMB cells, macrophages, as wells as the expression of human CD47 and PD-L1. Therefore, the spleen and bone marrow were dissociated with cell strainers in PBS and lysed with 5 ml ACK lysis buffer for 5 min at RT in the dark. Remaining cells were washed with PBS two times for 5 min at 300 g and again dissociated with cell strainers to avoid clumping of the cells. For the flow cytometry, samples were stained with anti-mouse F480 APC antibody (BioLegend, San Diego, USA, #123116), anti-human CD47 PE antibody (BioLegend, San Diego, USA, #323109) and anti-human PD-L1 BV antibody (BioLegend, San Diego, USA, #329713) for 20 min at 4 °C. Afterwards, unbound antibodies were washed off for 5 min at 300 g.

6.11 Graphical and statistical analysis

For the data analysis of ADCP assays Microsoft Excel (Microsoft corporation, Redmond, USA), MACSQuantify (Miltenyi Biotec, Berg. Gladbach, Germany), and FlowJo (FlowJo, LLC, Ashland, USA) was used. ELISAs were analysed in Microsoft Excel. Image analysis of western blots were done by Image Studio Lite version 5.2 (LI-COR Biosciences, Lincoln, USA) and phosphorylation status calculated with Microsoft Excel. The overall survival was evaluated using SPSS (IBM Deutschland GmbH, Ehningen, Germany).

Statistical comparison between groups was performed using the One-way ANOVA multiple comparison test in the ADCP assays and flowcytometry, the Kruskal–Wallis test for the non-

Gaussian distributed data, and the two-tailed unpaired student's t-test for the ELISA and flowcytometry data. Kaplan–Meier survival analysis was performed using pairwise Log-rank (Mantel–Cox) test. Differences were considered statistically significant at p-values less than 0.05 (ns = not significant, p > 0.05; *, p ≤ 0.05; **, p ≤ 0.01; ***, p ≤ 0.001).

For the Pam Station analysis, Bio Navigator software (PamGene International B. V., 's-Hertogenbosch, Netherlands) was used to calculate the cycle and time dependent signals into a single value for each peptide on the chip (exposure time scaling). Furthermore, outliers due to saturation or insufficient antibody binding were excluded. For further analysis, data were log transformed calculating the fold change between treated and untreated, and the p-value was calculated using an unpaired Students' two-tailed t-test. A p-value of p ≤ 0.05 was accepted as statistically significant. Individual peptides were matched to their representative kinases using a proprietary database (unpublished; PamGene International B. V., 's-Hertogenbosch, Netherlands). In brief, this database ranked the likelihood of peptides belonging to kinases using the public databases PhosphoNET, Phosphosite PLUS, Phospho.elm, UniPROT, Reactome, and Human Protein Reference Database identifying 384 kinases with 76,068 matches. Volcano plots were produced using the Enhanced Volcano package in RStudio (R version 3.3.1).

All graphs were generated using GraphPad Prism 8.00 (GraphPad Software, San Diego, USA) and Adobe Illustrator CS2 (Adobe Inc., San José , USA). Unless otherwise stated, bar graphs represent the mean +/- standard deviation (SD) of three biological replicates. Box plots show the minimal and maximal value, the 25th and 75th quartiles, and the median.

7 Results

Previously, Pallasch *et al.* could show that treatment of leukaemia bearing mice with anti-CD52 antibody alemtuzumab induce tumour cell clearance through activation of macrophage effector cell function and induction of phagocytosis [96]. In addition, they could overcome therapy resistant microenvironments such as the bone marrow by combining low-dose chemotherapy with antibody treatment. Since chemotherapeutics show high side effects, small molecule inhibitors become more and more important in the treatment of B cell malignancies. Here, S. Henschke ascertained a beneficial interaction of antibody treatment with inhibition of BTK in the BCR signalling pathway *via* ibrutinib in tumour cell clearance [225] (chapter 7.1).

Building on these findings, the work within this thesis has investigated and clarified the mechanisms of BCR inhibition and its interaction with the tumour microenvironment. Moreover, the work within this thesis focused on the role of BCR-inhibitor off target effects on B cell lymphoma clearance by macrophage-mediated ADCP.

The major part of this thesis is published in Barbarino *et al.* [225] as well as in Izquierdo and Vorholt *et al.* [231].

7.1 Ibrutinib enhances macrophage-mediated ADCP of hMB cells

In order to clarify the potential synergistic interaction between monoclonal therapeutic antibodies and BCR signalling inhibitors on B cell lymphoma clearance, ADCP assays were performed. To achieve this, J774A.1 macrophages were used as effector cells and co-cultured with hMB cells as target cells. Additionally, anti-CD52 antibody alemtuzumab and different concentrations of ibrutinib were utilised as treatment and added to the co-culture system. After 16-17 h incubation, the remaining GFP$^+$ hMB lymphoma cells were measured *via* flow cytometry. Here, it was observed that hMB lymphoma cells co-cultured with J774A.1 macrophages showed no basal phagocytosis rate (Appendix Figure 43A). Nevertheless, ADCP assays were normalised to the level of hMB cells co-cultured with macrophages. In the following ADCP set ups a concentration of 10 µg/ml alemtuzumab was used as this concentration was the lowest showing a significant tumour cell clearance by macrophages (Appendix Figure 43B).

Respective co-treatment of alemtuzumab and ibrutinib enhanced macrophage-mediated phagocytosis of lymphoma cells with increasing phagocytosis observed with increasing concentration of ibrutinib (Figure 8A). The increase in combination therapy seems to be

synergistic rather than additive, since the mean of the observed ADCP from the combination therapy (54.64 %) was 10 % higher than the expected ADCP (alemtuzumab monotherapy 29.28 % + ibrutinib monotherapy 14.93 % = 44.21 %). This increase in ADCP was not credited to cell toxicity induced by ibrutinib and alemtuzumab (Appendix Figure 43C and D). To prove that ibrutinib explicitly enhanced the phagocytosis of antibody targeted B cell lymphoma cells, engulfment of GFP+ hMB lymphoma cells into F4/80+ stained J774A.1 macrophages was measured (Figure 8B). As expected, increasing ibrutinib concentrations lead to a rising number of F4/80+/GFP+ double positive cells. Furthermore, the number of macrophages present under ibrutinib and alemtuzumab treatment stayed stable, indicating that the increased engulfment of hMB cells was not due to enhanced macrophage proliferation (Figure 8C).
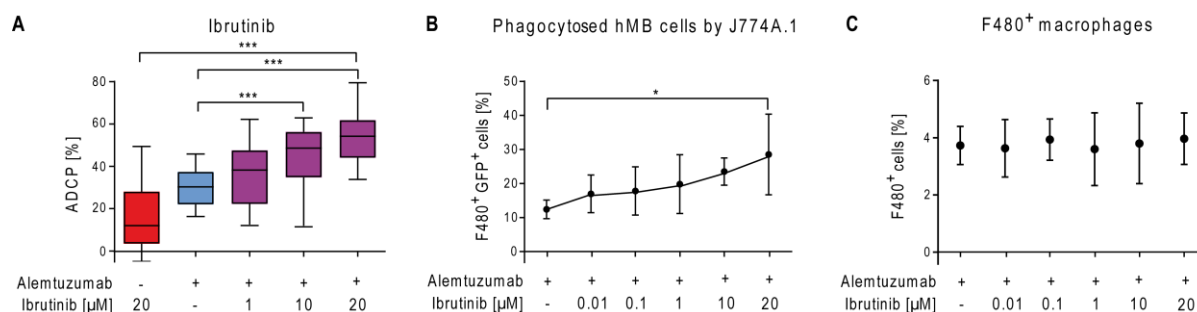

Figure 8 Ibrutinib enhance macrophage-mediated antibody-dependent cellular phagocytosis (ADCP).
(A) Box plot showing ADCP of hMB "double hit" lymphoma cells and J774A.1 macrophages treated with ibrutinib and alemtuzumab. Data are normalised to the co-culture without treatment. **(B)** Bar graph showing phagocyted hMB cells by J774A.1 macrophages, measuring GFP+ hMB lymphoma cells and F4/80+ macrophages in an ADCP model treated with ibrutinib and alemtuzumab. **(C)** Bar graph showing F4/80+ J774A.1 macrophages treated with alemtuzumab and different concentrations of ibrutinib. Box plots show the median, the 25th and 75th quartiles, and the minimal and maximal value. All bar graphs display the average and SEM. Experiments were performed of at least three biological replicates using flow cytometry. Data were performed together with S. Henschke. (* $p < 0.05$, *** $p \leq 0.001$)

To verify the role of the target cell line on ADCP, primary leukaemic cells from CLL patients were used as target cell line and pre-treated with ibrutinib for 24 h (Figure 9A). Comparing the ibrutinib treated co-culture with antibody to without antibody therapy exhibited a significantly enhanced ADCP using low ibrutinib concentrations of 0.01 µM (see calculation in 6.3.2). This corresponds to concentrations achieved with oral formulation of 420 mg ibrutinib daily [232]. Furthermore, to verify the role of macrophage effector cells on ibrutinib enhanced ADCP, murine primary peritoneal macrophages were used as effector cell line and revealed a similar increase in ADCP as measured with J774A.1 macrophages (Figure 9B).
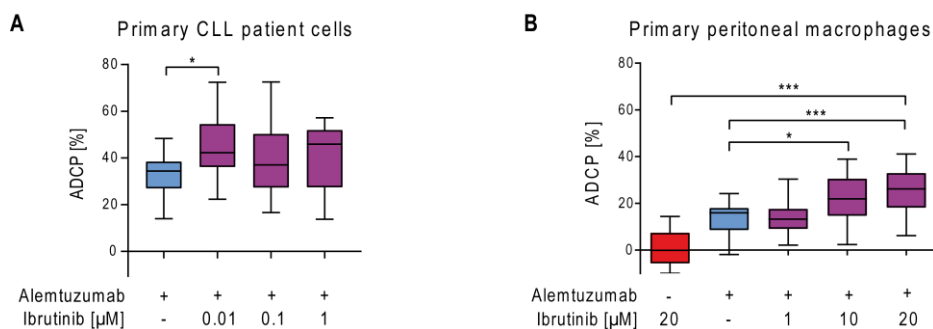
Figure 9 Ibrutinib increases ADCP using CLL patient cells or primary peritoneal macrophages.
(**A**) Box plot showing ADCP of CD19$^+$ primary chronic lymphocytic leukaemia (CLL) patient cells (N=6 patient samples) pre-treated *ex vivo* with ibrutinib for 24 h and co-cultured with J774A.1 macrophages. Alemtuzumab treatment was applied for 24 h. The graphic shows the relative macrophage-dependent cell death in the presence or absence of antibody. (**B**) Box plot showing ADCP of hMB "double hit" lymphoma cells and murine primary peritoneal macrophages (N=5 mice) as effector cells treated with ibrutinib and alemtuzumab. Data are normalised to the co-culture without treatment. Box plots show the median, the 25th and 75th quartiles, and the minimal and maximal value. Experiments were performed of at least three biological replicates using flow cytometry. Data were performed by S. Henschke. (* = p ≤ 0.05, *** = p ≤ 0.001)

To address the role of other clinically relevant B cell lymphoma antigen targeting antibodies, ADCP assays with J774A.1 macrophages, hMB cells, ibrutinib and antibodies targeting CD20 were performed. Here, the increase in ADCP of alemtuzumab in combination with 20 μM ibrutinib could be reproduced using anti-CD20 antibodies rituximab (Figure 10A) and obinutuzumab (Figure 10B), with obinutuzumab inducing an overall higher ADCP rate compared to rituximab.
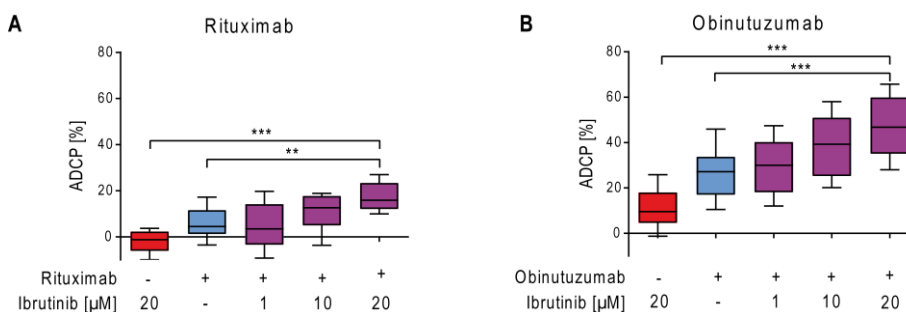

Figure 10 Ibrutinib increases ADCP using anti-CD20 antibodies.
Box plot showing ADCP of hMB "double hit" lymphoma cells and J774A.1 macrophages treated with anti-CD20 antibodies Rituximab (**A**) and Obinutuzumab (**B**). Data are normalised to the co-culture without treatment. Box plots show the median, the 25th and 75th quartiles, and the minimal and maximal value. Experiments were performed of at least three biological replicates using flow cytometry. Data were performed by S. Henschke. (** = p ≤ 0.01, *** = p ≤ 0.001)

Finally, to demonstrate the positive effect of combination therapy *in vivo*, hMB cells were transplanted into 8-14 weeks old male NSG mice resulting in a highly penetrant and aggressive *MYC/BCL2* "double hit" lymphoma. Ten days after transplantation mice were treated *i.p.* with

ibrutinib and alemtuzumab in combination or as mono therapy. For the control group mice were treated with PBS.

Pairwise Kaplan–Meier analysis to the PBS control group revealed a significant increase in overall survival with alemtuzumab mono therapy (alemtuzumab vs. PBS p = 0.049) as also previously shown by Pallasch *et al.* [96] (Figure 11A). In addition, combination treatment of ibrutinib with alemtuzumab significantly enhanced overall survival of hMB lymphoma carrying mice (ibrutinib + alemtuzumab vs. PBS p = 0.019). Furthermore, there was a clear but not significant shift of 1.5 days in the median overall survival comparing combination therapy (median = 12.5 days) with alemtuzumab mono therapy (median = 11 days), represented by a lower p-value compared to the PBS control group.

Besides assessment of overall survival the disease burden shortly after therapy onset was addressed by counting the total amount of GFP$^+$ hMB cells in spleen and bone marrow using flow cytometry (Figure 11B). Here, the number of hMB cells in the spleen was significantly decreased for the alemtuzumab mono therapy and alemtuzumab plus ibrutinib combination therapy. Moreover, both treatments nearly eliminated all hMB cells. In contrast, there was no reduction of hMB cells in the bone marrow with respective treatments, identifying the bone marrow as a treatment refractory niche as already described by Pallasch *et al.* 2014 [96]. Counting the amount of F480$^+$ macrophages in spleen and bone marrow revealed no change in macrophage number regarding the different treatments (Figure 11C). In addition, "don't eat me" cell surface markers CD47 (Figure 11D) and PD-L1 (Figure 11E) protecting lymphoma cells from phagocytosis were measured in spleen and bone marrow on hMB lymphoma cells. Here, the expression of CD47 in the spleen for the alemtuzumab and ibrutinib combination therapy exhibited a significant decrease. The expression of CD47 in the bone marrow was not altered. Moreover, PD-L1 expression was significantly increased in spleen with alemtuzumab mono therapy, whereas the combination with ibrutinib showed no difference to the control. Once again, the expression of PD-L1 in the bone marrow was not altered.
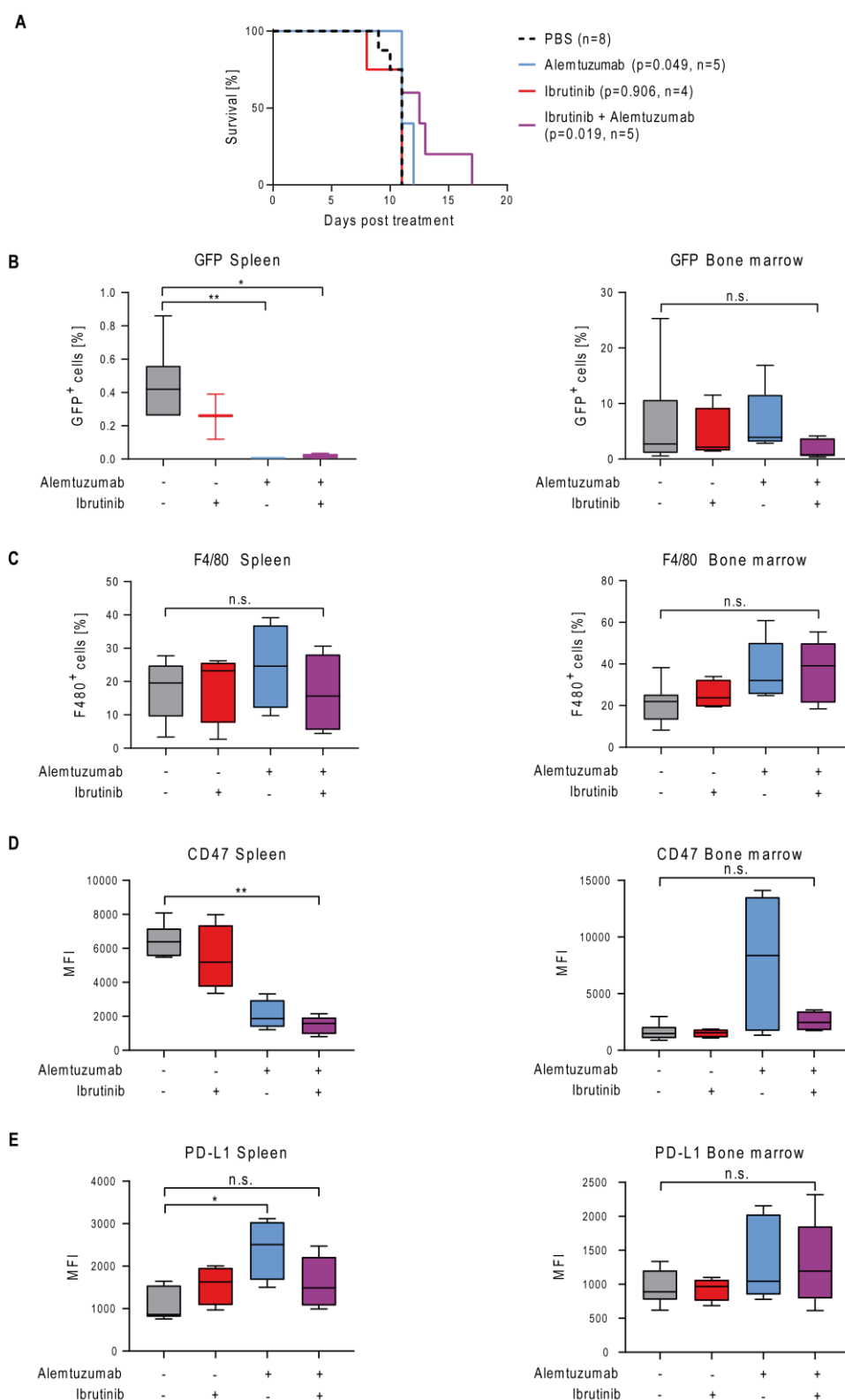
Figure 11 Combination treatment of hMB transplanted mice with ibrutinib and alemtuzumab prolongs survival.
(**A**) Kaplan-Meier analysis comparing the survival of male hMB transplanted NSG mice receiving ibrutinib and alemtuzumab as mono therapy or in combination. PBS was used as control. The treatment was given *i.p.* 10 days after *i.v.* hMB cell injection. (**B-E**) Box plots showing GFP+ (B), F4/80+ (C), CD47+ (D) and PD-L1+ (E) cells in spleen and bone marrow after survival of male hMB transplanted NSG mice treated with ibrutinib and alemtuzumab in combination or as mono therapy. Box plots (D) and (E) show the MFI on the x-axis. Experiments

were performed using flow cytometry. All box plots show the median, the 25th and 75th quartiles, and the minimal and maximal value. (* $p < 0.05$, ** $p \leq 0.01$ and n.s. = not significant)

In conclusion, the results demonstrate that combination therapy of ibrutinib with monoclonal antibodies increased macrophage-mediated phagocytosis of B cell lymphoma *in vitro* and improved overall survival *in vivo*.

7.2 Pre-treatment of hMB cells with ibrutinib can elicit increased ADCP *via* release of an acute secretory phenotype polarising and activating macrophages

To clarify the mechanism driving the beneficial effect of combination treatment with ibrutinib and monoclonal antibodies, the impact of combination therapy on lymphoma target cells helping in tumour cell clearance was examined.

To validate whether ibrutinib acts *via* hMB lymphoma target cells, ADCP assays with pre-treated hMB cells co-cultured with treatment naïve macrophages in fresh media were performed (Figure 12A). In contrast to pre-treating macrophage effector cells with ibrutinib (Figure 15), pre-treatment of hMB lymphoma cells with 1 and 10 µM ibrutinib significantly increased ADCP. Additionally, to analyse the influence of soluble factors released by malignant B cells, conditioned media from ibrutinib pre-treated hMB cells was generated and applied to ADCP co-culture of treatment naïve effector and target cells (Figure 12B). Here, applying the conditioned media of ibrutinib treated hMB cells could increase antibody-mediated phagocytosis by macrophages in a similar manner.
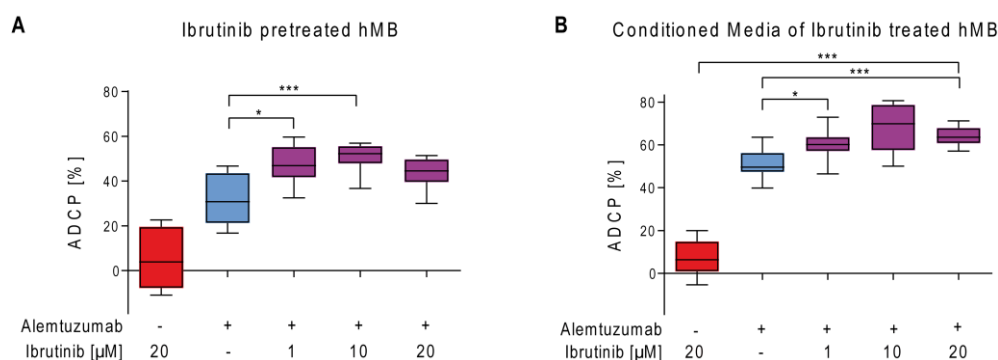

Figure 12 Ibrutinib-mediated improvement of ADCP is conciliated through B cells.
(A) Box plot showing ADCP of ibrutinib pre-treated hMB "double hit" lymphoma cells co-cultured with J774A.1 macrophages, both treated with alemtuzumab (N=2 biological replicates, n=10). **(B)** Box plot showing ADCP of hMB cells and J774A.1 macrophages treated with alemtuzumab and conditioned media of ibrutinib pre-treated hMB cells. Data are normalised to the co-culture without treatment. Box plots show the median, the 25th and 75th quartiles, and the minimal and maximal value. Unless otherwise stated, experiments were performed with at least three biological replicates using flow cytometry. Data were performed by S. Henschke. (* $p < 0.05$, *** $p \leq 0.001$)

To further unravel the impact of conditioned media of ibrutinib treated hMB cells on increased ADCP, respective media was analysed on secretory released cytokines *via* ELISA. Therefore, conditioned media of 20 µM ibrutinib was used to capture the whole spectrum of ibrutinib's action. Here, well characterised cytokines involved in pro- and anti-inflammatory responses by macrophages were selected, with IL-10 representing an anti-inflammatory and pro-tumoral response and IL-6 and TNF-α representing a pro-inflammatory and anti-tumoral response (see

introduction chapter 4.4.1.1). Measuring the amount of IL-10 (Figure 13A), IL-6 (Figure 13B) and TNF-α (Figure 13C) in conditioned media of ibrutinib treated hMB cells showed a decreased overall cytokine release compared to the control. Moreover, the effect of conditioned media of ibrutinib treated hMB cells on the cytokine release of macrophages was examined. Here, the expression of pro-tumoral IL-10 was not significantly altered, but showed a decreased tendency (Figure 13D). However, the expression of anti-tumoral IL-6 (Figure 13E) and TNF-α (Figure 13F) was significantly increased.
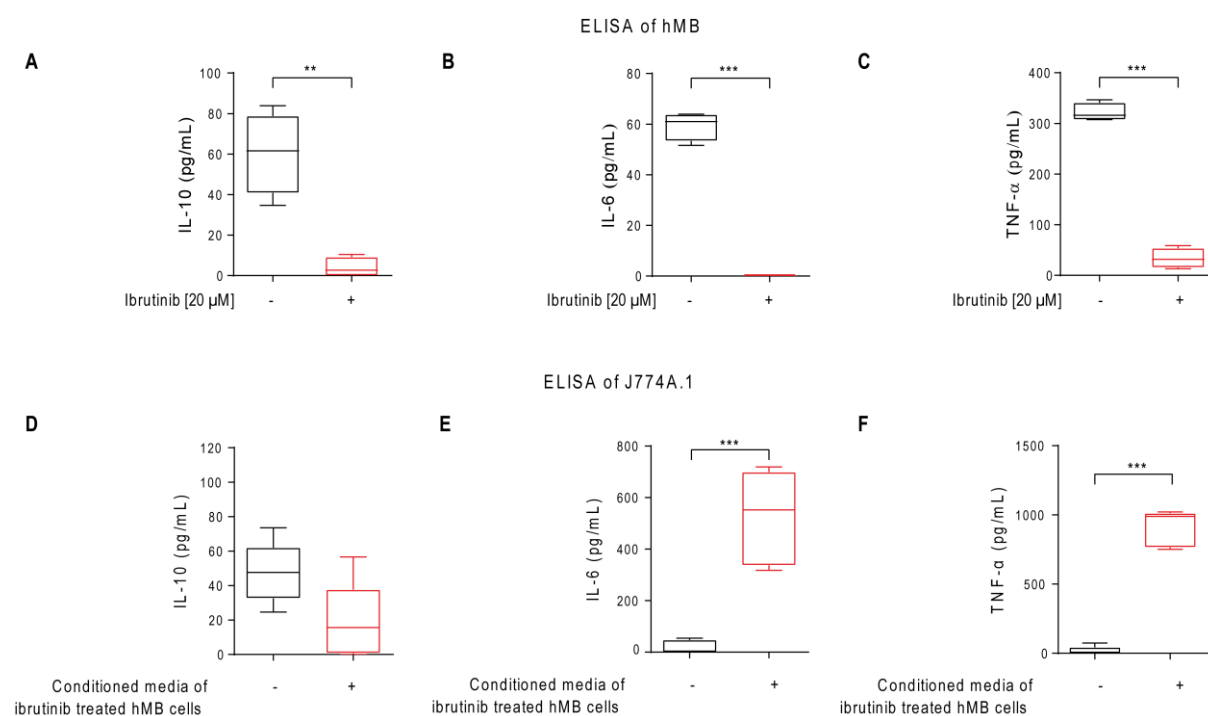

Figure 13 Ibrutinib decrease the cytokine release of hMB lymphoma cells that furthermore change macrophage polarisation.
(A-C) Box plots show the expression of IL-10 (A), IL-6 (B), and TNF-α (C) of hMB "double hit" lymphoma cells treated with ibrutinib. **(D-F)** Box plots show the expression of IL-10 (A), IL-6 (B), and TNF-α (C) of J774A.1 macrophages treated with conditioned media of hMB "double hit" lymphoma cells treated with 20 µM ibrutinib. Box plots show the median, the 25th and 75th quartiles, and the minimal and maximal value. Experiments were performed with four biological replicates using ELISA. (** $p < 0.01$, *** $p \leq 0.001$)

Besides the positive effect of conditioned media, the impact of ibrutinib on the expression of antibody antigens CD20 and CD52 needed to be addressed. Using flow cytometry for the analysis, there was no significant change in CD20 and CD52 percentage or MFI of ibrutinib treated hMB cells (Figure 14A). Moreover, testing the influence of ibrutinib on the expression level of the "don't eat me" signals CD47 and PD-L1 in hMB cells revealed no significant change in the percentage of positive cells or the MFI (Figure 14B).
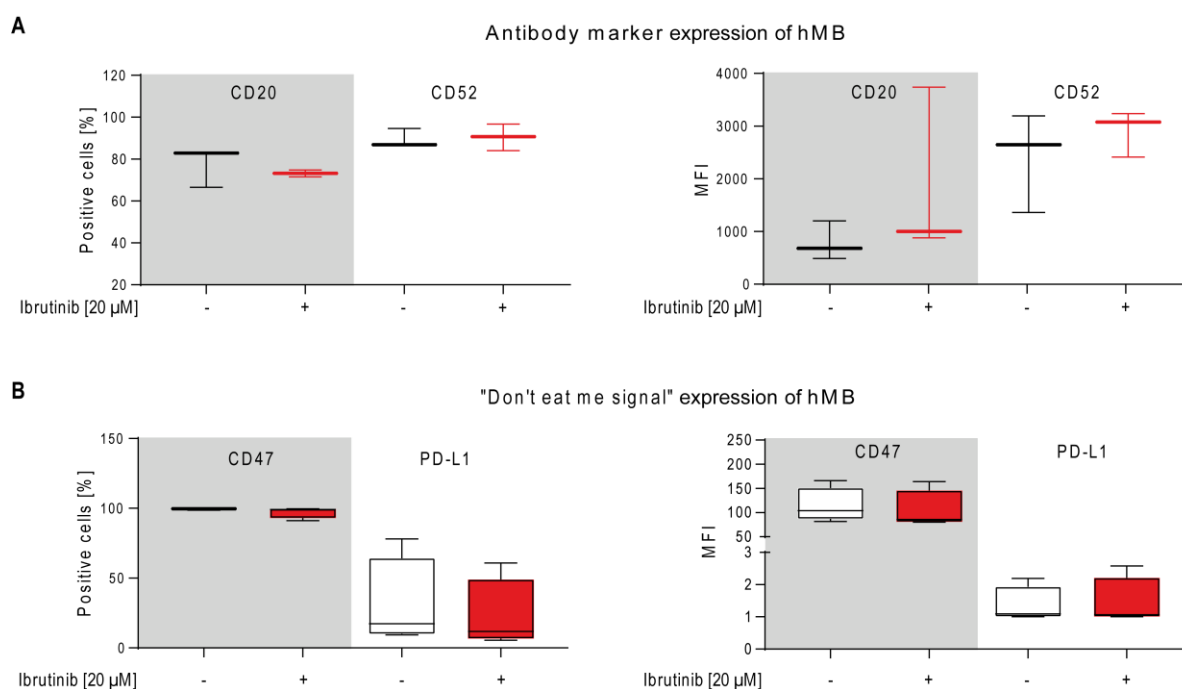
Figure 14 Ibrutinib does not alter the expression of CD20, CD52, CD47, and PD-L1.
Box plots showing the expression of **(A)** CD20 and CD52 and **(B)** CD47 and PD-L1 of hMB "double hit" lymphoma cells treated with ibrutinib. The x-axis displays the number of positive cells (left box plot) and the MFI (right box plot). Box plots show the median, the 25th and 75th quartiles, and the minimal and maximal value. Experiments were performed with three biological replicates using flow cytometry. Data of (A) were performed by S. Henschke.

Taken together, ibrutinib-mediated increase in ADCP depends on the influence of ibrutinib on hMB target cells. Thereby, ibrutinib induces a secretory component in the malignant B cells leading to an altered cytokine expression profile of hMB cells that furthermore induces an anti-tumoral cytokine release by macrophages. The expression of cell surface markers recognising antibodies and the expression of so called "don't eat me" signals was not changed on hMB lymphoma cells due to ibrutinib treatment.

7.3 Pre-treatment of macrophages with ibrutinib cannot increase ADCP

To further identify the mechanism of action on increased ADCP *via* ibrutinib it is important to check the role of treatment on the macrophage effector cell side. Therefore, J774A.1 macrophages were pre-treated with different concentrations of ibrutinib and afterwards co-cultured with treatment naïve hMB lymphoma cells and alemtuzumab (Figure 15). Here, it was observed that ibrutinib pre-treated macrophages could not further increase ADCP of lymphoma cells compared to alemtuzumab mono therapy.
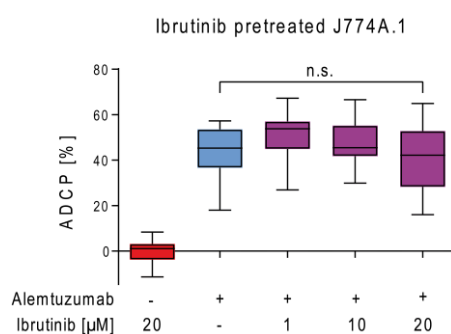

Figure 15 Ibrutinib pre-treatment of macrophages does not influence ADCP.
Box plot showing ADCP of hMB "double hit" lymphoma cells co-culture with ibrutinib pre-treated J774A.1 macrophages, both treated with alemtuzumab. Data are normalised to the co-culture without treatment. Box plots show the median, the 25th and 75th quartiles, and the minimal and maximal value. The experiment was performed with three biological replicates using flow cytometry. Data were performed by S. Henschke. (n.s. = not significant)

To determine the influence of ibrutinib on secretory released cytokines by macrophages, ELISAs were performed. Here, J774A.1 macrophages treated with 20 µM ibrutinib for 24 h showed a significant increase for IL-10 (Figure 16A) and no change in IL-6 and TNF-α release (Figure 16B and C).
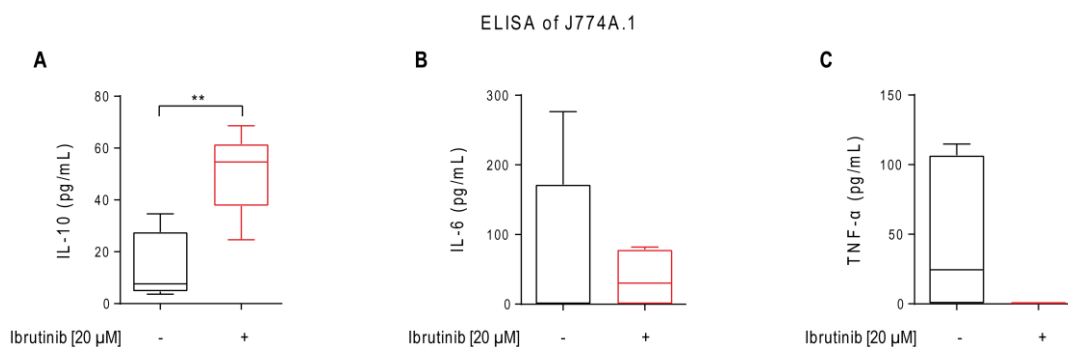

Figure 16 Influence of ibrutinib on J774A.1 macrophages.
Box plots show the expression of IL-10 (**A**), IL-6 (**B**), and TNF-α (**C**) of J774A.1 macrophages treated with ibrutinib. Box plots show the median, the 25th and 75th quartiles, and the minimal and maximal value. Experiments were performed with five biological replicates using ELISA. (** $p \leq 0.01$)

Moreover, the influence of ibrutinib on macrophage polarisation regarding tumour support was examined, where J774A.1 macrophages were treated with 20 µM ibrutinib for 24 h and checked for the anti-tumoral M1 and pro-tumoral M2 polarisation markers using flow cytometry (Figure 17). Testing the expression profile of the well characterised M1 polarisation markers CD64, CD86 and MHCII of J774A.1 macrophages, ibrutinib did not lead to a change in the number of positive cells nor the MFI (Figure 17A). Whereas the number of CD64 and CD86 expressing cells was already close to 100 % without treatment. Likewise, measuring the well-known M2 polarisation markers CD206 and ArgI showed no significant difference with ibrutinib treatment (Figure 17B).
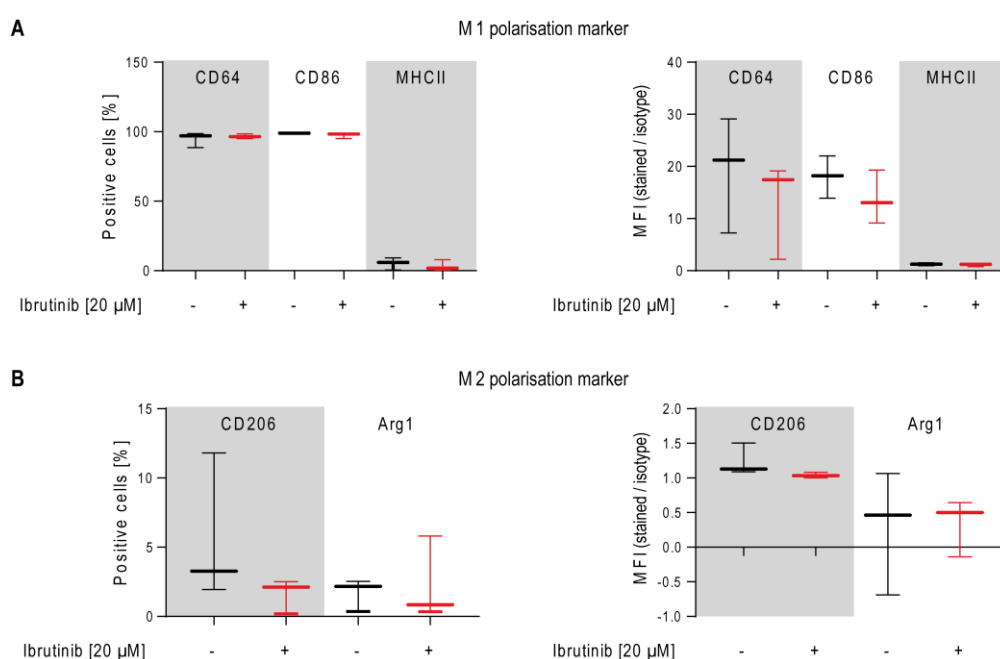
Figure 17 Ibrutinib does not alter macrophage polarisation.
Box plots showing M1 macrophage polarisation marker CD64, CD86 and MHCII (**A**) and M2 marker CD206 and ArgI (**B**) of J774A.1 macrophages treated with ibrutinib. The x-axis displays the number of positive cells (left box plot) and the MFI (right box plot). Here, the MFI is calculated by dividing the value of the stained sample by isotype control. Box plots show the median, the 25th and 75th quartiles, and the minimal and maximal value. Experiments were performed with three biological replicates using flow cytometry. Data were performed by S. Henschke.

These findings suggest that the effect of ibrutinib increased ADCP seems to be independent on the influence of ibrutinib on macrophage effector cells and their polarisation.

7.4   Second generation BTK-inhibitors fail to induce increased ADCP

To further confirm the role of BTK inhibition in increased ADCP, different concentrations of second generation BTK-inhibitors acalabrutinib (Figure 18A) and tirabrutinib (Figure 18B) were used to perform ADCP assays. Both inhibitors show a higher specificity to BTK resulting in less off-target inhibition compared to ibrutinib. Interestingly, the increase in ibrutinib's antibody-mediated phagocytosis could not be reproduced using second generation BTK-inhibitors, suggesting that ibrutinib increased ADCP independently of BTK inhibition. Moreover, acala- and tirabrutinib showed no toxicity to hMB lymphoma cells or J774A.1 macrophages (Appendix Figure 44A-C).
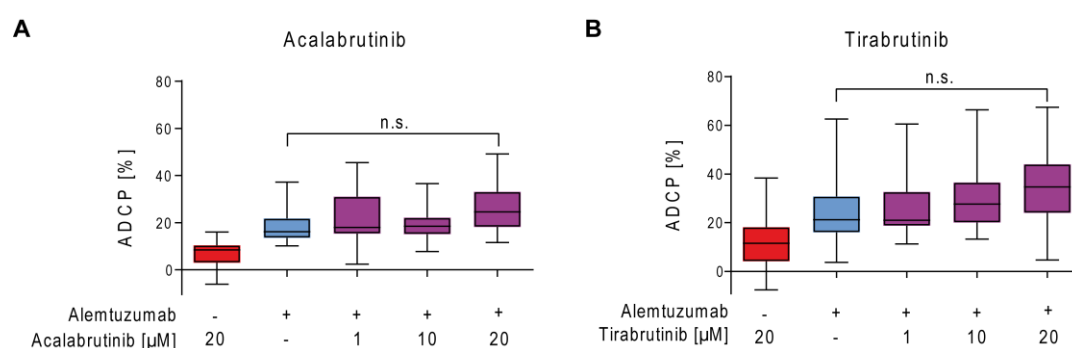
Figure 18 Second generation BTK-inhibitors does not enhance ADCP.
Box plot showing ADCP of hMB "double hit" lymphoma cells and J774A.1 macrophages treated with acalabrutinib (**A**) or tirabrutinib (**B**) and alemtuzumab. Data are normalised to the co-culture without treatment. Box plots show the median, the 25th and 75th quartiles, and the minimal and maximal value. Experiments were performed of at least three biological replicates using flow cytometry. Data were performed together with S. Henschke. (n.s. = not significant)

Furthermore, the expression of antibody antigens CD20 and CD52 of hMB lymphoma cells under acala- and tirabrutinib treatment, revealed no difference in the number of positive cells nor the MFI (Figure 19A). There was also no change in the expression profile of the "don't eat me" signal CD47 on hMB lymphoma cells under acala- or tirabrutinib treatment (Figure 19B). Moreover, the number of PD-L1 positive hMB cells treated with second generation BTK-inhibitors stayed the same, but the expression level per cell was significantly increased when treated with acalabrutinib.

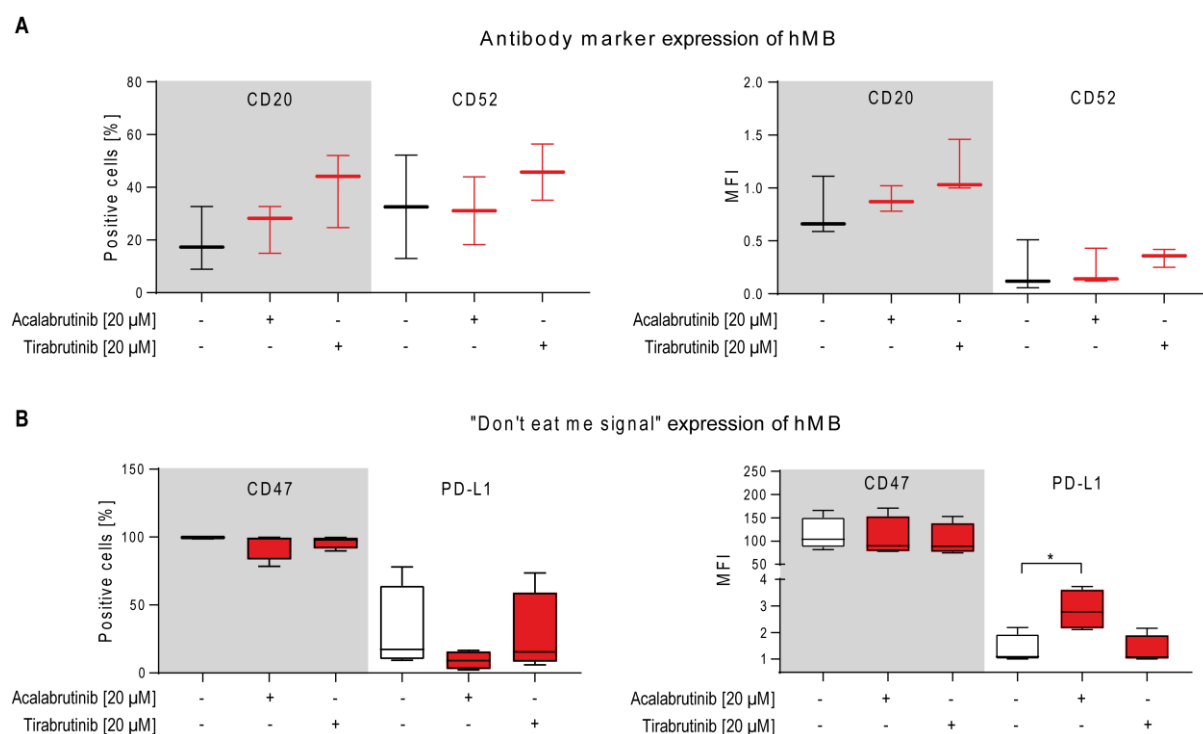**Figure 19 Second generation BTK-inhibitors do not alter the expression of CD20, CD52, CD47, and PD-L1.** Box plots showing the expression of **(A)** CD20 and CD52 and **(B)** CD47 and PD-L1 of hMB "double hit" lymphoma cells treated with acalabrutinib or tirabrutinib. The x-axis displays the number of positive cells (left box plot) and the MFI (right box plot). Box plots show the median, the 25th and 75th quartiles, and the minimal and maximal value. Experiments were performed with three biological replicates using flow cytometry. (* p < 0.05)

To evaluate the impact of second generation BTK-inhibitors *in vivo*, hMB cells were transplanted into 8-14 weeks old male NSG mice and treated with tirabrutinib alone or in combination with alemtuzumab ten days after transplantation. For the control group mice were treated with PBS. Here, combination treatment of tirabrutinib plus alemtuzumab did not lead to an increase of overall survival (Figure 20A). Moreover, the number of GFP⁺ hMB cells in the spleen and bone marrow of mice which received the combination therapy was not affected (Figure 20B). Besides, the different treatments did not influence the number of macrophages in the spleen and bone marrow (Figure 20C). Furthermore, combination therapy of tirabrutinib and alemtuzumab did not alter the expression of the "don't eat me" signals CD47 (Figure 20D) and PD-L1 (Figure 20E).
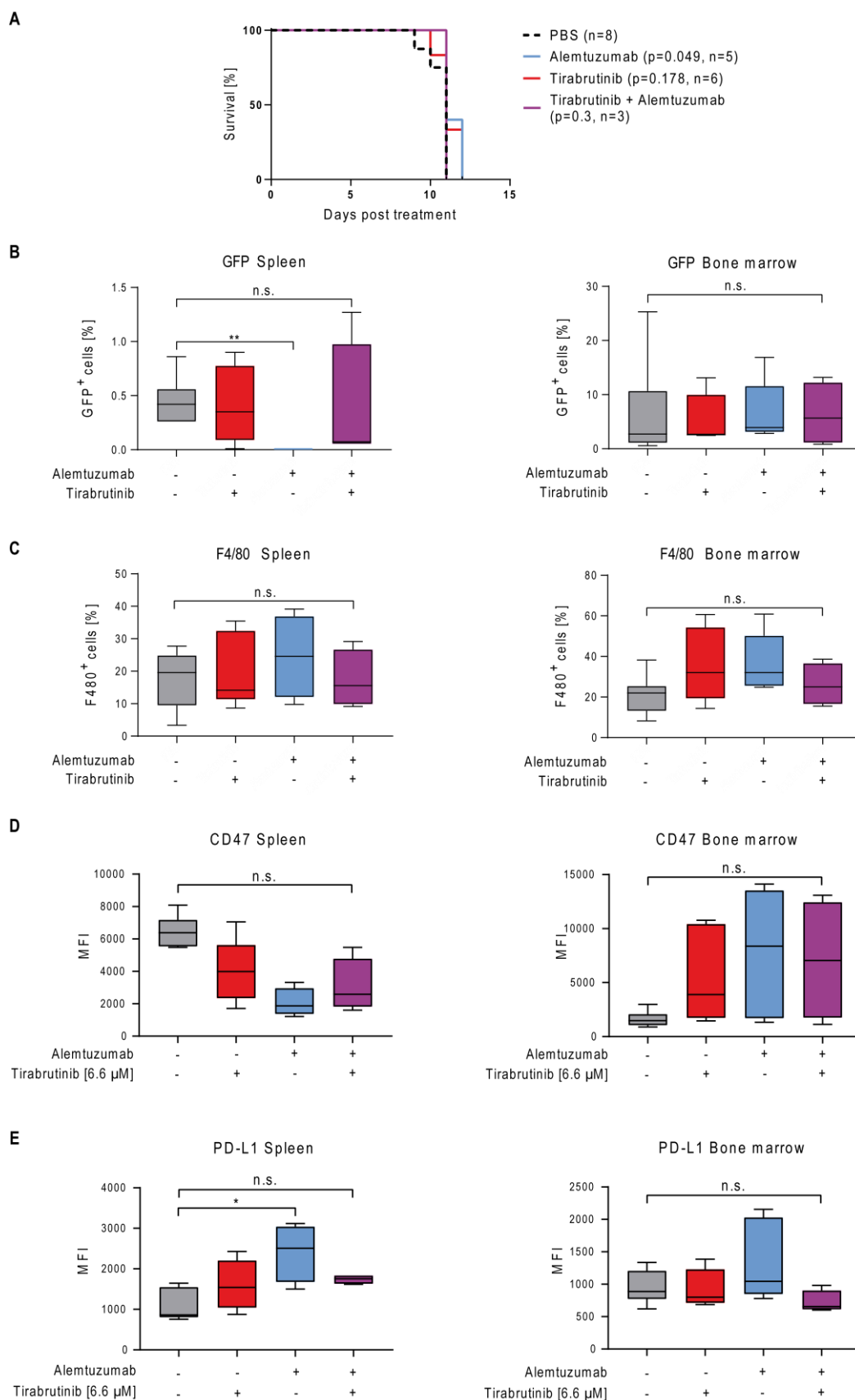
Figure 20 Combination treatment of hMB transplanted mice with tirabrutinib and alemtuzumab does not affect survival.
(**A**) Kaplan-Meier analysis comparing the survival of male hMB transplanted NSG mice receiving tirabrutinib and alemtuzumab as mono therapy or in combination. PBS was used as control. The treatment was given *i.p.* 10 days

after *i.v.* hMB cell injection. **(B-E)** Box plots showing GFP$^+$ (B), F4/80$^+$ (C), CD47$^+$ (D) and PD-L1$^+$ (E) cells in spleen and bone marrow after survival of male hMB transplanted NSG mice treated with tirabrutinib and alemtuzumab in combination or as mono therapy. Box plots (D) and (E) show the MFI on the x-axis. Experiments were performed using flow cytometry. All box plots show the median, the 25th and 75th quartiles, and the minimal and maximal value. (* p < 0.05, ** p ≤ 0.01 and n.s. = not significant)

Since ibrutinib as well as second generation BTK-inhibitors show affinity for other members of the TEC kinase family such as epidermal growth factor receptor (EGFR) or JAK3 [233], the next step was to assess *via* genetic depletion of *BTK via* KO or knock down (kd) in effector and target cell lines the role of BTK on ADCP.

Therefore, primary peritoneal macrophages from *BTK$^{-/-}$* C57BL/6 mice – gifted from O. Fedorchenko – were harvested and co-cultured with wt hMB lymphoma cells. Here, *BTK$^{-/-}$* macrophages exhibited a significant increase in ADCP under ibrutinib and alemtuzumab treatment compared to alemtuzumab mono therapy (Figure 21A). Moreover, performing an ADCP with hMB *BTK* kd lymphoma cells and J774A.1 wt macrophages (85 % kd efficiency, Appendix Figure 44D) revealed no significant difference between alemtuzumab treated wt hMB cells and alemtuzumab treated *BTK* kd cells (Figure 21B).
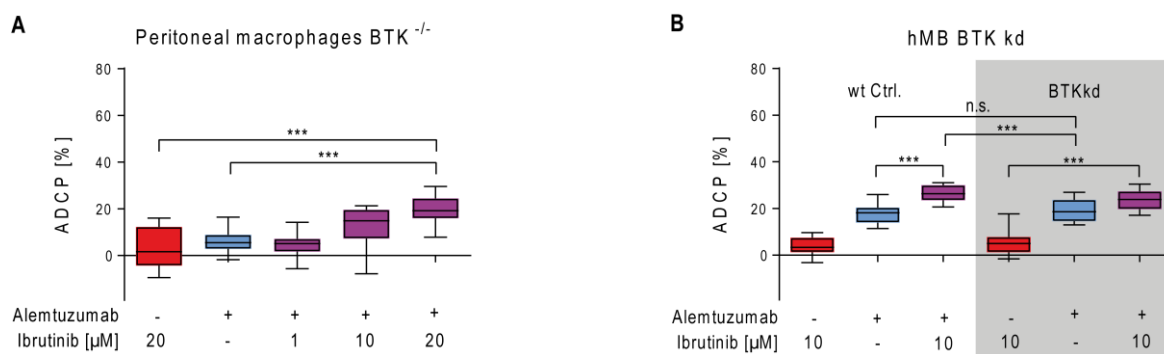
Figure 21 Ibrutinib elicits increased ADCP independent of BTK inhibition
(A) Box plot showing ADCP of hMB "double hit" lymphoma cells by combination of alemtuzumab with ibrutinib using primary peritoneal macrophages obtained from global *BTK$^{-/-}$* mice as effector cells. **(B)** Box plot showing ADCP by combination of alemtuzumab with ibrutinib and wild type (wt) hMB lymphoma cells and hMB with knock down in *BTK*. Data are normalised to the co-culture without treatment. Box plots show the median, the 25th and 75th quartiles, and the minimal and maximal value. Experiments were performed of at least three biological replicates using flow cytometry. Data were performed together with S. Henschke. (*** p ≤ 0.001)

In summary, the data indicate the ADCP-enhancing effects of ibrutinib to be independent of BTK inhibition in effector and target cells. Leading to the suggestion that one of ibrutinib's off-target kinases could be responsible for the observed effect.

7.5 Kinase activity profiling identifies Janus Kinase 2 & 3 as the main off-targets for ibrutinib vs. second generation BTK-inhibitors

To pin down the off-target effects of ibrutinib that might be responsible for the synergistic interaction of ibrutinib and alemtuzumab in increased ADCP, kinase activity profiles using peptide microarray chips from Pam Station were generated (see methods Figure 6).

To elucidate the reliability of PamChip peptide microarrays, a Bland-Altman plot of two repeated measurements was created. Thereby, both measurements are compared with each other by plotting the difference of both measurements (S_1-S_2) on the y-axis and the average ($\frac{S_1+S_2}{2}$) on the x-axis. The black line indicates the mean of the difference of both measurements and the red lines show the mean of the difference minus or plus 1.96 x SD.

Analysing the concordance of two repeated measurements of ibrutinib treated hMB lymphoma cells in a Bland-Altman plot exhibited most values distributed around the mean with only a few outliers (Figure 22). This indicates a reliable repetition of the experimental set-up.
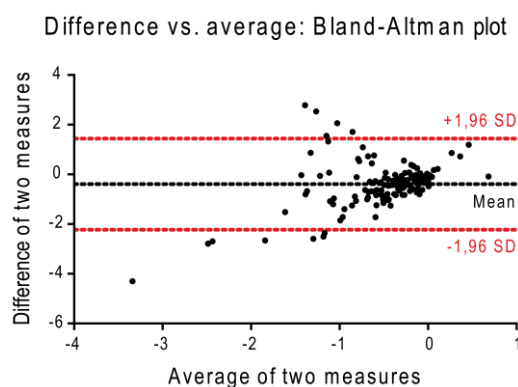
Figure 22 Bland-Altman plot of PamChip peptide microarrays.
The plot shows two repeated measurements of 1 µM ibrutinib treated hMB lymphoma cells measured with PamChip peptide microarrays. The black line indicates the mean of the difference of both measurements and the red lines show the mean of the difference minus or plus 1.96 x SD.

Another method to evaluate the suitability of high-throughput screenings like the PamChip peptide microarrays is the calculation of the Z-factor. Thereby, measurements of a positive and negative control are opposed to each other – here an untreated control against a treated one. The Z-factor is calculated with the SD (σ) and the median (µ) of the positive (p) and negative (n) control:

$$Z - factor = 1 - \frac{3(\sigma_p + \sigma_n)}{\mu_p - \mu_n}$$

A Z-factor over 0.5 indicates a good suitability of the method and a Z-factor lower than 0.5 a bad suitability.

Calculating the Z-factor of every peptide phosphorylation of hMB lymphoma cells treated with ibrutinib shows most peptides having a Z-factor over 0.5, suggesting a high suitability.

Figure 23 Z-factor of peptide phosphorylation of hMB lymphoma cells treated with 1 µM ibrutinib.
Every dot represents one peptide on the PamChip peptide microarray. The red line indicates a Z-factor of 0.5.

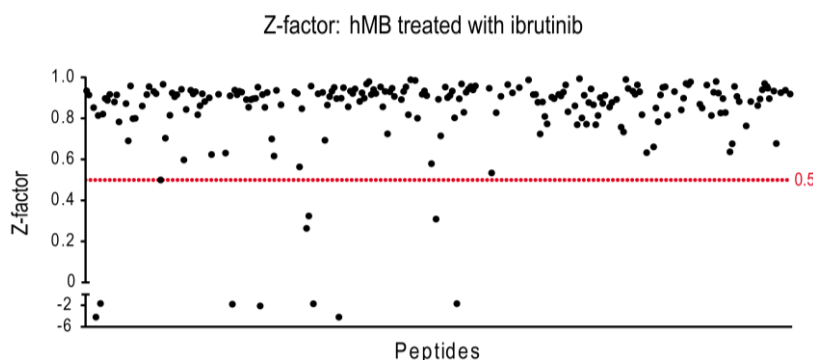In order to identify off-target effects of ibrutinib, hMB lymphoma cells were treated with different BTK-inhibitors for 6 h. To measure the phosphorylation of protein tyrosine as well as serine/threonine kinases, the treated cell lysates were applied to the peptide microarray chips (see methods Figure 6). Figure 24A illustrates a volcano plot of BTK-inhibitor treated hMB lymphoma cells. Every dot indicates a single peptide on the peptide microarray chip. Coloured dots represent significantly up- or downregulated ($\log_2$ fold change) peptides compared to the control. Treating hMB lymphoma cells with ibrutinib or tirabrutinib mainly reduced peptide phosphorylation (Figure 24A; left and right panel), whereas hMB cells treated with acalabrutinib showed an up and downregulation of peptides (Figure 24A; central panel). With bioinformatics processing using the databases PhosphoNET, Phosphosite PLUS, Phospho.elm, UniPROT, Reactome, and Human Protein Reference Database, the peptide phosphorylation status can be transformed into a kinase activity profile (Figure 24B). Displaying only the significantly changed kinases of respective treatments in a VENN diagram, it was observed that 78 significantly altered kinases were shared across all three BTK-inhibitors. Thereby, 176 kinases were only inhibited by ibrutinib, indicating the lower specificity of ibrutinib to BTK compared to second generation BTK-inhibitors. To find the most important off-targets, significantly altered kinases were filtered for the kinases having the same cysteine residue as BTK [233] (Figure 24C). These selected kinases were then attributed to their number of

significantly changed peptides displayed by the circle size of every kinase. Here, all three BTK-inhibitors targeted BTK in a similar way. Furthermore, the Janus Kinase (JAK) 2 and 3, as well as LYN and B lymphocyte kinase (BLK) revealed an enrichment of significantly changed peptides under ibrutinib treatment compared to second generation BTK-inhibitors. On the other hand, TEC kinases like SYK or EGFR showed only minimal changes between BTK-inhibitor treatments.
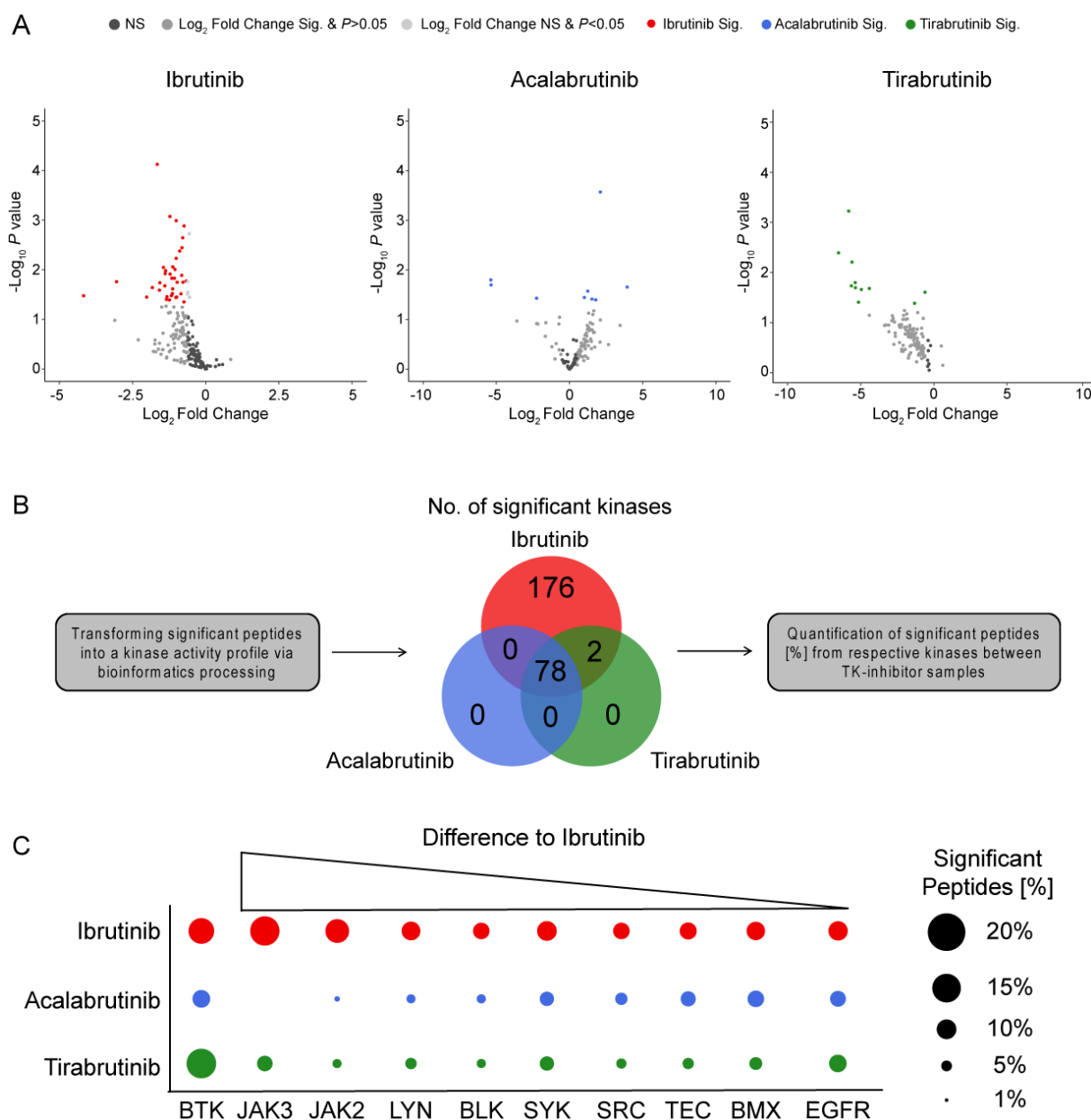
Figure 24 Kinase activity profiling identifies Janus Kinase 2 & 3 as the main off-targets for ibrutinib vs. second generation BTK-inhibitors.

(**A**) Volcano plots of significantly changed peptide phosphorylation after ibrutinib (red, n=6), acalabrutinib (blue, n=3) and tirabrutinib (green, n=3) treatment of hMB lymphoma cells. Each dot represents a kinase peptide substrate represented on the peptide microarray chip. Coloured dots indicate significantly altered peptides (two-sided student t-test, p $\leq$ 0.05; log$_2$ fold change $\leq$ or $\geq$ 0.5). A negative log$_2$ fold change stands for a downregulation of peptides and a positive log$_2$ fold change for an upregulation compared to the control. Acalabrutinib and

58

tirabrutinib treated lysates were only applied to PTK chips. **(B)** VENN diagram showing all significantly changed kinases of the PTK chips for the respective treatments. **(C)** Graphic showing ibrutinib (red) off target kinases and its number of significantly changed peptides. Kinase peptide numbers are sorted from the highest difference to acalabrutinib (blue) and tirabrutinib (green) to the lowest. Graphics show three biological replicates. Data were analysed together with S. J. Blakemore.

Likewise, treating CLL patient cells from three different patients with ibrutinib induced significant downregulation of peptides associated with BTK as well as off-target kinases JAK 2, LYN, BLK, and other TEC kinases (Figure 25A and B). Although the influence of ibrutinib seems to be generally weaker in CLL patient samples than in hMB lymphoma cells (Figure 24C), none of the ibrutinib treated CLL patient samples showed off-target inhibition of JAK3 as it was exhibited in hMB samples treated with ibrutinib (Figure 24C).
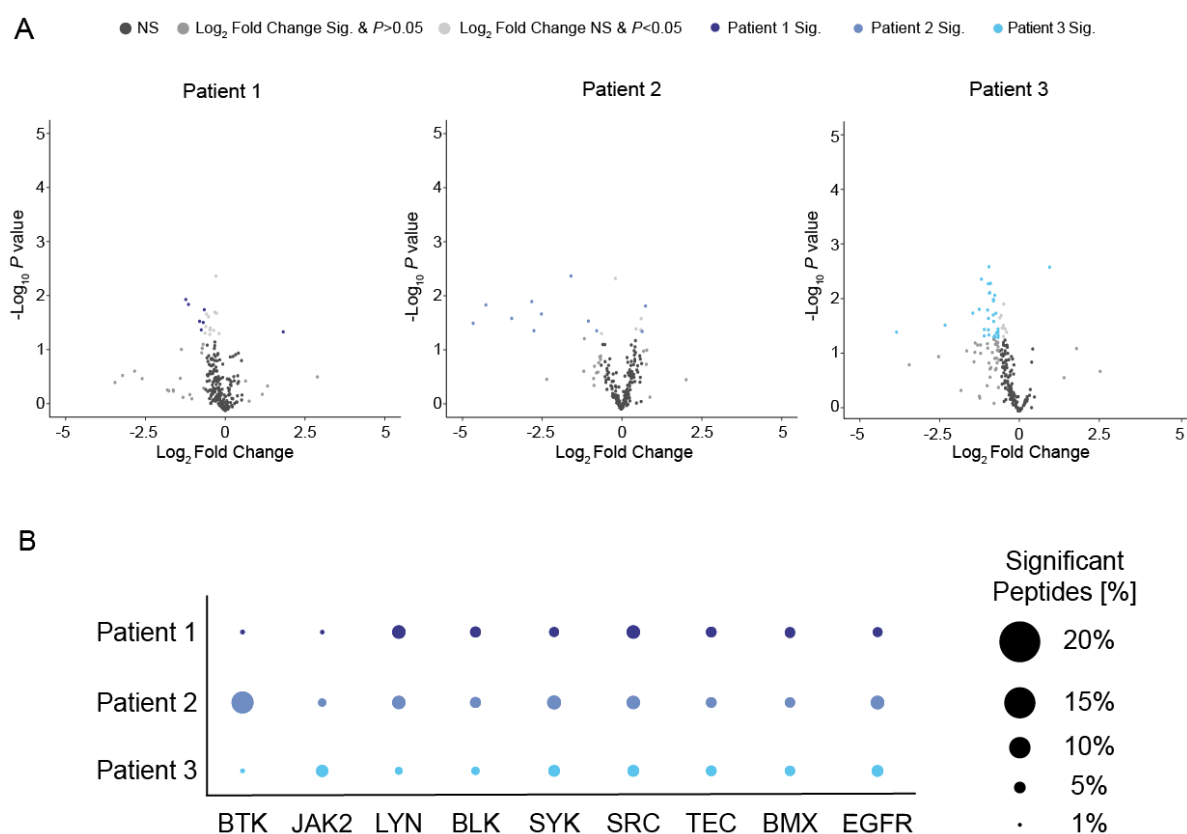
Figure 25 Kinase activity profiling of ibrutinib treated CLL patient cells.
(A) Volcanoplot of significantly changed peptide phosphorylation after treatment of CLL patient lymphoma cells with ibrutinib. Each dot represents a kinase peptide substrate on the peptide microarray chip. Couloured dots indicates significantly altered peptides (two-sided student t-test, $p \leq 0.05$; $\log_2$ fold change $\leq$ or ≥ 0.5). A negative $\log_2$ fold change stands for a downreagultion of peptides and a positive $\log_2$ fold change for an upregulation compared to the control. **(B)** Graphic showing ibrutinib off target kinases and its number of significantly changed peptides. Graphics show three technical replicates. Data were analysed together with S. J. Blakemore.

Testing off-target kinases in ibrutinib treated J774A.1 macrophage effector cells revealed only one significantly reduced peptide belonging to the kinase Ret (Figure 26). This data underlines the missing increase in ADCP when pre-treating macrophages with ibrutinib (Figure 15).
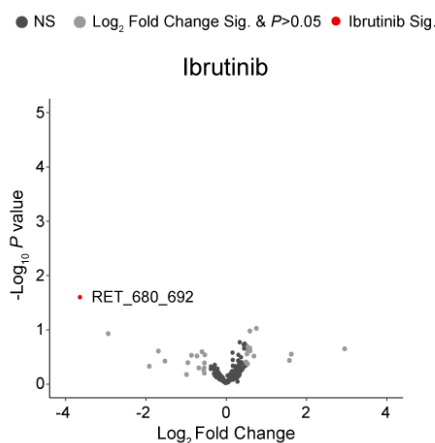
Figure 26 Kinase activity profiling of ibrutinib treated J774A.1 macrophages reveals one off target kinase. Volcanoplot of significantly changed peptide phosphorylation after treatment of J774A.1 macrophages with ibrutinib. Each dot represents a kinase peptide substrate represented on the peptide microarray chip. Couloured dots indicates significantly altered peptides (two-sided student t-test, $p \leq 0.05$; log_2 fold change $\leq$ or ≥ 0.5). A negative log_2 fold change stands for a downreagultion of peptides and a positive log_2 fold change for an upregulation compared to the control. Graphics show three biological replicates. Data were analysed together with S. J. Blakemore.

In conclusion, ibrutinib shows off-target inhibition that is not present in second generation BTK-inhibitors. Thereby, suggesting JAK2 amongst others to be an important off-target kinase of ibrutinib, and therefore potentially be the responsible kinase for the increased macrophage-mediated phagocytosis of lymphoma cells.

7.6 JAK inhibition enhances macrophage-mediated ADCP

In order to elucidate which off-target kinase of ibrutinib plays a role in macrophage-mediated ADCP, a TEC kinase inhibitor library was generated and *in vitro* ADCP assays were performed with respective inhibitors.

As expected from the results of the kinase activity profiling, inhibition of bone marrow kinase on chromosome X (BMX; CHMFL-BMX-078, Figure 27A), EGFR (erlotinib, Figure 27B) and SYK (entospletinib, Figure 27C) in hMB and J774A.1 co-culture, did not influence ADCP. In addition, none of the kinase inhibitors showed toxicity to the hMB lymphoma cells in the used concentrations (Appendix Figure 45A, B and C). However, inhibition of JAK1/2 *via* ruxolitinib (Figure 27D) induced a significant increase in macrophage-mediated ADCP. Moreover, inhibition of JAK2/3 with tofacitinib (Figure 27E) and inhibition of pan-JAK with SP600125 (Figure 27F) led to a significant improvement of ADCP with increasing phagocytosis observed with increasing concentrations. Notably, none of the inhibitors displayed direct cytotoxicity or induction of apoptosis to hMB lymphoma cells at the used concentrations (Appendix Figure 45D, E and F).
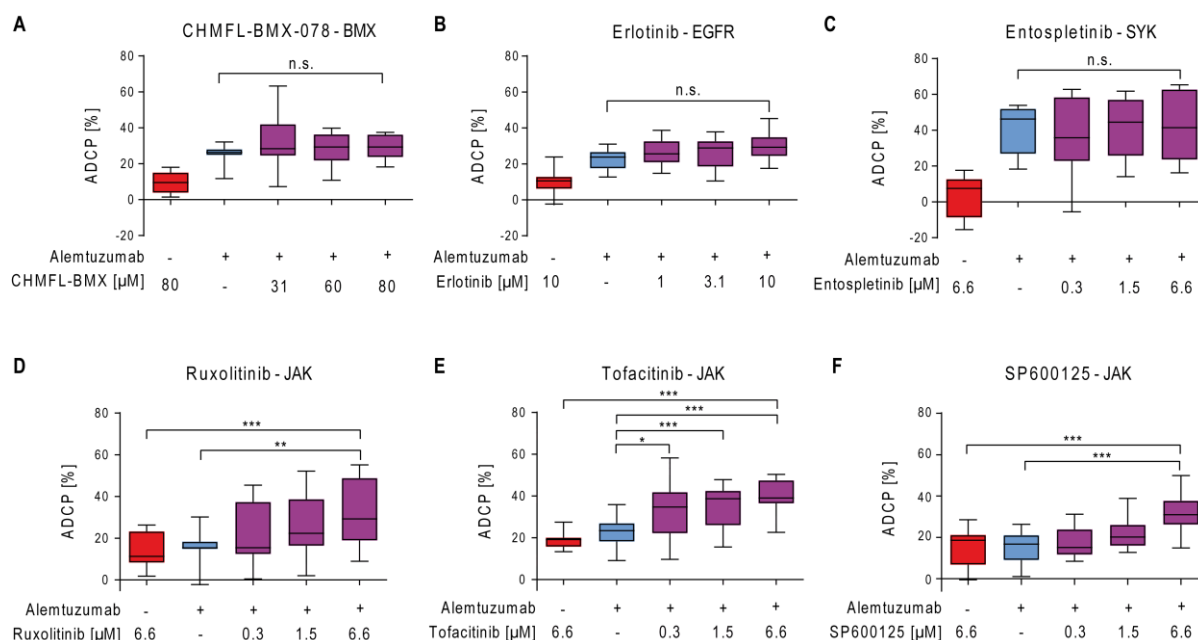
Figure 27 JAK inhibition enhances macrophage-mediated ADCP.
Box plots showing ADCP of hMB "double hit" lymphoma cells and J774A.1 macrophages treated with alemtuzumab and CHMFL-BMX-078 (BMX-inhibitor, N=2 biological replicates, n=10) **(A)**, erlotinib (EGFR-inhibitor) **(B)**, entospletinib (SYK-inhibitor, N=2 biological replicates, n=10) **(C)**, ruxolitinib (JAK1/2-inhibitor) **(D)**, tofacitinib (JAK2/3-inhibitor) **(E)**, or SP600125 (pan-JAK-inhibitor) **(F)**. Data are normalised to the co-culture without treatment. All box plots show the median, the 25th and 75th quartiles, and the minimal and maximal value. Unless otherwise stated experiments were performed of at least three biological replicates. (n.s. = not significant, * $p < 0.05$, ** $p \leq 0.01$ and *** $p \leq 0.001$)

To validate the influence of the different BTK and JAK-inhibitors on the JAK/STAT signalling pathway and their effect on ADCP (see introduction 4.4.1.3), western blot analysis with phosphorylation of downstream STAT3 in hMB lymphoma cells was performed (Figure 28A). Thereby pSTAT3 and STAT3 have an atomic mass unit of 86 kDa. Illustrating the percentage of phosphorylated STAT3 in hMB treated with respective inhibitors, showed no or just a slight change in pSTAT3 for the second generation BTK-inhibitors acalabrutinib and tirabrutinib compared to the untreated control (Figure 28B). On the other hand, hMB cell treatment with BTK-inhibitor ibrutinib led to less activated STAT3, indicating its off target interaction with the JAK/STAT signalling pathway. Moreover, treating hMB cells with tofacitinib and ruxolitinib decreased the phosphorylation of STAT3 the most.
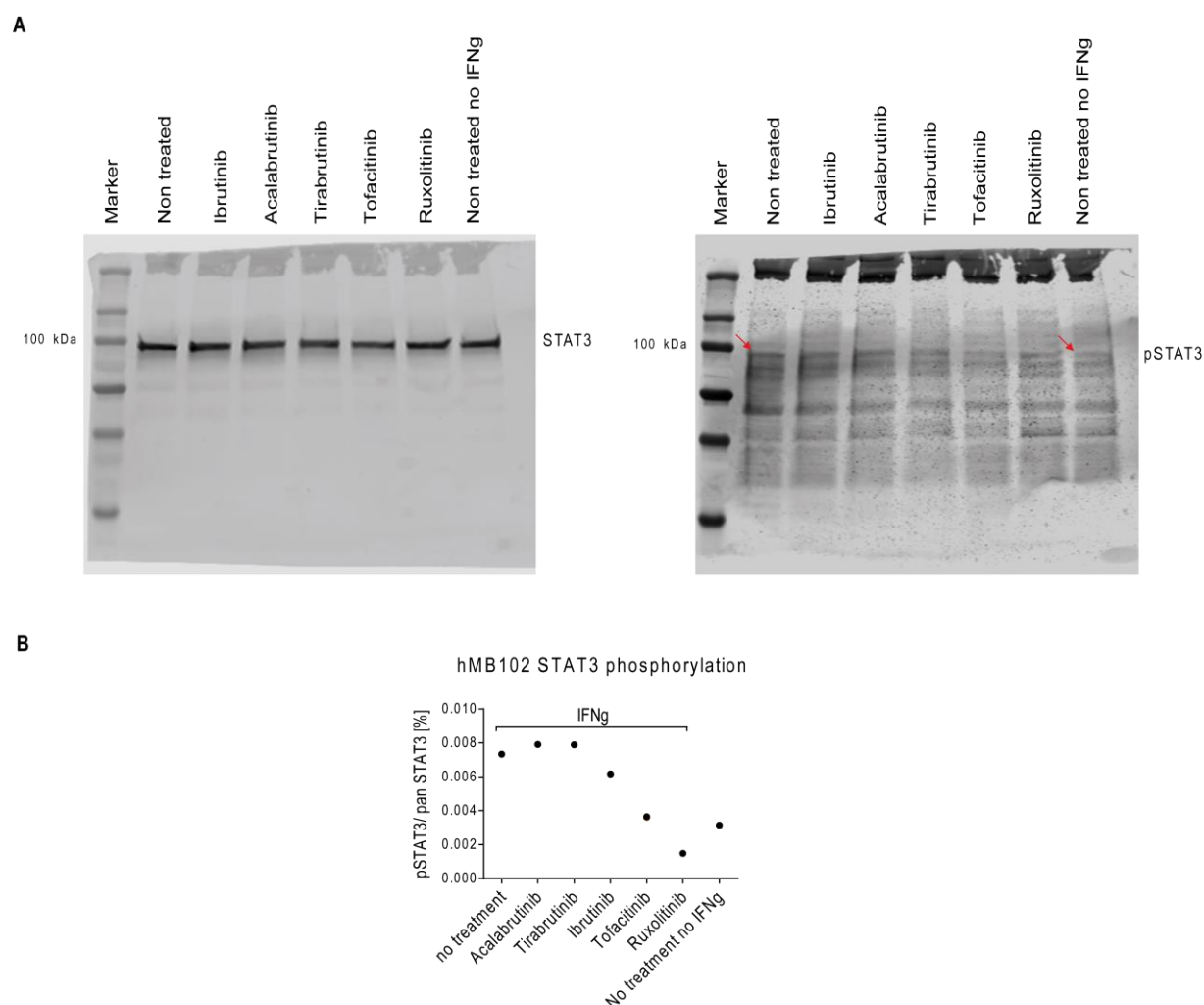

Figure 28 Phosphorylation of STAT3 in B cells differs between BTK-inhibitors of the first and second generation and JAKis.
(A) Representative western blot image displaying the expression of STAT3 and pSTAT3 (86 kDa) of hMB "double hit" lymphoma cells treated with 20 µM acalabrutinib, tirabrutinib, ibrutinib, and 10 µM tofacitinib and ruxolitinib.

hMB cells were stimulated with rh IFN-γ. **(B)** Graph comparing the percentage of phosphorylated STAT3 of (A) between different treatments.

In summary, JAK seems to be an important off-target of ibrutinib playing a central role in enhancing macrophage-mediated ADCP.

7.6.1 *JAK2* KO in hMB cells improves ADCP *via* release of an acute secretory phenotype and downregulation of PD-L1

To verify the mechanistic influence of JAK inhibition on enhanced macrophage-mediated ADCP, hMB lymphoma cells were pre-treated with ruxolitinib (Figure 29A) or tofacitinib (Figure 29B) and co-cultured with J774A.1 macrophages and alemtuzumab. Here, only pre-treatment of hMB lymphoma cells with ruxolitinib leads to significantly enhanced tumour cell clearance.

Since the kinase activity profile of ibrutinib treated hMB cells indicated JAK2 as a potential off-target (Figure 24 and Figure 25), the specific JAK2 influence on increased ADCP needed to be addressed. Therefore, JAK2 deficient hMB lymphoma target cells were generated using the CRISPR/Cas9 system (Appendix Figure 45G). Thereby, *JAK2* KO and non-target (NT) lymphoma cells co-cultured with J774A.1 macrophages showed no basal phagocytosis rate (Appendix Figure 45H). In the ADCP assay, *JAK2* KO cells treated with alemtuzumab were significantly enhanced phagocyted compared to *JAK2* wt cells treated with alemtuzumab (Figure 29C). Furthermore, the enhanced ADCP of *JAK2* KO hMB and alemtuzumab could not be improved by co-treatment with either ibrutinib or tofacitinib.
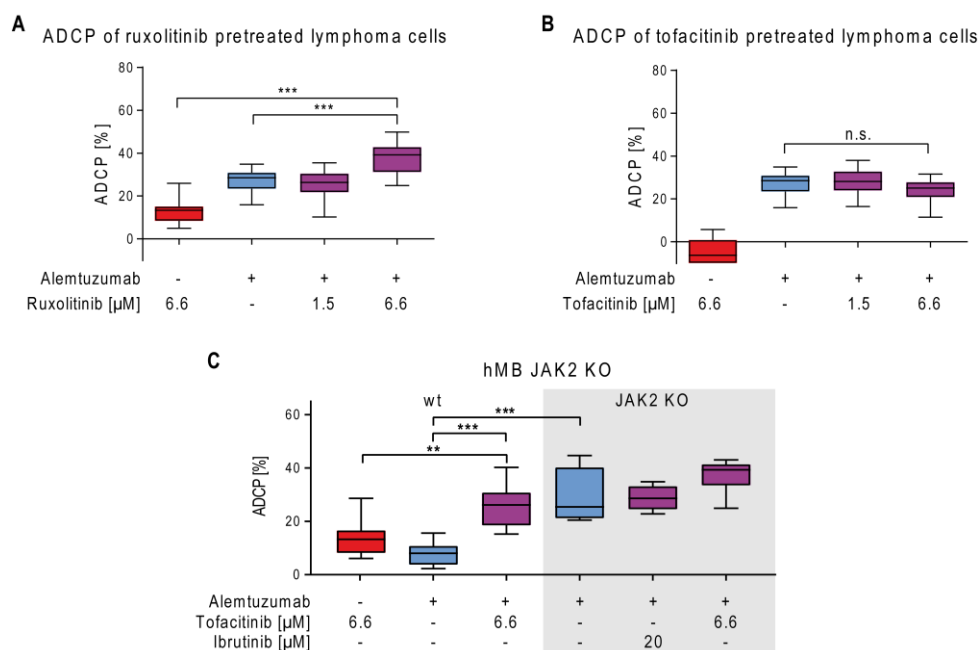
Figure 29 JAK2 in B cells is responsible for the increase in ADCP.
Box plots showing ADCP of ruxolitinib **(A)** and tofacitinib **(B)** pre-treated hMB "double hit" lymphoma cells co-cultured with J774A.1 macrophages, both treated with alemtuzumab. **(C)** Box plot showing ADCP of *JAK2* KO vs. empty vector control transduced, wild type (wt) hMB lymphoma target cells and J774A.1 macrophages treated or not treated with JAK2-inhibitor tofacitinib, BTK-inhibitor ibrutinib and alemtuzumab (N=2 biological replicates, n=10). Data are normalised to the co-culture without treatment. Box plots show the median, the 25th and 75th quartiles, and the minimal and maximal value. Unless otherwise stated experiments were performed with at least three biological replicates using flow cytometry. (** $p \leq 0.01$, *** $p \leq 0.001$ and n.s. = not significant)

To validate these findings *in vivo*, hMB wt and hMB *JAK2* KO cells were transplanted into 8-14 weeks old male NSG. Ten days after transplantation mice were treated *i.p.* with alemtuzumab or PBS for the control group. Here, mice transplanted with *JAK2* KO hMB lymphoma cells showed an increased survival compared to mice transplanted with hMB NT empty vector control cells (PBS *JAK2* KO vs. PBS NT p = 0.013) (Figure 30). Moreover, alemtuzumab treatment of *JAK2* KO hMB transplanted mice induced a moderate but not significant increase in survival (alemtuzumab *JAK2* KO median = 28.5 days vs. PBS *JAK2* KO median = 24 days, p = 0.277). Additionally, one *JAK2* KO hMB transplanted mouse treated with alemtuzumab was alive until day 182 – the end of the experimental set up. This data shows an additional effect of *JAK2* KO hMB cells *in vivo*.
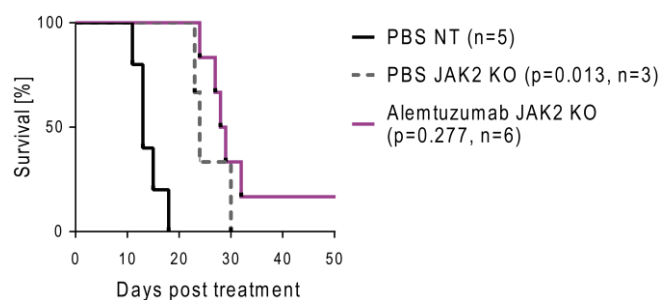
Figure 30 Combination treatment of hMB *JAK2* KO transplanted mice with alemtuzumab prolongs survival.
Kaplan-Meier analysis comparing the survival of male hMB non-target (NT) or hMB *JAK2* KO transplanted NSG mice receiving alemtuzumab. PBS was used as control. The treatment was given *i.p.* 10 days after *i.v.* hMB cell injection.

Since treating lymphoma cells and macrophages only with conditioned media of ibrutinib treated hMB cells increased ADCP (Figure 12B), ADCP assays with conditioned media of ruxolitinib (Figure 31A) or tofacitinib (Figure 31B) treated hMB lymphoma cells were performed. Here, conditioned media of ruxolitinib and tofacitinib treated hMB could not enhance ADCP. However, treating the co-culture with conditioned media generated from *JAK2* KO hMB increased ADCP (Figure 31C). These data indicate that *JAK2* KO hMB cells release an acute secretory activating phenotype that increase ADCP.
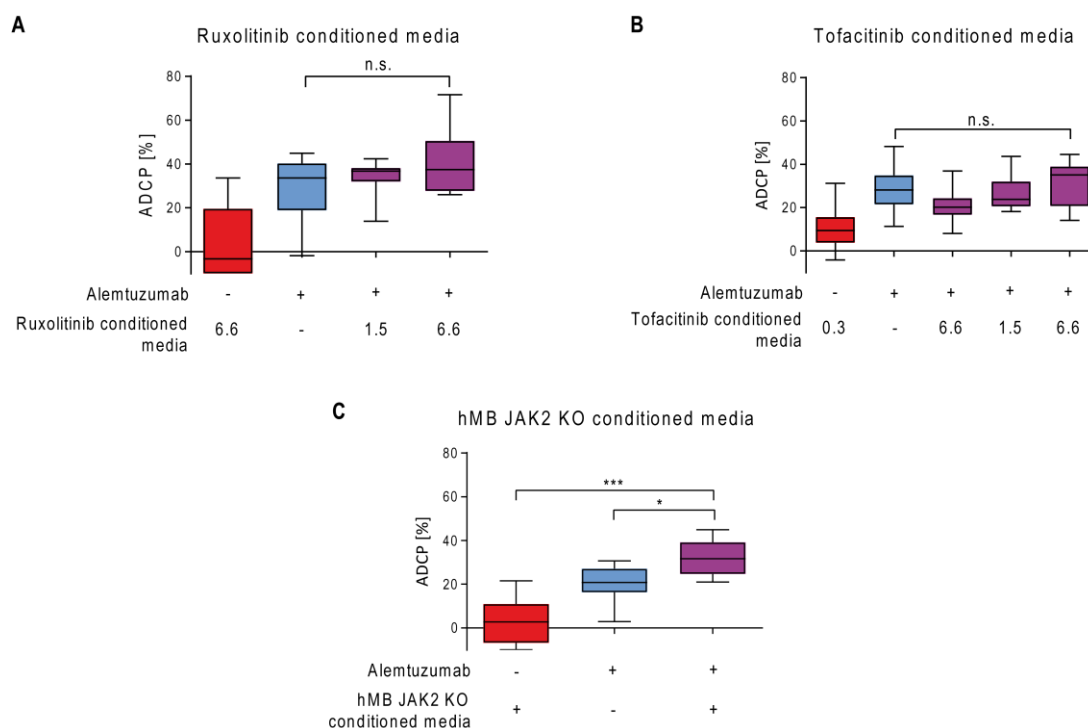
Figure 31 Conditioned media of *JAK2* KO cells improve ADCP.
(A) Box plot showing ADCP of hMB "double hit" lymphoma cells and J774A.1 macrophages treated with alemtuzumab and conditioned media of ruxolitinib **(A)** and tofacitinib **(B)** treated hMB cells and conditioned media of hMB *JAK2* KO cells **(C)** (N=2 biological replicates, n=10). Data are normalised to the co-culture without treatment. Box plots show the median, the 25th and 75th quartiles, and the minimal and maximal value. Unless

otherwise stated experiments were performed with three biological replicates using flow cytometry. (* $p < 0.05$, *** $p \leq 0.001$ and n.s. = not significant)

To further analyse the impact of conditioned media used in Figure 31 on ADCP, tumour supporting IL-10 and anti-tumoral IL-6 and TNF-α was measured. Conditioned media of ruxolitinib treated hMB cells presented a decreased expression of all cytokines (Figure 32). The same effect was observed when analysing respective cytokines in conditioned media of ibrutinib treated hMB cells (Figure 13). Moreover, checking the expression of cytokines released from *JAK2* KO hMB lymphoma cells revealed an increased expression of TNF- α (Figure 32C).
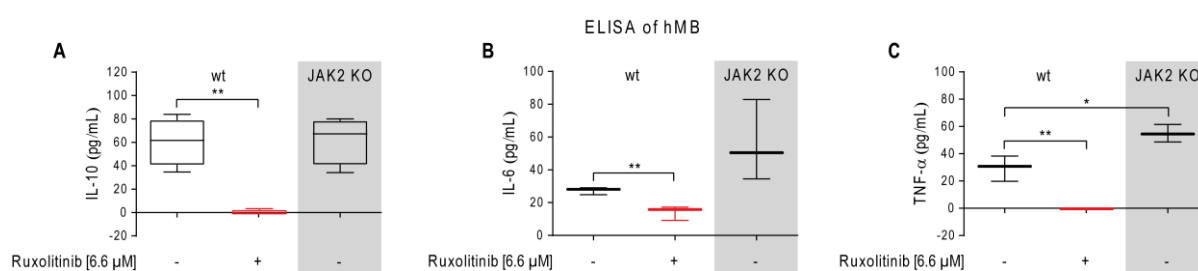
Figure 32 JAK2 inhibition and KO in B cells leads to a change of IL-10, IL-6 and TNF-α expression.
Box plots show the expression of IL-10 (**A**), IL-6 (**B**), and TNF-α (**C**) of hMB "double hit" lymphoma cells treated with ruxolitinib and hMB *JAK2* KO cells. Box plots show the median, the 25th and 75th quartiles, and the minimal and maximal value. Experiments were performed with four biological replicates using ELISA. (* $p < 0.05$ and ** $p \leq 0.01$)

Furthermore, analysing the expression of antibody antigens CD20 and CD52 on hMB lymphoma cells under ruxolitinib and tofacitinib treatment, revealed no difference in the number of positive cells or the MFI compared to the untreated control (Figure 33A). Moreover, *JAK2* KO hMB cells showed no change in the expression of CD20 (Figure 33B) whereas the number of CD52 positive cells and the expression per cell (MFI) was significantly downregulated compared to wt hMB.
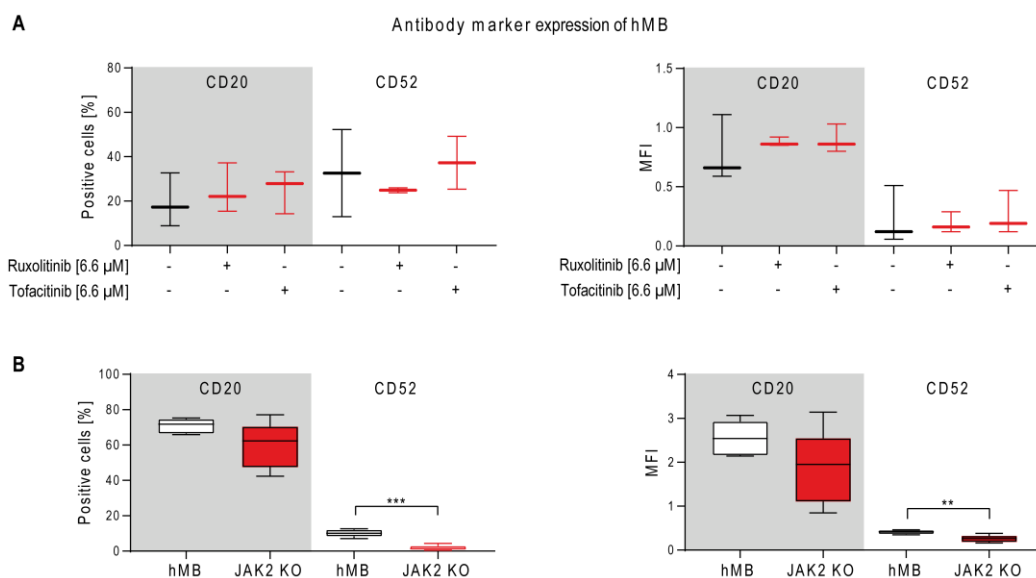
Figure 33 JAK2 inhibition in B cells does not alter the expression of CD20 and CD52.
(**A**) Box plots showing the expression of CD20 and CD52 of hMB "double hit" lymphoma cells treated with ruxolitinib or tofacitinib. (**B**) Box plots showing the expression of CD20 and CD52 of hMB *JAK2* KO lymphoma cells. The x-axis displays the number of positive cells (left box plot) and the MFI (right box plot). Box plots show the median, the 25th and 75th quartiles, and the minimal and maximal value. Experiments were performed with five biological replicates using flow cytometry.

To examine the role of "don't eat me" signals, the expression of CD47 and PD-L1 on hMB cells under JAK2 inhibition and the expression of respective markers on hMB *JAK2* KO cells was measured (Figure 34). Treating hMB lymphoma cells with ruxolitinib or tofacitinib revealed no altered expression of CD47 or PD-L1 (Figure 34A). However, the expression of CD47 in number of positive cells was slightly increased in *JAK2* KO hMB (Figure 34B). In contrast, the number of positive PD-L1 cells was strongly decreased in *JAK2* KO hMB cells. The expression of CD47 and PD-L1 per *JAK2* KO hMB cell was unaltered compared to wt hMB cells.
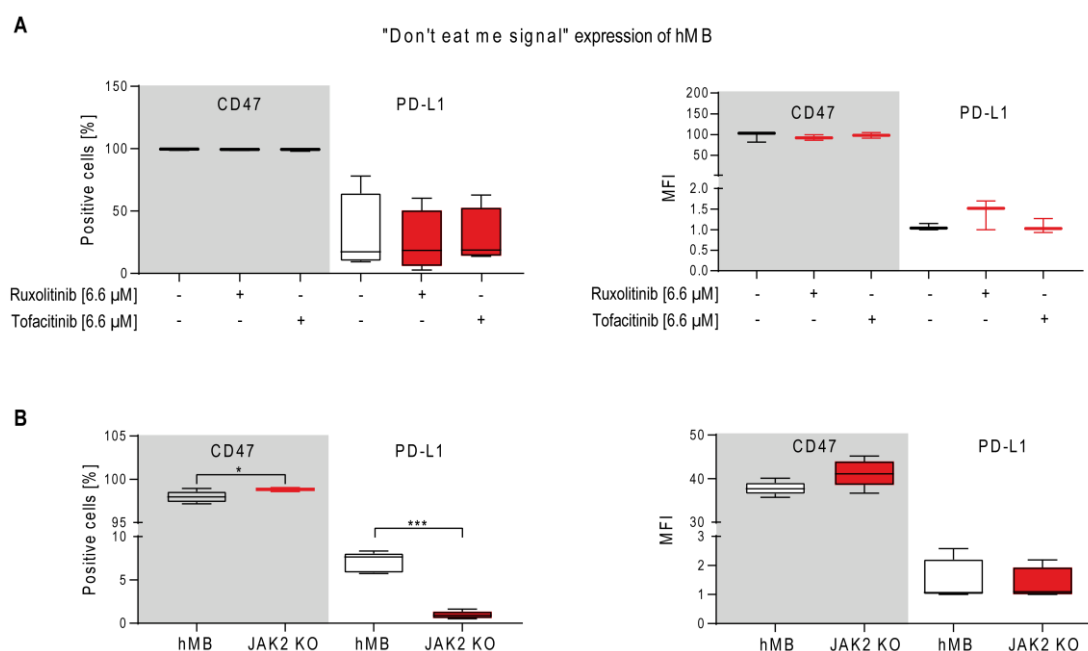
Figure 34 *JAK2* KO in B cells decrease the expression of PD-L1.
(**A**) Box plots showing the expression of CD47 and PD-L1 of hMB "double hit" lymphoma cells treated with ruxolitinib or tofacitinib. (**B**) Box plots showing the expression of CD47 and PD-L1 of hMB *JAK2* KO cells. The x-axis displays the number of positive cells (left box plot) and the MFI (right box plot). Box plots show the median, the 25th and 75th quartiles, and the minimal and maximal value. Experiments were performed with three biological replicates using flow cytometry.

In conclusion, the synergistic effect of ibrutinib and monoclonal antibody therapy on ADCP is caused by JAK2 off-target inhibition. Thereby, JAK2 influence hMB lymphoma cells due to altered cytokine release and decreased PD-L1 expression. Moreover, the impact of JAK2 deficiency and combined monoclonal antibody therapy could improve *in vivo* overall survival of NSG mice.

7.6.2 Pre-treatment of macrophages with JAK-inhibitors improve ADCP and change macrophage polarisation and activity

To verify the role of macrophage effector cells on increased ADCP with JAK inhibition, J774A.1 macrophages were pre-treated with ruxolitinib (Figure 35A) or tofacitinib (Figure 35B) and co-cultured with treatment naïve hMB lymphoma cells and alemtuzumab. Pre-treating macrophages with both JAK-inhibitors enhanced ADCP of lymphoma cells.
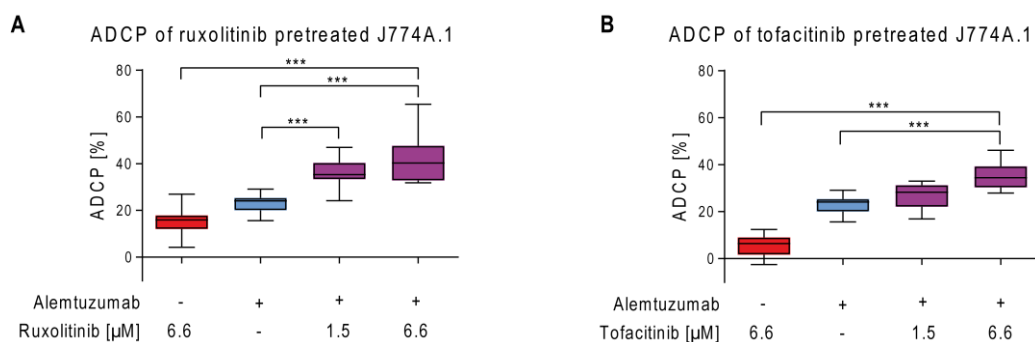
Figure 35 JAK inhibition only in macrophages leads to an increase in ADCP.
Box plots showing ADCP of ruxolitinib (**A**) or tofacitinib (**B**) pre-treated J774A.1 macrophages co-cultured with hMB "double hit" lymphoma cells, both treated with alemtuzumab. Data are normalised to the co-culture without treatment. Box plots show the median, the 25th and 75th quartiles, and the minimal and maximal value. Experiments were performed with at least three biological replicates using flow cytometry. (*** $p \leq 0.001$)

Furthermore, to identify the mechanism of JAK inhibition on macrophages and the impact on increased ADCP, J774A.1 macrophages were treated with ruxolitinib and the conditioned media was analysed on secretory released cytokines performing an ELISA (Figure 36). Treating macrophages with ruxolitinib decreased the expression of tumour supporting IL-10 (Figure 36A) and increased the expression of anti-tumoral IL-6 (Figure 36B) and TNF-α (Figure 36C).
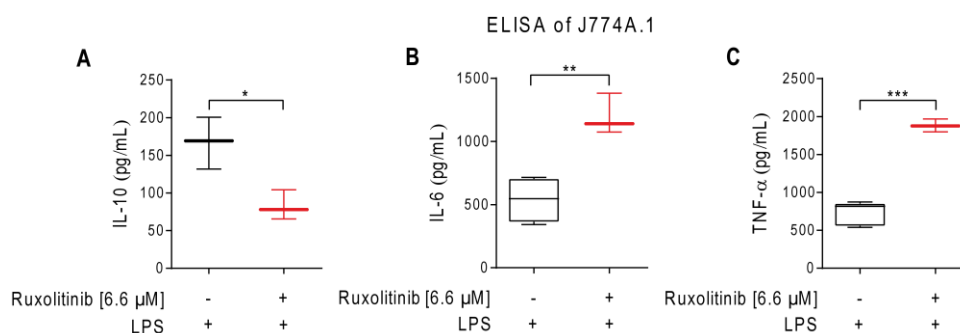
Figure 36 JAK inhibition in macrophages leads to a change of IL-10, IL-6 and TNF-α.
Box plots show the expression of IL-10 (**A**), IL-6 (**B**), and TNF-α (**C**) of J774A.1 macrophages treated with ruxolitinib. Box plots show the median, the 25th and 75th quartiles, and the minimal and maximal value. Experiments were performed with three biological replicates using ELISA. (* $p < 0.05$, ** $p \leq 0.01$ and *** $p \leq 0.001$)

Moreover, checking M1 and M2 polarisation markers on J774A.1 macrophages treated with ruxolitinib showed a slightly decreased number of M1 CD80 positive macrophages (Figure 37A). However, there was no change in the expression of M1 marker CD86. Furthermore, ruxolitinib increased the MFI of M2 marker CD206 (Figure 37B).
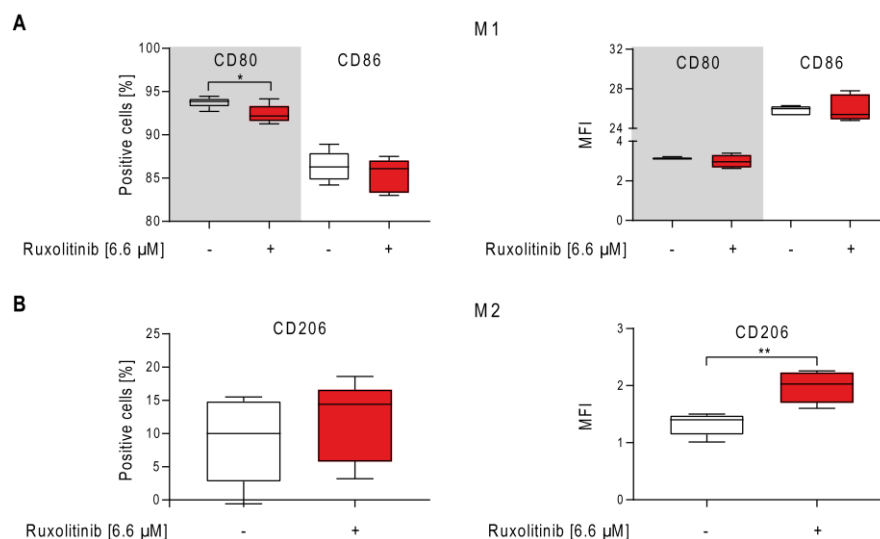
Figure 37 JAK inhibition slightly affects macrophage polarisation.
Box plots showing M1 macrophage polarisation marker CD80 and CD86 **(A)** and M2 marker CD206 **(B)** of J774A.1 macrophages treated with ruxolitinib. The x-axis displays the number of positive cells (left box plot) and the MFI (right box plot). Box plots show the median, the 25th and 75th quartiles, and the minimal and maximal value. Experiments were performed with three biological replicates using flow cytometry. (* $p < 0.05$)

Taken together, JAK inhibition influence ADCP in modifying the phagocytic activity of macrophages and their release of cytokines.

7.7 Resistance of *TP53* deficient B cell lymphoma to chemoimmunotherapy is mediated through EV release and PD-L1 expression

Independently of this thesis, we – the Prof. Pallasch laboratory – have evaluated the importance of *TP53* loss on macrophage phagocytic capacity under chemoimmunotherapy, identifying *via in vitro* experiments and a multi-omics approach upregulation of PD-L1 on lymphoma B-cells. Considering the loss of PD-L1 expression on *JAK2* KO hMB cells, it was relevant to this thesis to undertake *in vivo* experiments to validate these findings, since at least within lymphoma B cells PDL-1 might represent a central mechanism of inhibiting macrophage phagocytic capacity.

Chemoimmunotherapy is one standard treatment for B cell malignancies [14]. Thereby, one important mechanism is the induction of tumour cell clearance by macrophage activation [96], [234], [235]. However, resistance to chemoimmunotherapy occurs – mainly induced by additional mutations like the loss of *TP53* [195], [196]. Recently, we demonstrated that the loss of *TP53* in B cell lymphoma leads to a reduced macrophage phagocytic function by repressing genes responsible for the phagocytosis [231], [236]. Furthermore, we showed *via* proteomic analysis that in *TP53* B cell lymphoma the actin cytoskeleton formation and the release of EVs is altered. Thereby, EVs secreted by *TP53* deficient B cell lymphoma reduced anti-tumour effector function of macrophages.

In order to validate the role of EVs on tumour cell clearance in *TP53* B cell lymphoma *in vivo*, the NSG mouse model was used. Therefore, *TP53* B cell lymphoma with a KO in *RAB27A* were generated – losing the ability to release EVs [237]. For the *in vivo* experiments, *shTP53/RAB27A*-KO hMB cells and *shTP53/RAB27A*-wt hMB cells were transplanted into 8-14 weeks old NSG mice. Ten days after transplantation mice were treated *i.p.* with CTX and alemtuzumab or PBS as control. Here, mice transplanted with *RAB27A*-KO cells (green lines) exhibited a significant longer overall survival compared to *RAB27A*-wt mice (black lines) (Figure 38). Moreover, mice transplanted with *shTP53/RAB27A*-KO hMB treated with chemoimmunotherapy (green dashed line) revealed a significant longer survival than mice transplanted with *shTP53/RAB27A*-wt hMB treated with chemoimmunotherapy (black dashed line, *RAB27A* KO + CTX + alemtuzumab vs. *RAB27A* wt + CTX + alemtuzumab p < 0.0001).
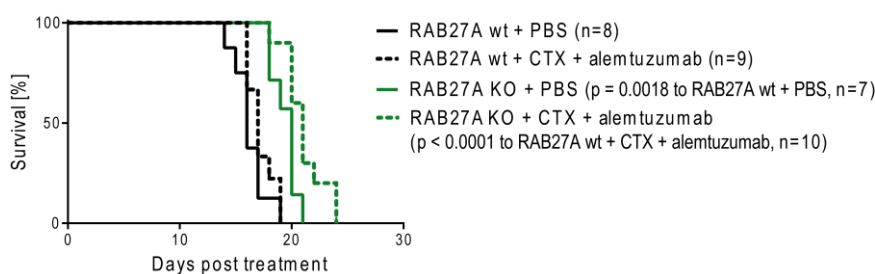
Figure 38 EV secretion from *TP53* deficient lymphoma B cells reduce overall survival and response to chemoimmunotherapy.
Kaplan-Meier analysis comparing the survival of *shTP53/RAB27A*-KO or wt hMB transplanted NSG mice receiving CTX and alemtuzumab in combination therapy. PBS was used as control. The treatment was given *i.p.* 10 days after *i.v.* hMB cell injection. Data were performed together with E. Izquierdo.

The next step was to understand the mechanism behind the reduced anti-tumour effector function of macrophages induced by EVs derived from *TP53* deficient B cell lymphoma. Here, we showed that EVs derived from *TP53* deficient B cell lymphoma express high levels of PD-L1 [231]. Moreover, blocking respective PD-L1 with atezolizumab restores the chemoimmunotherapy induced phagocytic capacity of macrophages [231]. To underline the *in vitro* generated data *in vivo*, *shTP53* deficient hMB cells were transplanted into 8-14 weeks old mice and treated after ten days with CTX, alemtuzumab and anti-PD1 (aPD1, GS-696882) antibody to block the PD-L1/PD1 axis (Figure 39). NSG mice that got the triple therapy (orange line) revealed a significantly prolonged survival compared to NSG mice only treated with the combination of CTX and alemtuzumab (grey line, aPD1 + CTX + alemtuzumab vs. CTX + alemtuzumab p = 0.023).
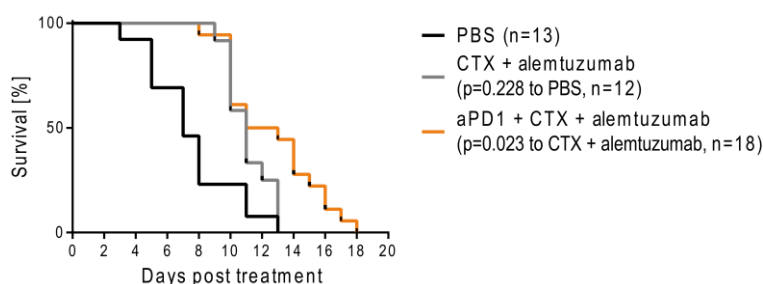
Figure 39 Blocking PD1 improves CTX and alemtuzumab combination therapy of NSG mice transplanted with *TP53* deficient B cells.
Kaplan-Meier analysis comparing the survival of *shTP53* transplanted NSG mice receiving anti-PD1 (aPD1), CTX and, alemtuzumab in combination therapy. PBS was used as control. The treatment was given *i.p.* 10 days after *i.v.* hMB cell injection. Data were performed together with E. Izquierdo.

Moreover, we generated a *shTP53* hMB cell line with a *PD-L1* KO [231]. Respective cell line was transplanted into NSG mice and treated with CTX and alemtuzumab or PBS as control (Figure 40). In general, mice transplanted with *shTP53/PD-L1*-KO hMB cells (orange lines)

showed a significant longer overall survival than mice transplanted with *shTP53/PD-L1*-wt hMB (black lines). Notably, the overall survival of mice treated with CTX and alemtuzumab was highly increased in *shTP53/PD-L1*-KO lymphoma (orange dashed line) compared to *shTP53/PD-L1*-wt lymphoma (black dashed line, *PD-L1* KO + CTX + alemtuzumab vs. *PD-L1* wt + CTX + alemtuzumab p = 0.005).
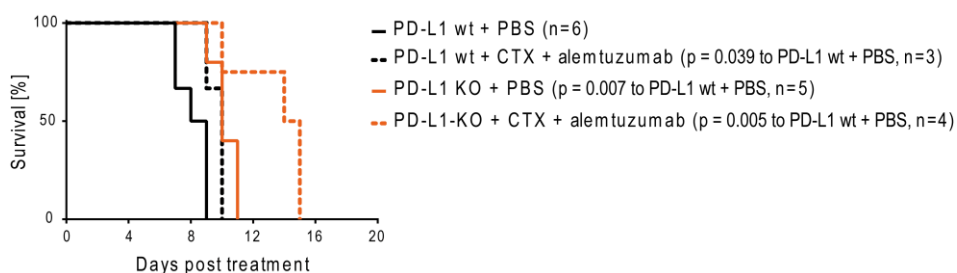
Figure 40 NSG mice transplanted with *TP53* and *PD-L1* deficient B cells improve CTX and alemtuzumab combination therapy.
Kaplan-Meier analysis comparing the survival of *shTP53/PD-L1*-KO or wt hMB transplanted NSG mice receiving CTX and alemtuzumab in combination therapy. PBS was used as control. The treatment was given *i.p.* 10 days after *i.v.* hMB cell injection. Data were performed together with E. Izquierdo.

Taken together, the *in vivo* data demonstrated the resistant mechanism from *TP53* deficient lymphoma to chemoimmunotherapy to be mediated due to EVs. In detail, this resistance is dependent on the expression of PD-L1 in *shTP53* lymphoma and can be supressed by combining chemoimmunotherapy with PD-1/PD-L1 inhibition.

7.8   JAK2 inhibition mediated increase in ADCP is independent of EVs

Taken into account, that EVs isolated from *shTP53* lymphoma cells inhibited macrophage phagocytic capacity and JAK2 inhibition in lymphoma cells increased ADCP, the role of EVs derived from hMB *JAK2* KO cells on macrophage-mediated ADCP was examined. Therefore, EVs from *JAK2* KO and NT hMB cells were isolated and co-cultured with alemtuzumab, hMB cells, and J774A.1 macrophages. Neither EVs derived from NT hMB cells, nor EVs derived from *JAK2* KO hMB cells improved ADCP (Figure 41A). Moreover, EVs of both lymphoma lines showed no toxicity to hMB cells (Figure 41B).
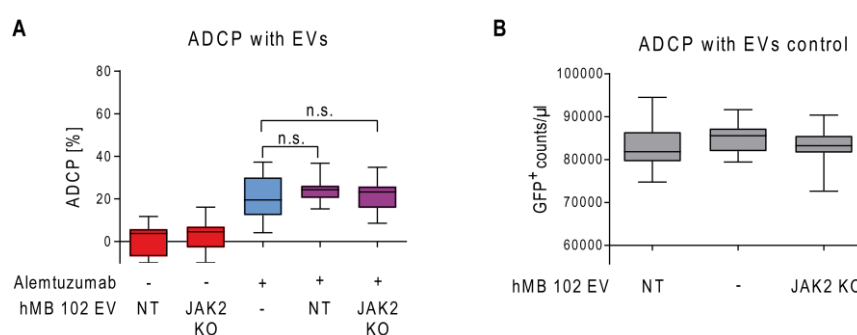
Figure 41 JAK2 inhibition mediated increase in ADCP is independent of EVs.
(A) Box plot showing ADCP of hMB "double hit" lymphoma cells and J774A.1 macrophages treated with alemtuzumab and EVs generated from hMB, hMB *JAK2* KO cells and cells with the non-target (NT) control. Data are normalised to the respective co-culture without treatment. **(B)** Box plot showing GFP+ hMB cells treated with EVs generated from hMB, hMB *JAK2* KO cells and hMB cells with the non-target (NT) control. Box plots show the median, the 25th and 75th quartiles, and the minimal and maximal value. Experiments were performed with three biological replicates using flow cytometry. (n.s. = not significant)

8 Discussion

In B cell malignancies inhibition of the BCR signalling pathway using BTK-inhibitors like ibrutinib became a very important therapeutic strategy [56]. Additional combination of small molecule inhibitors with monoclonal antibodies have been used in clinical trials with the molecular understanding of their synergistic interaction lagging behind [211]–[214]. The mechanisms of beneficial treatment combination need to be addressed not only on the tumour cell side but also in context of the TME. Here, phagocytosis of antibody-opsonized tumour cells by macrophages play a major role in the treatment of cancer with immunotherapeutics [144], [163], [164]. Accordingly, Pallasch *et al.* could demonstrate that treatment of leukaemia bearing mice with anti-CD52 antibody alemtuzumab induce tumour cell clearance through activation of macrophage effector cell function and induction of phagocytosis [96].

Therefore, the work of this thesis clarifies the important role of macrophages in the tumour microenvironment and their ability to induce phagocytosis of tumour cells influenced by combination therapy with small molecule inhibitors and monoclonal antibodies.

8.1 Ibrutinib enhances macrophage-mediated ADCP of lymphoma cells

Since, BTK plays a major role in the BCR signalling pathway which promotes the proliferation and survival of B cells, the inhibition of BTK using ibrutinib was introduced as frontline therapy for patients with relapsed CLL or small lymphocytic lymphoma (SLL) [206], [212], [238]–[246]. Moreover, ibrutinib was tested in clinical trials to improve chemoimmunotherapy such as R-CHOP or bendamustin and rituximab or ofatumumab [209], [214], [247]. Because chemotherapy shows high side effects in patients, clinical trials were initiated using combinations such as ibrutinib and anti-CD20 antibody rituximab [211], [212], [248], [249]. Here, the most recent phase III clinical trial of Shanafelt *et al.* demonstrated improved progression free survival (PFS) in CLL patients treated with ibrutinib and rituximab compared to patients who received FCR chemoimmunotherapy [211]. Likewise, Dimopoulos *et al.* showed a higher PFS with ibrutinib and rituximab combination in patients suffering from Waldenström's macroglobulinemia [248]. Although, Woyach *et al.* and Burger *et al.* revealed no benefit in PFS treating CLL patients with ibrutinib and rituximab combination [212], [249], Burger *et al.* exhibited that patients receiving the combination therapy showed a faster remission and achieved lower residual disease levels [249]. Taken together, these clinical trials demonstrate that the understanding of molecular mechanisms in combination therapies like

ibrutinib and monoclonal antibodies is important to investigate therapeutic strategies. Moreover, understanding the molecular mechanisms and targeting more specifically could help in overcoming treatment resistance or preventing side effects.

The work of this thesis has identified a synergistic interaction between monoclonal antibodies and ibrutinib leading to increased macrophage-mediated ADCP in B cell lymphoma (Figure 8). Already in the 1980s, researchers demonstrated that monoclonal antibodies stimulate macrophage infiltration and macrophage-mediated destruction of tumours *in vitro* and *in vivo* [250]–[252]. Subsequently, more recent studies exhibited that anti-CD20 and anti-CD52 antibodies induce macrophage-mediated ADCP in leukaemia and lymphoma [96], [253]–[259]. Here, Church *et al.* observed the highest increase in phagocytosis using the anti-CD52 antibody alemtuzumab [253]. However, previous studies have provided conflicting results about the influence of monoclonal antibodies in combination with ibrutinib on macrophage-mediated phagocytosis [260]. On the one hand combination of ibrutinib with anti-CD38 antibody daratumumab increased ADCP in CLL cells [261]. Moreover, TG-1701 – a novel irreversible BTK-inhibitor – supported anti-CD20-mediated ADCP of ibrutinib resistant mantle cell lymphoma [262]. On the other hand combination of ibrutinib with anti-CD20 antibodies impaired ADCP even though, Borge *et al.* still observed an increased binding of rituximab opsonized CLL cells to ibrutinib pre-treated macrophages [263], [264]. These contrary results should be independent of the antibody selection since the work of this thesis demonstrated that the increase in ibrutinib's ADCP can be mediated by targeting CD52 with alemtuzumab as well as CD20 using rituximab and obinutuzumab (Figure 10). However, measuring phagocytosis in co-culture systems is technically challenging and requires high levels of standardisation regarding target and effector cell lines as well as suitable treatments.

Addressing the influence of ibrutinib and alemtuzumab combination on different target cell lines, using hMB "double hit" lymphoma as well as primary CLL patient cells increased ADCP (Figure 8A and Figure 9A). Importantly, pre-treatment of CLL patient cells showed an increase in ADCP using low ibrutinib concentrations of 0.01 µM which corresponds to the dose of 420 mg ibrutinib daily used for patients [232]. In contrast, ADCP of hMB cells was improved with increasing ibrutinib concentrations emphasising the different behaviour of hMB "double hit" lymphoma and CLL patient cells. The better response of CLL patient cells to low ibrutinib concentrations might be explained due to their high dependency on BCR signalling, whereas hMB cells keep the ability to proliferate and avoid apoptosis due to overexpression of the *MYC*

and *BCL-2* oncogenes [3], [48]. Moreover, hMB cells can proliferate independently, whereas primary CLL patient cells are strongly reliant on the TME and therefore challenging to keep in culture [19], [43]. Additionally, performing ADCP assays with primary "double hit" lymphoma cells to exclude the influence of origin being cell line derived or primary would give further insights. However, acquiring primary cells from patients is difficult due to disease rarity and high genetical aberrations.

Although Da Roit and Engelberts *et al.* as well as Borge *et al.* used CLL patient cells to perform phagocytosis assays they could not detect any effect on ADCP [263], [264]. However, in contrast to this work, they have used different effector cells that might explain the missing effect in increased ADCP. Prior performing the experiments, they differentiated human monocytes into macrophages thereby potentially affecting macrophage polarisation and subsequently FcγR-induced phagocytic activity. In this work both murine J774A.1 macrophages and primary peritoneal macrophages were used for ADCP assays in which both macrophage types showed increased ADCP with ibrutinib combination (Figure 8A and Figure 9B).

In general, different types of macrophages can show different ability of phagocytic potential [265]. Especially, the macrophage polarisation status and subsequent cytokine release altering macrophage phenotype is one important factor (chapter 4.4.1.1) [106]. Furthermore, it was reported that BTK is important for phagocytosis, therefore blocking BTK with ibrutinib should antagonise ADCP by macrophages [263], [266], [267]. Nonetheless, the work of this thesis observed that the ibrutinib-mediated increase in ADCP is independent on BTK in primary peritoneal macrophages (Figure 21A). Moreover, kinase activity profiling of J774A.1 macrophages revealed limited effects under ibrutinib treatment (Figure 26). Considering the findings of the literature, different types of macrophage effector cells could show diverse dependency on BTK and its influence on phagocytic activity.

Emphasising the beneficial combination of ibrutinib and alemtuzumab *in vitro*, combination therapy also improved survival of the humanised mouse model of *MYC/BCL-2* "double hit" lymphoma *in vivo* (Figure 11A) [226]. Since the used immune deficient NSG mice lack of mature T cells, B cells, and NK cells, the main effector cells mediating tumour cell depletion display macrophages [268]. Moreover, it was shown that alemtuzumab binds to the vast majority of tumour cells in different compartments such as the spleen and bone marrow of NSG mice and is dependent on the Fc-portion of alemtuzumab [96]. During the experiments, a difference in the overall survival between male and female mice was observed. This effect could be explained by the general lower weight of female mice causing a stronger tumour burden and

disease progression. Additionally, female mice injected with hMB lymphoma cells displayed bigger ovaries that contained high amounts of GFP⁺ hMB cells of around 38 %. Therefore, in the following experiments only male mice were considered.

Since B cells circulate between the bone marrow and lymphoid organs, the bone marrow and spleen were analysed for remaining hMB cells influenced by therapy (Figure 11). Here, combination treatment of ibrutinib and alemtuzumab as well as alemtuzumab mono therapy vastly reduced hMB lymphoma in the spleen but not in the bone marrow. The different response of the spleen and bone marrow was not influenced by a change in macrophage number but can be explained by the circumstance that the bone marrow represents a niche being refractory towards therapy. Here, Pallasch *et al.* supposed that the higher expression of Fc-γ receptor IIB in the bone marrow contributes to the different responses in various organ sites [96], [269]. However, Pallasch *et al.* could overcome therapy resistance of the bone marrow by combining alemtuzumab with the cytotoxic agent CTX. Although, other studies observed that ibrutinib induce an efflux of tumour cells from organ compartments into the blood in CLL patients [270], this was not detected in the here used mouse model by weekly blood analysis.

Importantly, hMB cells harvested from the spleen showed a significant decrease in the expression of "don't eat me signal" CD47 only under combination therapy. This could explain the beneficial effect of combination therapy *in vivo* since CD47 prevents phagocytosis of macrophages by binding to the signal regulatory protein alpha (SIRPα) [143]. In general, targeting CD47 with therapeutic antibodies becomes more and more relevant in cancer therapies [271], [272]. Furthermore, combining anti-CD47 antibodies with rituximab revealed synergistic effects in lymphoma and leukaemia models [255], [273] and would be interesting to test in the humanised "double hit" lymphoma mouse model as well.

Regarding the "don't eat me" signal PD-L1, Kondo and Shaim *et al.* measured a reduced PD-L1 expression on CLL patient cells under ibrutinib treatment [53]. In the "double hit" lymphoma model used in this work, no positive influence of PD-L1 expression on hMB cells under ibrutinib or ibrutinib and alemtuzumab combination therapy was observed. Alemtuzumab mono therapy even exhibited an increased PD-L1 expression. Since, Kondo and Shaim *et al.* revealed a durable downregulation of PD-L1 after three month post treatment [53] the effect might not be detected in the NSG mouse model since mice reached humane endpoint before a possible recovery. Moreover, Breinholt *et al.* reported that TAMs exhibit the highest PD-L1 expression, whereas B cells rarely express PD-L1 especially in *MYC/BCL-2* "double hit" lymphoma [274]. In general, blocking the PD-1/PD-L1 axis with therapeutic antibodies alone

or in combination with ibrutinib would be interesting to test as it showed already initial success in B cell malignancies [222], [275]–[280].

To visualize the observed effects, *in vitro* phagocytosis could be detected by live cell imaging as already shown for alemtuzumab mono therapy [96] and human derived macrophages. Moreover, *in vivo* mouse numbers should be increased to improve reliability, and *in vivo* phagocytosis could be measured by analysing F480/GFP double positive cells in the different compartments. Additionally, to verify the macrophage-mediated effect of combination therapy *in vivo*, clodronate containing liposomes could be used to deplete macrophages in transplanted NSG mice [281]. For alemtuzumab mono therapy this was already shown in the "double hit" lymphoma mouse model by Pallasch *et al.* [96]. A second mouse model like SCID-BEIGE mice (C.B-17/IcrHsd-Prkdc^{scid}Lys^{bg}) could be used to give further insights into tumour development in different compartments by assessing tumour growth using bioluminescence imaging [164]. Another key model to test the influence of combination treatment would be the CLL Eµ-TCL1 mouse model, since it reproduces leukaemia with a certain phenotype that is similar to the human B-CLL including the responses of the TME [282]. Together with testing different animal models, unravelling the molecular interactions of phagocytosis mediated by ibrutinib and antibody combination is important to improve future therapies.

8.2 Ibrutinib increases ADCP *via* release of an acute secretory phenotype of lymphoma target cells that polarises and activates macrophages

Phagocytosis can be triggered and improved through a variety of mechanisms including macrophage polarisation, cell surface marker expression of "don't eat me" signals or antigens, cytokine release, exosomes, hypoxia and opsonins [107], [139], [140], [283], [284]. In order to get a better overview of the individual inhibitors influencing ADCP as wells as cytokine and surface marker expression Figure 42 summarizes the most important results of this work.
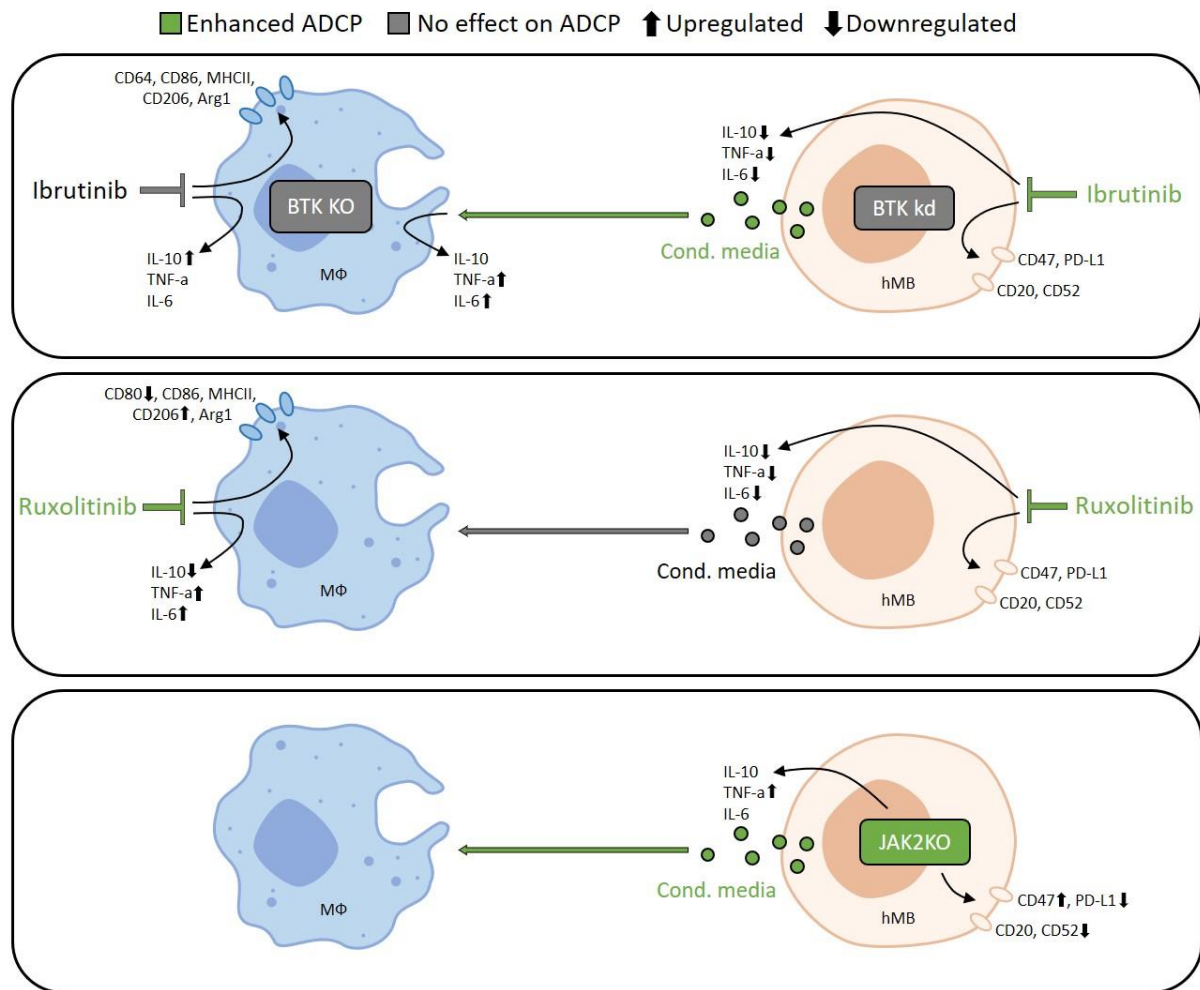
Figure 42 Overview of the influence of inhibitors on ADCP, cytokine release, and cell surface marker expression.
(Upper box) Ibrutinib pre-treated macrophages co-cultured with treatment naïve hMB cells revealed no increase in ADCP. Here, ibrutinib did not influence the expression of M1 and M2 cell surface markers but enhanced the release of IL-10 by macrophages. In contrast, ibrutinib pre-treated hMB cells co-cultured with treatment naïve macrophages increased ADCP. Likewise, conditioned media of ibrutinib treated hMB cells increased ADCP showing an overall decreased cytokine expression. Respective conditioned media of ibrutinib treated hMB cells enhanced the release of TNF-α and IL-6 by macrophages. Treatment of hMB cells with ibrutinib did not influence the expression of the immune checkpoints CD47 and PD-L1 nor of the antibody markers CD20 and CD52. Importantly, macrophages and hMB cells with a *BTK* KO/kd did not affect ADCP. **(Middle box)** Ruxolitinib pre-treated macrophages co-cultured with treatment naïve hMB cells enhanced ADCP and influenced the cell surface marker expression as well as the cytokine release of macrophages. Similarly, ruxolitinib pre-treated hMB cells co-cultured with treatment naïve macrophages increased ADCP and influenced the cytokine release of hMB cells. However, ruxolitinib did not influence the immune checkpoint and antibody marker expression of hMB cells. Moreover, conditioned media of ruxolitinib treated hMB cells revealed no influence on ADCP. **(Lower box)** hMB cells with a KO in *JAK2* co-cultured with wt macrophages increased ADCP and influenced the cytokine release as well as the expression of immune checkpoints and antibody markers of hMB cells. Furthermore, conditioned media of *JAK2* KO hMB cells enhanced ADCP of wt hMB cells. Green coloured shapes indicate an enhanced effect on ADCP, grey coloured shapes indicate no effect on ADCP, bold arrows describe an up- or down-regulation of cell surface marker expression and cytokine release.

In our ADCP assays, ibrutinib improved ADCP by directly affecting the hMB target cells (Figure 12A). Treatment of hMB cells with ibrutinib led to a decreased release of the cytokines IL-10, TNF- α, and IL-6 (Figure 13A-C). In general, patients suffering from CLL show

increased cytokine levels that support tumour growth and development [285]. In line with the results of this work Niemann *et al.* reported a decrease of respective cytokine levels such as IL-10 and TNF-α under ibrutinib treatment suggesting ibrutinib to inhibit the tumour supportive role of the TME [286]. However, it was reported that IL-10 secreted from B cell lymphoma stimulates macrophage-mediated phagocytosis of rituximab-opsonized B-CLL cells [287]. Moreover, others reported that TNF-α and IL-6 also positively influence the phagocytic activity of macrophages [288], [289]. Consequently, the observed reduction of respective cytokines under ibrutinib treatment should negatively influence phagocytosis in this set up. Nevertheless, using only the conditioned media of ibrutinib treated hMB cells increased ADCP (Figure 12B) and stimulated macrophage polarisation by enhancing the secretion of pro-inflammatory TNF-α and IL-6 by macrophages (Figure 13D-F). In addition, with the observed effect of conditioned media of ruxolitinib treated hMB cells that exhibited a similar cytokine secretion profile as ibrutinib treated hMB cells (Figure 32) but did not increased ADCP (Figure 31) the effect seems to be mediated through independent secretory components (Figure 42). Therefore, performing a screening of the secretory elements from ibrutinib treated lymphoma cells using multiple cytokine arrays would give further insights. Moreover, identifying changed pathways of macrophages treated with conditioned media from ibrutinib treated and untreated lymphoma cells using proteomic analysis would further clarify the influence of soluble factors on macrophage polarisation.

Besides the activation of macrophages *via* secretory released factors, direct activation by reprogramming macrophage phenotypes was already initiated using radio- or chemo- and immunotherapy [284]. There are two strategies to reprogram macrophages: First, blocking M2 stimulating factors *via* inhibition of STAT3 and 6 [290]–[293] and second, inducing M1 activating factors *via* stimulation of STAT1, NFκB, and CD40 or PI3Kγ deletion [284], [294]–[300]. Nevertheless, polarising macrophages simply towards an M1-like phenotype does not necessarily have to induce phagocytosis. Although M1-like macrophages are meant to act anti-tumoral and M2-like macrophages pro-tumoral. Amongst others, Leidi *et al.* demonstrated that M2 macrophages stimulate rituximab-opsonised leukaemic cells more efficiently than M1 macrophages [287], [301], [302]. Here, stimulation of macrophages with the M2-associated cytokine IL-10 increased their phagocytic ability. In contrast, stimulation with the M2-associated cytokine IL-4 decreased their phagocytic capacity.

In this work direct treatment of macrophages with ibrutinib revealed no increase in ADCP and did not change the expression of M1 or M2 polarisation markers on macrophages (Figure 17).

However, ibrutinib changed the cytokine secretion profile slightly towards an M2-like phenotype *via* upregulation of IL-10 (Figure 16). In line with these findings three independent studies revealed similar impacts on macrophage polarisation under ibrutinib treatment. First, Colado *et al.* exhibited that ibrutinib impairs human macrophage polarisation towards M1 [303]. Second, Fiorcari and Maffei *et al.* exhibited an increased IL-10 release of ibrutinib treated nurse-like cells protecting CLL cells from apoptosis and phagocytosis [304]. And third, patients getting ibrutinib treatment showed an enhanced expression of the M2 marker CD206 in monocytic populations in peripheral blood after one month. In contrast, another study reported a reprogramming of TAMs towards an M1-like phenotype under ibrutinib treatment in pancreatic cancer [305]. In summary, the findings observed here and the current literature indicate that every factor influencing phagocytosis needs to be considered separately and in a continuum of the macrophage polarisation profile.

Besides ibrutinib treatment, monoclonal antibodies *per se* can also lead to a release of cytokines influencing treatment response [306]. Therefore, future experiments could include the influence of monoclonal antibodies on cytokine secretion and macrophage polarisation. Moreover, the impact of ibrutinib on further cytokines and polarisation markers like TGF-β or CD163 could be investigated.

Since soluble factors and macrophage polarisation might display only a part of the mechanistic interactions of ibrutinib and monoclonal antibodies other factors like antigen expression were addressed. It was reported that BCR-inhibitors including ibrutinib downregulate the expression of CD20 on tumour cells leading to decreased antibody binding [307], [308]. However, the influence of ibrutinib on CD20 and CD52 expression on hMB lymphoma cells was unaffected (Figure 14A). Besides, it was reported that B cells expressing high or low CD20 levels exhibited no difference in macrophage-mediated phagocytosis of rituximab-opsonised B cells [287].

Likewise, the expression of "don't eat me" signals CD47 and PD-L1 on hMB cells were not changed under ibrutinib treatment *in vitro* (Figure 14B). Studies have reported that on the one hand ibrutinib reduced the expression of PD-L1 on CLL patient cells mediated through STAT3 inhibition [53] and on the other hand increased PD-L1 expression on CLL cells [309]. Incorporating the *in vivo* results, the expression of CD47 on hMB cells seems to be only influenced under combination therapy of ibrutinib plus alemtuzumab. This result demonstrate the importance of analysing the expression of immune checkpoints like PD-L1 and CD47 in future clinical studies.

8.3 Ibrutinib's increase in ADCP is mediated *via* off target effects involving JAK2

For the first time, the work of this thesis demonstrated that the synergy of ibrutinib with monoclonal antibodies leading to increased ADCP was not primarily mediated by BTK inhibition but rather by targeting off-target kinases such as JAK2 (chapter 7.4-7.6). Using JAK2-inhibitors instead of ibrutinib could recapitulate the increase in ADCP, identifying the JAK/STAT signalling pathway as an important mediator for macrophage-mediated phagocytosis synergising with monoclonal antibodies.

Although, combination therapy of the more specific BTK-inhibitor acalabrutinib with obinutuzumab showed initial success in CLL patients [310], [311], this work revealed no synergistic effect *in vitro* as well as *in vivo* using acalabrutinib or tirabrutinib in combination with monoclonal antibodies (Figure 18, Figure 19, and Figure 20). Besides, acalabrutinib increased the expression of PD-L1 on B cell lymphoma cells preventing macrophage-mediated phagocytosis as shown in this thesis (Figure 19B) and by M. Schwarzbich [309]. One explanation for the different response of acalabrutinib plus monoclonal antibodies in CLL patients could be the lower dependency of the here used aggressive "double hit" lymphoma cell line on BTK and subsequently sustained BCR signalling. Moreover, the effect of acalabrutinib with obinutuzumab combination therapy in CLL patients might be mediated through ADCP-independent mechanisms [312].

Addressing possible off-targets of ibrutinib, Berglöf *et al.* reviewed a set of kinases holding a cysteine residue in the ATP-binding site that correlates with cysteine 481 of BTK binding to ibrutinib [233]. Furthermore, using differential kinobeads profiling identified TEC kinase family members including TEC and BLK as the most potently bound off-target kinases [313]. These off-targets have been reported to play a role in many B cell malignancies and the TME synergising with BTK inhibition or acting independently [233]. For example, it has already been shown that ibrutinib inhibits ITK that further abrogate the formation of Th2 cells and potentiate the anti-tumour immune responses of Th1 cells [314], [315].

Many of the known ibrutinib off-target kinases such as BMX, EGFR, or JAK2 and 3 were identified in this work in "double hit" lymphoma cells as well as CLL patient cells using the PamStation platform (Figure 24 and Figure 25). Here, JAK2 and 3 exhibited the most significantly changed target peptides under ibrutinib treatment compared to second generation

BTK-inhibitors. In contrast, the number of significantly altered peptides belonging to the kinases BMX or EGFR were similar in all three BTK-inhibitors. Since second generation BTK-inhibitors revealed no increase in ADCP, this could explain why the inhibition of BMX and EGFR showed no additional effect on ADCP as well (Figure 27). However, this thesis only revealed an increase in macrophage-mediated ADCP *via* inhibition of JAK – specifically JAK2 (Figure 27 and Figure 29). The special role of JAK2 was further confirmed as it was measured as an ibrutinib off-target in hMB as well as CLL patient cells, whereas off-target JAK3 was only observed in hMB cells treated with ibrutinib (Figure 24 and Figure 25).

Kinase activity profiling of ibrutinib treated macrophages barely influenced peptide phosphorylation (Figure 26) supporting ibrutinib's influence on ADCP mainly *via* targeting lymphoma cells as already discussed in chapter 8.2.

Comparing the volcano plots of hMB treated cells, ibrutinib and tirabrutinib showed a primarily downregulation of peptide phosphorylation whereas acalabrutinib induced and an up- and downregulation. These results underline that BTK-inhibitors can show different off-target profiles and therefore potentially act in a different way. Nevertheless, increasing the number of replicates would give further clarification. Additionally, using other methods such as proteomic analysis, RNA-sequencing, or microarrays would increase and clarify the spectrum of off-target inhibition and related pathways. The better ibrutinib's influence on ADCP and off-target inhibition is understood, the more precisely ADCP can be achieved for therapy of B cell malignancies.

In line with the results of this thesis, it has already been shown that ibrutinib modulates the TME through JAK2 downstream target STAT3 and mediates the suppression of B cell function in CLL [53]. STAT3 signalling induced by the prognostic CLL biomarker β_2-microglobulin was also suggested to support the TME and therefore the tumour through elevated MDSC levels [316]. In general, signalling cascade *via* IL-6, JAK2, and STAT3 was reported to be active in many types of cancer [317]–[319] showing a correlation between increased levels of IL-6 and shorter survival of CLL patients [318]. Dysregulation of the JAK/STAT signalling was also shown by genetic alterations in multiple genes including, *STAT3/5B/6*, *JAK1/2*, and *protein tyrosine phosphatase non-receptor type 1* (*PTPN1*) in classical Hodgkin lymphoma [320]. In addition, *MYC* alterations in plasmablastic lymphoma cooperated with dysregulation of the JAK/STAT signalling pathway [321]. It was further reported that stimulation of the BCR in CLL *via* anti-IgM antibodies activates the JAK2/STAT3 signalling pathway [322]. However,

in contrast to ibrutinib second generation BTK-inhibitors showed no influence on STAT3 phosphorylation (Figure 28) facilitating ibrutinib's influence through off-target inhibition.

To further validate that the increase in ADCP with JAK-inhibitors is mediated through the deactivation of the IL-6/JAK2/STAT3 signalling, tocilizumab could be used. Tocilizumab is a humanised monoclonal antibody that binds to the IL6R and therefore blocks the stimulation *via* IL-6 and downstream activation of JAK2 and STAT3 and tocilizumab is already used as therapeutic antibody for rheumatoid arthritis [323].

Using JAK-inhibitors such as tofacitinib showed already proven effects in rheumatoid arthritis and is approved by the FDA (Food and Drug Administration) [324]–[326]. Following, JAK-inhibitors are investigated as treatment options for B cell malignancies. Here, Hofland and de Weerdt *et al.* demonstrated that inhibition of JAK blocked the proliferation of CLL cells [327]. Moreover, it was shown that ruxolitinib improved disease-related symptoms in CLL patients, induced apoptosis, and decreased lymph node size [328], [329]. However, the concentrations of JAK-inhibitors used for this thesis did not lead to increased apoptosis and showed no toxicity on hMB lymphoma cells (Figure 45). Ruxolitinib was also tested in a phase II clinical trial for CLL patients but was stopped after high incidences of anaemia and no evidence of reduced lymphocytosis [329].

As another treatment strategy, direct inhibition of STAT3 was investigated for lymphoma and leukaemia and revealed tumour regression due to cell cycle arrest or apoptosis [328], [330], [331]. It was shown that active STAT3 increase the transcription of *MYC* and anti-apoptotic *BCL-2*, therefore regulating proliferation and apoptosis of B cells [161], [332]. In contrast, Rozovski *et al.* reported that at very high levels constitutively activated STAT3 can also lead to apoptosis of CLL cells due to activation of caspase-3 that plays a role in apoptosis [333]. Nevertheless, due to the promising effects of JAK/STAT pathway inhibition in B cell malignancies, combinatorial treatment options should be further investigated in clinical trials.

Overall, besides JAK2 further kinases could play a supportive role in ADCP such as LYN or BLK. The kinase activity of LYN in the TME was already reported to play a role in CLL progression [334]. Here, macrophages with a KO in LYN showed reduced nursing capacity for CLL cells. This effect was mainly mediated through direct cell contacts. Likewise, it was reported that reduced BLK expression in C57BL/6-*lpr/lpr* mice enhance the production of proinflammatory cytokines [335] potentially stimulating the phagocytic capacity of

macrophages. Performing ADCP assays with inhibitors for LYN or BLK might reveal additional kinases that influence macrophage-mediated ADCP.

8.3.1 Increased ADCP of *JAK2* KO hMB cells is mediated *via* release of an acute secretory phenotype and downregulation of PD-L1

The mechanism of increased ADCP with JAK – specifically JAK2 – inhibition was mediated through hMB target cells as well as macrophage effector cells (Figure 29 and Figure 35; overview Figure 42). Here, hMB *JAK2* KO target cells mediated ADCP *via* an acute secretory phenotype showing an increased expression of pro-inflammatory and anti-tumoral TNF-α (Figure 31 and Figure 32). This effect was not observed using the JAK-inhibitors ruxolitinib and tofacitinib that led to an overall decreased cytokine expression.

Decreased expression of pro-inflammatory cytokines such as IL-6 or TNF-α under ruxolitinib and tofacitinib treatment was also reported by others [328], [336], [337]. Here, the different reactions of *JAK2* KO and JAK2 inhibition on cytokine secretion could be explained due to long-term effects triggered by the KO but not the inhibitors. Moreover, inhibitors show off-target effects. For example, ruxolitinib binds to other JAK family members like JAK1 thereby blocking the release of pro-inflammatory cytokines [338]. Since ibrutinib also mediated ADCP *via* the release of an acute secretory phenotype, once more the importance of soluble factors on influencing macrophage phagocytic activity is emphasised.

Besides the changed cytokine secretion, *JAK2* KO hMB cells showed a slight increased expression of CD47 (Figure 34). However, since the expression of CD47 on wt hMB cells was already nearly 100 %, the increased CD47 expression on *JAK2* KO hMB cells might not affect phagocytosis in this set up.

Interestingly, *JAK2* KO lymphoma cells exhibited a strong decrease of PD-L1 expression that might further influence macrophage phagocytic activity. Although, ruxolitinib and tofacitinib revealed no influence on PD-L1 expression after 17 h, Green *et al.* exhibited a reduction of the PD-L1 counterpart PD-1 ligand transcription after 24 h in Hodgkin lymphoma cells using JAK2-inhibitors [339]. Moreover, recent studies showed a correlation of JAK2 activity and increased PD-L1 expression in tumours [339]–[341]. Here, loss-of-function mutations in *JAK1/2* and the subsequent lack of PD-L1 expression led to a resistance towards anti-PD1 antibody therapy [341]. As reported by Kondo and Shaim *et al.*, JAK2 downstream target and transcription factor STAT3 mediates the expression of PD-L1 [53]. They also reported that

ibrutinib decrease the expression of PD-L1 through STAT3 [53]. Although in this work ibrutinib and JAK-inhibitors revealed no effect on PD-L1 expression, *JAK2* KO did. It can be hypothesised that the inhibition of downstream STAT3 *via* ibrutinib and JAK-inhibitors was too short or week to influence PD-L1 expression.

To further examine the influence of PD-L1 on increased ADCP, the PD-1/PD-L1 axis could be blocked using anti-PDL1 antibody atezolizumab or anti-PD1 antibody GS-696882. In general, blocking PD-L1 in Eµ-TCL1 mice was shown to prevent CLL development [278]. Likewise, PD-1/PD-L1 block increased macrophage-mediated phagocytosis *in vivo* suggesting the effect to be dependent on blocking PD-1 of TAMs [140]. Furthermore, it was reported that TAMs display the main source of PD-L1 expression [274] mediated *via* IL-10 [118]. Therefore, checking the influence of JAK2 inhibition or *JAK2* KO on the expression of PD-1/PD-L1 on macrophages would give further insights.

Interestingly, *JAK2* KO hMB lymphoma cells revealed a decreased expression of CD52 (Figure 33) hypothesising alemtuzumab treatment to increase phagocytosis despite very low levels of CD52 expression.

The beneficial combination of JAK2 deficient lymphoma target cells combined with monoclonal antibody treatment was also observed *in vivo* exhibiting increased survival (Figure 30). Likewise, Hao *et al.* revealed a decreased growth of Hodgkin lymphoma and mediastinal large B cell lymphoma with selective inhibition of JAK2 *in vivo* [342]. Here, additional treatment with monoclonal antibodies could further increase the effect of JAK2 inhibition. Supporting the benefit of JAK inhibition and antibody treatment, tofacitinib showed an increased delivery of antibody-based agents to solid tumours and a reduction of tumour-associated inflammatory cells [336]. Moreover, it was reported that inhibition of the JAK/STAT pathway led to CLL cell death unaffected by the protective bone marrow microenvironment suggesting a combination therapy of ibrutinib plus JAK/STAT-inhibitors [318], [337].

Although, complete KO of *JAK2* in a mouse model resulted in embryonic lethality at day 12.5 [343], other mouse models like the EµTCL1 model could be tested for JAK2-inhibitor and alemtuzumab combination therapy.

8.3.2 Increased ADCP with JAK inhibition in macrophages is mediated through macrophage activation and polarisation

In contrast to ibrutinib, JAK inhibition in macrophages using ruxolitinib and tofacitinib increased ADCP by affecting macrophage polarisation. Here, ruxolitinib slightly decreased the number of CD80 positive macrophages and increased the MFI of CD206 (Figure 37). CD80 is a known M1 macrophage polarisation marker [344]. Although many studies showed the importance of CD80 expression on influencing B cell activity, nothing is known about the its role on macrophage activation [345]. CD206 is an M2 associated polarization marker that recognises mannose glycoproteins of pathogens [346]. Therefore increased CD206 expression can lead to increased phagocytosis. Besides cell surface marker expression, macrophages exhibited a decreased expression of IL-10 and increased expression of TNF-α and IL-6 under ruxolitinib treatment (Figure 36). Since, IL-10 was reported to positively influence macrophage phagocytosis, the here observed increase in ADCP could be supported *via* IL-6 production that further upregulates the expression of CD206 [288]. Moreover, the increased production of TNF-α can upregulate the phagocytic activity of macrophages [289].

In general, for macrophage polarisation and cytokine production the JAK/STAT signalling pathway plays a major role. Activation of the JAK/STAT pathway leads to the transcription of either anti- or pro-inflammatory genes influencing macrophage activity and cytokine production [147], [148] (chapter 4.4.1.3). The JAK/STAT signalling cascade *via* IL-6, JAK2, and STAT3 was described to be active in many types of cancer including CLL [317]–[319]. Ruxolitinib as well as tofacitinib seem to inhibit the IL-6/JAK2/STAT3 signalling in macrophages leading to less anti-inflammatory and more pro-inflammatory cytokine production. This effect was also observed by Chen *et al.* demonstrating a reduced anti-inflammatory, M2 polarisation of macrophages under ruxolitinib treatment in a multiple myeloma mouse model [347]. The M2 polarisation was documented *via* increased expression of the M1 markers CD86 and iNOS as well as decreased expression of the M2 markers Arg1 and CD36. Moreover, blocking the M2 phenotype of TAMs *via* JAK2 downstream targets STAT3 and STAT6 using inhibitors like sorafenib, resveratrol, or fenretinide revealed tumour regression and inhibited angiogenesis [290]–[293]. In contrast, studies also reported that deletion of STAT3 or inhibition of the JAK/STAT pathway *via* ruxolitinib in macrophages promotes therapeutic resistance *via* increased expression of the pro-tumorigenic factor cyclooxygenase-2 (COX-2) [348].

8.4 Chemoimmunotherapy resistance of TP53 deficient B cell lymphoma is mediated through secretion of EVs and increased PD-L1 expression

Interestingly, we also observed in other projects of the Prof. Pallasch laboratory that PD-L1 plays an important role on treatment response in lymphoma and leukaemia. Previously, Pallasch et al. reported that chemoimmunotherapy activates macrophage phagocytic capacity through an acute secretory activating phenotype [96]. Afterwards, we demonstrated that the loss of *TP53* prevents the chemoimmunotherapy-induced phagocytic capacity due to increased release of EVs and PD-L1 expression of *shTP53* hMB lymphoma cells [231]. Subsequently, the work of this thesis further validated that the resistant mechanism from *shTP53* lymphoma to chemoimmunotherapy is also mediated by EVs *in vivo* (Figure 38). Furthermore, the *in vivo* experiments demonstrated that the expression of PD-L1 in *shTP53* lymphoma can be suppressed by combining chemoimmunotherapy with PD-1/PD-L1 inhibition leading to prolonged overall survival (Figure 39 and Figure 40).

In general, the loss of TP53 is one of the most important resistant mechanism towards chemoimmunotherapy in B cell malignancies [35], [349]. TP53 plays a major role in the DDR pathway that regulates cell cycle arrest and apoptosis [64], [65]. Therefore, mutations in the *TP53* gene leads to increased proliferation and tumorigenesis. Moreover, others reported that loss of *TP53* influence the innate immune system promoting a pro-tumoral TME [66], [231], [350].

In line with the findings of this thesis, the influence of TP53 on the TME can be conciliated through the release of exosomes that communicate with adjacent cells and cells of the immune system [283], [351]. It was described that cancer cells with a mutation in *TP53* release EVs including the mutated TP53 protein and subsequently convert fibroblasts into CAFs promoting tumour growth [352]. Besides tumour cells, tissue-infiltrating macrophages were also reported to secrete high amounts of EVs after DNA damage [353]. The important role of EVs was already investigated while observing that EVs derived cancer cells support tumour growth by polarising macrophages towards an tumour supportive M2-like phenotype [354], [355]. Likewise, miR-1246-enriched exosomes derived from *TP53* mutated cancer cells were taken up by macrophages leading to an M2 polarisation [356].

Importantly, Chen *et al.* also showed that EVs derived from metastatic melanoma carry the immune checkpoint ligand PD-L1 that subsequently suppress the immune system [357]. Likewise, Haderk *et al.* demonstrated that CLL-derived exosomes modulate PD-L1 expression and cytokine release such as IL-6 on monocytes [358]. Furthermore, PD-L1 was increased in a

murine DLBCL model with lost TP53 causing immune evasion [359]. Subsequently, blocking PD-1 activated immune cells like T cells and improved overall survival of respective mice. Moreover, the upregulation of PD-L1 by lost TP53 and the following immune evasion was also described in other types of cancer such as lung cancer [360]. Monitoring tumours for *TP53* mutations and PD-L1 expression could improve treatment strategies using immune checkpoint inhibitors as already shown in non-small-cell lung cancer [361], [362].

In general, targeting immune checkpoints like PD-1/PD-L1 with antibodies can reprogram the immune system and mediate cancer regression [363]. As observed in this work, one important effect of blocking PD-1/PD-L1 is to activate the phagocytic capacity of TAMs and repress tumour immunity [140]. Moreover, patients with DLBCL and high expression of PD-L1 on macrophages or T cells revealed significantly poorer survival after chemoimmunotherapy [364]. Therefore, in line with the findings of this thesis treatment strategies using anti-PD-L1 antibodies in combination with chemoimmunotherapy should be investigated for patients with a mutation in *TP53* and resulting expression of PD-L1.

Although EVs derived from *JAK2* KO "double hit" lymphoma cells revealed no influence on ADCP (Figure 41), EVs derived from *shTP53* lymphoma with an additional KO in *JAK2* might support ADCP since *JAK2* KO lymphoma showed less PD-L1 expression (Figure 34B). Therefore, the role of JAK2 inhibition on TP53 deficient lymphoma cells and the influence on chemoimmunotherapy resistance should be evaluated. Moreover, it could be tested if NSG mice engrafted with *shTP53* lymphoma cells and additional KO in *JAK2* could overcome the TP53-mediated resistance towards chemoimmunotherapy. In the future, clinical trials could further investigate the combination of JAK2-inhibitors and chemoimmunotherapy in patients with mutated *TP53*.

9   Conclusion and Outlook

In conclusion, the combination of ibrutinib and monoclonal antibody therapy in B cell malignancies synergistically interacted with each other increasing macrophage-mediated ADCP. This increase was independent of the inhibition of BTK. Subsequently, this thesis demonstrates ibrutinib's off-target JAK2 to mediate the increase in ADCP *via* inhibition of the JAK/STAT signalling pathway – to be more precise *via* the inhibition of downstream phosphorylation of STAT3 leading to altered transcription of macrophage phenotype genes [147]. Moreover, JAK2 deficient B cells showed a decreased PD-L1 expression and an altered cytokine release that further contributed to increased ADCP and stimulated anti-tumour responses in the TME.

Besides the macrophage immune response, combination therapy of JAK2 inhibition and monoclonal antibodies should be further investigated on other cells of the TME such as T cells, MDSCs, or CAFs. Here, the role of PD-L1 expression on T cells was already reported influencing neighbouring macrophages and effector T cells in cancer [365]. Therefore, inhibition of the JAK/STAT signalling pathway *via* JAK2 or STAT3 inhibition might play an important role for T cell activation as well. Subsequently, other mechanisms like T cell-mediated cytotoxicity, chemokine, and interleukin release could contribute to therapeutic response of B cell lymphoma. Therefore, future clinical trials should consider combination therapies of JAK/STAT signalling inhibitors such as ruxolitinib with monoclonal antibodies as new potential treatment strategies for B cell malignancies activating macrophage immune response.

The important role of PD-L1 on treatment response in lymphoma and leukaemia was also observed in TP53 mutated lymphoma inducing resistance towards CIT. The work of this thesis demonstrated that the resistance of TP53 mutated lymphoma cells towards CIT is induced *via* the release of extracellular vesicles and PD-L1 expression *in vivo*. Therefore, combining CIT with PD-1/PD-L1 checkpoint inhibitors would investigate treatment responses of lymphoma patients with an additional mutation in *TP53*. Here, clinical trials investigated already the combination of R-CHOP with pembrolizumab in PD-L1 expressing DLBCL tumours showing improved PFS [366]. In general, future clinical trials should include monitoring the expression of immune checkpoints and EVs regarding possible treatment resistances and to improve individual treatment strategies.
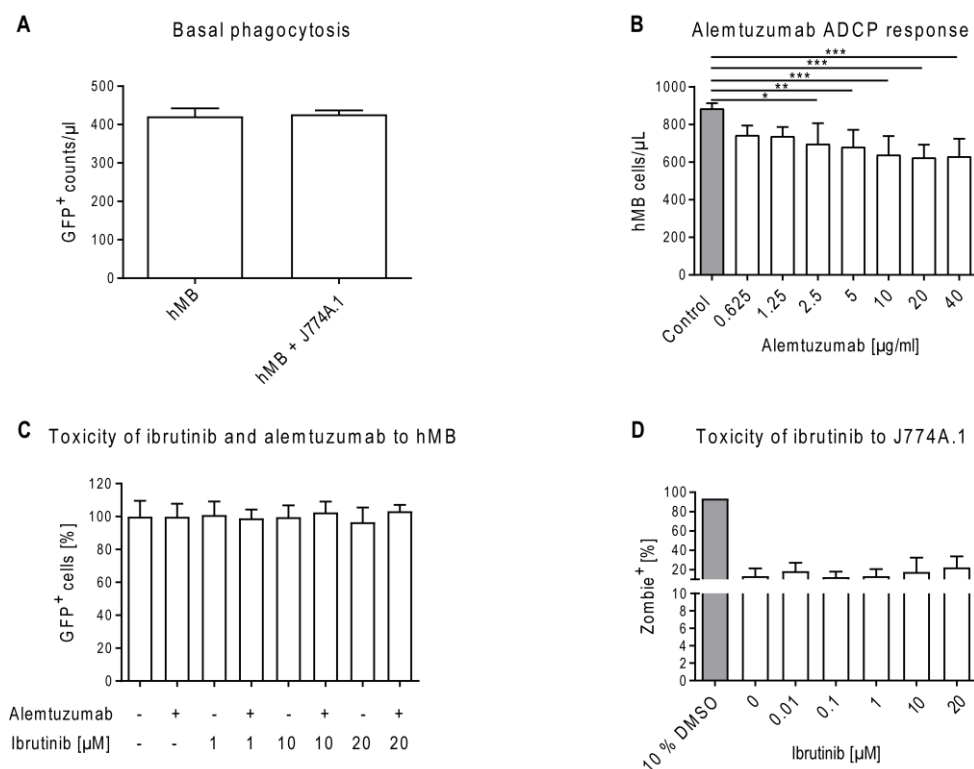
10 Appendix

10.1 Supplementary data

Figure 43 Toxicity of ibrutinib and concentration dependent ADCP response of alemtuzumab.
(**A**) Viability of GFP⁺ hMB "double hit" lymphoma cells co-cultured with J774A.1 macrophages. (**B**) ADCP assay with co-culture of hMB lymphoma cells and J774A.1 macrophages treated with different concentrations of alemtuzumab. (**C**) Viability of GFP⁺ hMB lymphoma cells treated with ibrutinib and alemtuzumab in combination or alone. (**D**) Toxicity staining of ibrutinib treated J774A.1 macrophages with Zombie staining. 10 % DMSO concentration was used as a negative control. All bar graphs display the average and SEM. Data were performed together with L. Müller and S. Henschke. (* $p < 0.05$, ** $p \leq 0.01$ and *** $p \leq 0.001$)
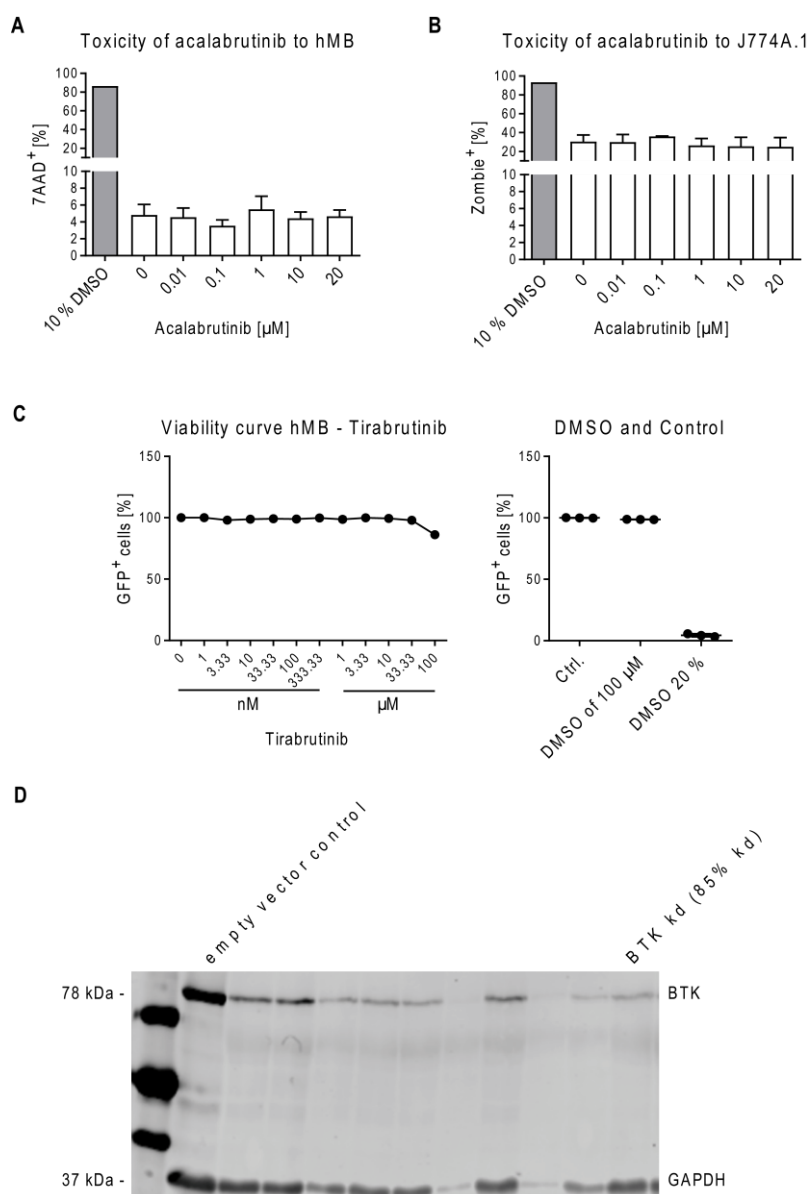
Figure 44 Toxicity of acalabrutinib and western blot of hMB BTK kd.
(**A**) Toxicity staining of acalabrutinib treated hMB "double hit" lymphoma cells with 7AAD. 10 % DMSO concentration was used as a negative control. (**B**) Toxicity staining of acalabrutinib treated J774A.1 macrophages with Zombie staining. 10 % DMSO concentration was used as a negative control. (**C**) Viability curve of GFP+ hMB lymphoma cells treated with Tirabrutinib. Tirabrutinib was diluted in DMSO. Therefore, toxicity of DMSO of 100 µM inhibitor concentration was used as a control. Additionally, 20 % DMSO concentration was used as a negative control. (**D**) Western blot of BTK expression in mCHERRY+-sorted empty vector control versus *BTK* vector infected hMB cells. GAPDH serves as loading control. hMB cells showed a knock down of 85 %. All bar graphs display the average and SEM. Data (A) and (B) were performed by S. Henschke.
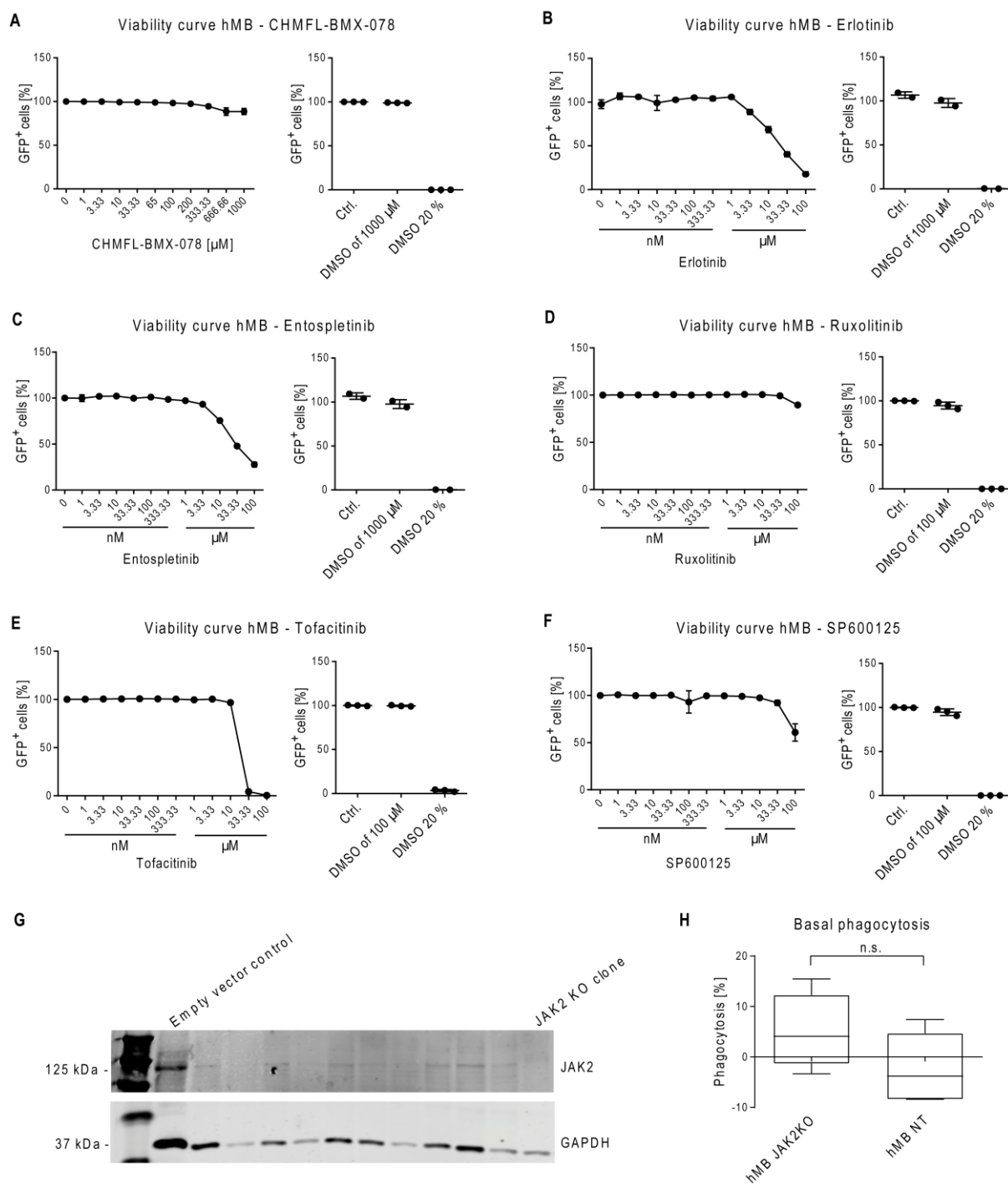
Figure 45 Toxicity of TEC kinase inhibitors and western blot of hMB JAK2 KO.
(A-F) Viability curve of GFP+ hMB "double hit" lymphoma cells treated with (A) CHMFL-BMX-078, (B) erlotinib, (C) entospletinib, (D) ruxolitinib, (E) tofacitinib and (F) SP600125. All inhibitors were diluted in DMSO. Therefore, toxicity of DMSO of 100 µM inhibitor concentration was used as a control. Additionally, 20 % DMSO concentration was used as a negative control. **(G)** Western blot of JAK expression in mCHERRY+-sorted empty vector control versus *JAK2* KO vector infected hMB cells. GAPDH serves as loading control. **(H)** Basal phagocytosis of GFP+ hMB *JAK2* KO and NT cells co-cultured with J774A.1 macrophages. Viability curves show the mean and SEM. Box plots show the median, the 25th and 75th quartiles, and the minimal and maximal value. (n.s.=not significant)

94

10.2 List of abbreviations

7AAD	7-Aminoactinomycin D
ACK	Ammonium-chloride-potassium
ADCC	Antibody-dependent cell-mediated cytotoxicity
ADCP	Antibody-dependent cellular phagocytosis
AKT	Protein kinase B
ALK	Anaplastic lymphoma kinase
ALL	Acute lymphocytic leukaemia
AML	Acute myeloid leukaemia
APC	Allophycocyanin
aPD1	Anti-PD1
APRIL	A proliferation-inducing ligand
Arg1	Arginase 1
BAFF	B cell activating factor
BCL	B cell lymphoma gene
BCM	B cell medium
BCR	B cell receptor
BLK	B lymphocyte kinase
BLNK	B cell linker protein
BMX	Bone marrow kinase on chromosome X
BSA	Bovine serum albumin
BTK	Bruton's tyrosine kinase
BV	Brilliant violet
$CaCl_2$	Calcium Chloride Dihydrate
CAF	Cancer-associated fibroblast
CART	Chimeric antigen receptor T
CCD	Charge coupled device
CD	Cluster of differentiation
CHK2	Checkpoint kinase 2
CLL	Chronic lymphocytic leukaemia
CLL-IPI	CLL International Prognostic Index
CML	Chronic myeloid leukaemia

COX-2	Cyclooxygenase-2
CRISPR	Clustered regularly interspaced short palindromic repeats
CSF-1	Colony stimulating factor 1
CTX	Cyclophosphamide monohydrate
CXCL	C-X-C motif chemokine
DDR	DNA damage response
DLBCL	Diffuse large B cell lymphoma
DMEM	Dulbecco's Modified Eagle Medium
DMSO	Dimethyl sulfoxide
DNA	Deoxyribonucleic acid
ECM	Extracellular matrix
EDTA	Ethylenediaminetetraacetic acid
EGF	Epidermal growth factor
EGFR	Epidermal growth factor receptor
ELISA	Enzyme-linked immunosorbent assay
ERK	Extracellular signal-regulated kinase
EV	Extracellular vesicle
Fab	Antigen-binding fragment
FBS	Fetal bovine serum
Fc	Crystallisable fragment
FcR	Fc receptors
FCR	Fludarabine, cyclophosphamide, and rituximab
FDA	Food and Drug Administration
FGF	Fibroblast growth factor
FITC	Fluorescein isothiocyanate
GAPDH	Glyceraldehyde 3-phosphate dehydrogenase
GFP	Green fluorescent protein
GM-CSF	Granulocyte-macrophage colony-stimulating factor
HBS	HEPES buffered saline
HGBCL	High-grade B cell lymphoma
hMB	Humanised *MYC*/*BCL-2* "double hit" lymphoma
HSC	Haematopoietic stem cell
i.p.	Intra peritoneal

i.v.	Intravenous
IFN	Interferon
IFNAR	Interferon-α/β receptor
IFNGR	Interferon-gamma receptor
IGF	Insulin-like growth factor
IGHV	Ig heavy chain variable region
IL	Interleukin
IL10R	IL-10 receptor
IL4R	IL-4 receptor
IL6R	IL-6 receptor
IMDM	Iscove's Modified Dulbecco's Medium
iNOS	Inducible nitric oxide synthases
ITAM	Immunoreceptor tyrosine-based activation motif
JAK	Janus kinase
JNK	C-Jun N-terminal kinase
kd	Knock down
KO	Knock out
LPS	Lipopolysaccharide
MAPK	Mitogen-activated protein kinase
MDM2	Mouse double minute protein 2
MDSC	Myeloid-derived suppressor cell
MFI	Median fluorescence intensity
MHC	Major histocompatibility complex
M-MDSC	Monocyte-related myeloid-derived suppressor cell
mTOR	Mechanistic target of rapamycin
NFκB	Nuclear factor kappa-light-chain-enhancer of activated B cells
NK cells	Natural killer cells
NO	Nitric oxide
NSG	NOD.Cg-Prkdc^{scid}II2rg^{tm1Wjl}/SzJ
P/S	Penicillin/Streptomycin
PBS	Phosphate buffered saline
PD-1	Programmed cell death protein 1
PD-L1	Programmed cell death ligand 1

PE	Phycoerythrin
PEG	Polyethylenglykol
PFS	Progression free survival
PI3K	Phosphatidylinositol-3-kinase
PIP2	Phosphatidylinositol-4,5-bisphosphate
PIP3	Phosphate-idylinositol-3,4,5-triphosphate
PKC	Protein kinase C
PLCγ2	Phospholipase gamma 2
pRB	Retinoblastoma protein
PTK	Protein tyrosine kinase
PTPN1	Protein tyrosine phosphatase non-receptor type 1
R-CHOP	Rituximab, cyclophosphamide, hydroxydaunorubicin, vincristine, and prednisone
RIPA	Radioimmunoprecipitation assay
RNA	Ribonucleic acid
ROS	Reactive oxygen species
RPMI	Roswell Park Memorial Institute
RT	Room temperature
SD	Standard deviation
SDS	Sodium dodecyl sulphate
SDS-Page	SDS polyacrylamide gel electrophoresis
SIRPα	Signal regulatory protein α
SLL	Small lymphocytic lymphoma
SNARE	N-ethylmaleimide-sensitive-factor attachment receptor
SOCS	Suppressor of cytokine signalling
STAT	Signal transducer and activator of transcription
STK	Serine/threonine kinase
SYK	Spleen tyrosine kinase
TAM	Tumour associated macrophage
TBS	Tris buffered saline
TBS-T	Tris buffered saline with Tween-20
TGF-β	Transforming growth factor-β
T_h cells	T helper cells

TK	Tyrosine kinase
TLR	Toll-like receptor
TME	Tumour microenvironment
TNF-α	Tumour necrose factor-α
T$_{reg}$ cells	Tegulatory T cells
TVA	Tierversuchsantrag
TYK2	Tyrosine kinase 2
VEGF	Vascular endothelial growth factor
ZAP-70	Zeta-chain-associated protein kinase 70

10.3 List of figures

10.4 List of tables

11 References

[1]   J. Ferlay *et al.*, "Estimating the global cancer incidence and mortality in 2018: GLOBOCAN sources and methods," *International Journal of Cancer*, vol. 144, no. 8. Wiley-Liss Inc., pp. 1941–1953, Apr. 15, 2019, doi: 10.1002/ijc.31937.

[2]   D. Hanahan and R. A. Weinberg, "Hallmarks of Cancer: The Next Generation," *Cell*, vol. 144, no. 5, pp. 646–674, Mar. 2011, doi: 10.1016/j.cell.2011.02.013.

[3]   R. A. Weinberg, *The biology of cancer*. Garland science, 2013.

[4]   NCI Dictionary of Cancer Terms, "Definition of leukemia - NCI Dictionary of Cancer Terms - National Cancer Institute." https://www.cancer.gov/publications/dictionaries/cancer-terms/def/leukemia (accessed Jan. 29, 2021).

[5]   NCI Dictionary of Cancer Terms, "Definition of leukocyte - NCI Dictionary of Cancer Terms - National Cancer Institute." https://www.cancer.gov/publications/dictionaries/cancer-terms/def/leukocyte (accessed Jan. 29, 2021).

[6]   H. Greten; T. Greten; Rinninger, *Innere Medizin*. Georg Thieme Verlag, 2010.

[7]   NCI Dictionary of Cancer Terms, "Adult Acute Lymphoblastic Leukemia Treatment (PDQ®)–Patient Version - National Cancer Institute." https://www.cancer.gov/types/leukemia/patient/adult-all-treatment-pdq (accessed Jan. 29, 2021).

[8]   NCI Dictionary of Cancer Terms, "Chronic Myelogenous Leukemia Treatment (PDQ®)–Patient Version - National Cancer Institute." https://www.cancer.gov/types/leukemia/patient/cml-treatment-pdq (accessed Jan. 29, 2021).

[9]   NCI Dictionary of Cancer Terms, "Definition of myeloid - NCI Dictionary of Cancer Terms - National Cancer Institute." https://www.cancer.gov/publications/dictionaries/cancer-terms/def/myeloid (accessed Jan. 29, 2021).

[10]   NCI Dictionary of Cancer Terms, "Definition of lymphocyte - NCI Dictionary of Cancer Terms - National Cancer Institute." https://www.cancer.gov/publications/dictionaries/cancer-terms/search/lymphocyte/?searchMode=Begins (accessed Jan. 29, 2021).

[11]   NCI Dictionary of Cancer Terms, "Lymphoma - NCI Dictionary of Cancer Terms -

National Cancer Institute." https://www.cancer.gov/publications/dictionaries/cancer-terms/search/lymphoma/?searchMode=Begins (accessed Jan. 29, 2021).

[12] R. Küppers and M. L. Hansmann, "The Hodgkin and Reed/Sternberg cell," *International Journal of Biochemistry and Cell Biology*, vol. 37, no. 3. Elsevier Ltd, pp. 511–517, 2005, doi: 10.1016/j.biocel.2003.10.025.

[13] J. O. Armitage, R. D. Gascoyne, M. A. Lunning, and F. Cavalli, "Non-Hodgkin lymphoma," *The Lancet*, vol. 390, no. 10091. Lancet Publishing Group, pp. 298–310, Jul. 15, 2017, doi: 10.1016/S0140-6736(16)32407-2.

[14] M. Hallek, "Chronic lymphocytic leukemia: 2020 update on diagnosis, risk stratification and treatment," *Am. J. Hematol.*, vol. 94, no. 11, pp. 1266–1287, Nov. 2019, doi: 10.1002/ajh.25595.

[15] C. Rozman and E. Montserrat, "Chronic Lymphocytic Leukemia," *N. Engl. J. Med.*, vol. 333, no. 16, pp. 1052–1057, Oct. 1995, doi: 10.1056/NEJM199510193331606.

[16] A. Rosenthal and A. Younes, "High grade B-cell lymphoma with rearrangements of MYC and BCL2 and/or BCL6: Double hit and triple hit lymphomas and double expressing lymphoma," *Blood Rev.*, vol. 31, no. 2, pp. 37–42, Mar. 2017, doi: 10.1016/j.blre.2016.09.004.

[17] V. Phuoc, J. Sandoval-Sus, and J. C. Chavez, "Drug therapy for double-hit lymphoma," *Drugs Context*, vol. 8, pp. 1–13, Dec. 2019, doi: 10.7573/dic.2019-8-1.

[18] S. H. Swerdlow, "Diagnosis of 'double hit' diffuse large B-cell lymphoma and B-cell lymphoma, unclassifiable, with features intermediate between DLBCL and Burkitt lymphoma: When and how, FISH versus IHC," *Hematol. (United States)*, vol. 2014, no. 1, pp. 90–99, Dec. 2014, doi: 10.1182/asheducation-2014.1.90.

[19] S. M. Aukema *et al.*, "Double-hit B-cell lymphomas.," *Blood*, vol. 117, no. 8, pp. 2319–31, Feb. 2011, doi: 10.1182/blood-2010-09-297879.

[20] C. E. Nesbit, J. M. Tersak, and E. V. Prochownik, "MYC oncogenes and human neoplastic disease," *Oncogene*, vol. 18, no. 19, pp. 3004–3016, May 1999, doi: 10.1038/sj.onc.1202746.

[21] N. Meyer and L. Z. Penn, "Reflecting on 25 years with MYC," *Nature Reviews Cancer*, vol. 8, no. 12. Nat Rev Cancer, pp. 976–990, Dec. 2008, doi: 10.1038/nrc2231.

[22] J. E. Krull *et al.*, "Somatic copy number gains in MYC, BCL2, and BCL6 identifies a subset of aggressive alternative-DH/TH DLBCL patients," *Blood Cancer J.*, vol. 10, no. 11, p. 117, Nov. 2020, doi: 10.1038/s41408-020-00382-3.

[23] C. V. Dang, K. A. O'Donnell, K. I. Zeller, T. Nguyen, R. C. Osthus, and F. Li, "The c-

Myc target gene network," *Semin. Cancer Biol.*, vol. 16, no. 4, pp. 253–264, Aug. 2006, doi: 10.1016/j.semcancer.2006.07.014.

[24] A. V. Grinberg, C.-D. Hu, and T. K. Kerppola, "Visualization of Myc/Max/Mad Family Dimers and the Competition for Dimerization in Living Cells," *Mol. Cell. Biol.*, vol. 24, no. 10, pp. 4294–4308, May 2004, doi: 10.1128/MCB.24.10.4294-4308.2004.

[25] D. Hockenbery, G. Nuñez, C. Milliman, R. D. Schreiber, and S. J. Korsmeyer, "Bcl-2 is an inner mitochondrial membrane protein that blocks programmed cell death," *Nature*, vol. 348, no. 6299, pp. 334–336, Nov. 1990, doi: 10.1038/348334a0.

[26] A. Strasser, A. W. Harris, M. L. Bath, and S. Cory, "Novel primitive lymphoid tumours induced in transgenic mice by cooperation between myc and bcl-2," *Nature*, vol. 348, no. 6299, pp. 331–333, Nov. 1990, doi: 10.1038/348331a0.

[27] N. Tomita *et al.*, "Clinicopathological features of lymphoma/leukemia patients carrying both BCL2 and MYC translocations," *Haematol. /*, vol. 94, no. 7, 2009, doi: 10.3324/haematol.2008.005355.

[28] J. W. Friedberg, "How I treat double-hit lymphoma," *Blood*, vol. 130, no. 5, pp. 590–596, Aug. 2017, doi: 10.1182/blood-2017-04-737320.

[29] A. Jemal, R. Siegel, E. Ward, T. Murray, J. Xu, and M. J. Thun, "Cancer Statistics, 2007," *CA. Cancer J. Clin.*, vol. 57, no. 1, pp. 43–66, Jan. 2007, doi: 10.3322/canjclin.57.1.43.

[30] S. Molica, "Sex differences in incidence and outcome of chronic lymphocytic leukemia patients.," *Leuk. Lymphoma*, vol. 47, no. 8, pp. 1477–80, Aug. 2006, doi: 10.1080/10428190600555819.

[31] L. M. Morton, S. S. Wang, S. S. Devesa, P. Hartge, D. D. Weisenburger, and M. S. Linet, "Lymphoma incidence patterns by WHO subtype in the United States, 1992-2001," *Blood*, vol. 107, no. 1, pp. 265–276, Jan. 2006, doi: 10.1182/blood-2005-06-2508.

[32] L. Watson, P. Wyld, and D. Catovsky, "Disease burden of chronic lymphocytic leukaemia within the European Union," *Eur. J. Haematol.*, vol. 81, no. 4, pp. 253–258, Oct. 2008, doi: 10.1111/j.1600-0609.2008.01114.x.

[33] M. Hallek, B. Eichhorst, and D. Catovsky, *Chronic Lymphocytic Leukemia*, First edit. Springer Nature, 2019.

[34] M. Hallek *et al.*, "iwCLL guidelines for diagnosis, indications for treatment, response assessment, and supportive management of CLL," *Blood*, vol. 131, no. 25, pp. 2745–2760, Jun. 2018, doi: 10.1182/blood-2017-09-806398.

[35] H. Döhner *et al.*, "Genomic Aberrations and Survival in Chronic Lymphocytic

Leukemia," *N. Engl. J. Med.*, vol. 343, no. 26, pp. 1910–1916, Dec. 2000, doi: 10.1056/nejm200012283432602.

[36]   H. Döhner *et al.*, "p53 Gene deletion predicts for poor survival and non-response to therapy with purine analogs in chronic B-cell leukemias," *Blood*, vol. 85, no. 6, pp. 1580–1589, Mar. 1995, doi: 10.1182/blood.v85.6.1580.bloodjournal8561580.

[37]   T. Zenz *et al.*, "TP53 mutation profile in chronic lymphocytic leukemia: Evidence for a disease specific profile from a comprehensive analysis of 268 mutations," *Leukemia*, vol. 24, no. 12, pp. 2072–2079, 2010, doi: 10.1038/leu.2010.208.

[38]   D. A. Landau *et al.*, "Mutations driving CLL and their evolution in progression and relapse," *Nature*, vol. 526, no. 7574, pp. 525–530, Oct. 2015, doi: 10.1038/nature15395.

[39]   X. S. Puente *et al.*, "Whole-genome sequencing identifies recurrent mutations in chronic lymphocytic leukaemia," *Nature*, vol. 475, no. 7354, pp. 101–105, Jul. 2011, doi: 10.1038/nature10113.

[40]   X. S. Puente *et al.*, "Non-coding recurrent mutations in chronic lymphocytic leukaemia," *Nature*, vol. 526, no. 7574, pp. 519–524, Oct. 2015, doi: 10.1038/nature14666.

[41]   S. P. Jackson and J. Bartek, "The DNA-damage response in human biology and disease," *Nature*, vol. 461, no. 7267. Nature, pp. 1071–1078, Oct. 22, 2009, doi: 10.1038/nature08467.

[42]   N. Tsukada, J. A. Burger, N. J. Zvaifler, and T. J. Kipps, "Distinctive features of 'nurselike' cells that differentiate in the context of chronic lymphocytic leukemia," *Blood*, vol. 99, no. 3, pp. 1030–1037, Feb. 2002, doi: 10.1182/blood.V99.3.1030.

[43]   J. A. Burger, P. Ghia, A. Rosenwald, and F. Caligaris-Cappio, "The microenvironment in mature B-cell malignancies: A target for new treatment strategies," *Blood*, vol. 114, no. 16. American Society of Hematology, pp. 3367–3375, 2009, doi: 10.1182/blood-2009-06-225326.

[44]   I. M. Pedersen *et al.*, "Protection of CLL B cells by a follicular dendritic cell line is dependent on induction of Mcl-1," *Blood*, vol. 100, no. 5, pp. 1795–1801, Sep. 2002, doi: 10.1182/blood.v100.5.1795.h81702001795_1795_1801.

[45]   N. Chiorazzi, K. R. Rai, and M. Ferrarini, "Chronic lymphocytic leukemia.," *N. Engl. J. Med.*, vol. 352, no. 8, pp. 804–815, Feb. 2005, doi: 10.1056/NEJMra041720.

[46]   M. H. A. van Attekum, E. Eldering, and A. P. Kater, "Chronic lymphocytic leukemia cells are active participants in microenvironmental cross-talk," *Haematologica*, vol. 102, no. 9. Ferrata Storti Foundation, pp. 1469–1476, Aug. 31, 2017, doi: 10.3324/haematol.2016.142679.

[47]   K. L. Owen, N. K. Brockwell, and B. S. Parker, "JAK-STAT Signaling: A Double-Edged Sword of Immune Regulation and Cancer Progression," *Cancers (Basel).*, vol. 11, no. 12, p. 2002, Dec. 2019, doi: 10.3390/cancers11122002.

[48]   C. U. Niemann and A. Wiestner, "B-cell receptor signaling as a driver of lymphoma development and evolution," *Seminars in Cancer Biology*, vol. 23, no. 6 Part A. Academic Press, pp. 410–421, Dec. 01, 2013, doi: 10.1016/j.semcancer.2013.09.001.

[49]   K. R. Rai, A. Sawitsky, E. P. Cronkite, A. D. Chanana, R. N. Levy, and B. S. Pasternack, "Clinical staging of chronic lymphocytic leukemia.," *Blood*, vol. 46, no. 2, pp. 219–234, Aug. 1975.

[50]   J. L. Binet *et al.*, "A new prognostic classification of chronic lymphocytic leukemia derived from a multivariate survival analysis.," *Cancer*, vol. 48, no. 1, pp. 198–206, Jul. 1981, doi: 10.1002/1097-0142(19810701)48:1<198::aid-cncr2820480131>3.0.co;2-v.

[51]   N. Pflug *et al.*, "Development of a comprehensive prognostic index for patients with chronic lymphocytic leukemia," *Blood*, vol. 124, no. 1, pp. 49–62, Jul. 2014, doi: 10.1182/blood-2014-02-556399.

[52]   International CLL-IPI working Group, "An international prognostic index for patients with chronic lymphocytic leukaemia (CLL-IPI): a meta-analysis of individual patient data.," *Lancet. Oncol.*, vol. 17, no. 6, pp. 779–790, Jun. 2016, doi: 10.1016/S1470-2045(16)30029-8.

[53]   K. Kondo *et al.*, "Ibrutinib modulates the immunosuppressive CLL microenvironment through STAT3-mediated suppression of regulatory B-cell function and inhibition of the PD-1/PD-L1 pathway," *Leukemia*, vol. 32, no. 4, pp. 960–970, Apr. 2018, doi: 10.1038/leu.2017.304.

[54]   F. K. Stevenson, S. Krysov, A. J. Davies, A. J. Steele, and G. Packham, "B-cell receptor signaling in chronic lymphocytic leukemia," *Blood*, vol. 118, no. 16, pp. 4313–4320, 2011, doi: 10.1182/blood-2011-06-338855.

[55]   R. E. Davis *et al.*, "Chronic active B-cell-receptor signalling in diffuse large B-cell lymphoma," *Nature*, vol. 463, no. 7277, pp. 88–92, Jan. 2010, doi: 10.1038/nature08638.

[56]   J. A. Burger and A. Wiestner, "Targeting B cell receptor signalling in cancer: preclinical and clinical advances," *Nat. Rev. Cancer*, vol. 18, no. 3, pp. 148–167, Mar. 2018, doi: 10.1038/nrc.2017.121.

[57]   Y. Baba *et al.*, "BLNK mediates Syk-dependent Btk activation," *Proc. Natl. Acad. Sci.*, vol. 98, no. 5, pp. 2582–2586, Feb. 2001, doi: 10.1073/pnas.051626198.

[58]   J. A. Burger and N. Chiorazzi, "B cell receptor signaling in chronic lymphocytic

leukemia," *Trends Immunol.*, vol. 34, no. 12, pp. 592–601, Dec. 2013, doi: 10.1016/j.it.2013.07.002.

[59] T. Zenz, D. Mertens, R. Küppers, H. Döhner, and S. Stilgenbauer, "From pathogenesis to treatment of chronic lymphocytic leukaemia," *Nat. Rev. Cancer*, vol. 10, no. 1, pp. 37–50, Jan. 2010, doi: 10.1038/nrc2764.

[60] R. Rosenquist, D. Cortese, S. Bhoi, L. Mansouri, and R. Gunnarsson, "Prognostic markers and their clinical applicability in chronic lymphocytic leukemia: where do we stand?," *Leuk. Lymphoma*, vol. 54, no. 11, pp. 2351–2364, Nov. 2013, doi: 10.3109/10428194.2013.783913.

[61] L. Z. Rassenti *et al.*, "ZAP-70 Compared with Immunoglobulin Heavy-Chain Gene Mutation Status as a Predictor of Disease Progression in Chronic Lymphocytic Leukemia," *N. Engl. J. Med.*, vol. 351, no. 9, pp. 893–901, Aug. 2004, doi: 10.1056/NEJMoa040857.

[62] L. Chen *et al.*, "Expression of ZAP-70 is associated with increased B-cell receptor signaling in chronic lymphocytic leukemia," *Blood*, vol. 100, no. 13, pp. 4609–4614, Dec. 2002, doi: 10.1182/blood-2002-06-1683.

[63] J. W. Harper and S. J. Elledge, "The DNA Damage Response: Ten Years After," *Mol. Cell*, vol. 28, no. 5, pp. 739–745, Dec. 2007, doi: 10.1016/j.molcel.2007.11.015.

[64] R. Cui *et al.*, "Central Role of p53 in the Suntan Response and Pathologic Hyperpigmentation," *Cell*, vol. 128, no. 5, pp. 853–864, Mar. 2007, doi: 10.1016/j.cell.2006.12.045.

[65] S. Gasser and D. H. Raulet, "The DNA Damage Response Arouses the Immune System: Figure 1.," *Cancer Res.*, vol. 66, no. 8, pp. 3959–3962, Apr. 2006, doi: 10.1158/0008-5472.CAN-05-4603.

[66] W. Xue *et al.*, "Senescence and tumour clearance is triggered by p53 restoration in murine liver carcinomas," *Nature*, vol. 445, no. 7128, pp. 656–660, Feb. 2007, doi: 10.1038/nature05529.

[67] A. Torgovnick and B. Schumacher, "DNA repair mechanisms in cancer development and therapy," *Front. Genet.*, vol. 6, no. APR, p. 157, Apr. 2015, doi: 10.3389/fgene.2015.00157.

[68] T. Riley, E. Sontag, P. Chen, and A. Levine, "Transcriptional control of human p53-regulated genes," *Nat. Rev. Mol. Cell Biol.*, vol. 9, no. 5, pp. 402–412, May 2008, doi: 10.1038/nrm2395.

[69] J. M. Ford, "Regulation of DNA damage recognition and nucleotide excision repair:

Another role for p53," *Mutat. Res. Mol. Mech. Mutagen.*, vol. 577, no. 1–2, pp. 195–202, Sep. 2005, doi: 10.1016/j.mrfmmm.2005.04.005.

[70] M. H. G. Kubbutat, S. N. Jones, and K. H. Vousden, "Regulation of p53 stability by Mdm2," *Nature*, vol. 387, no. 6630, pp. 299–303, May 1997, doi: 10.1038/387299a0.

[71] S. W. Lowe, E. Cepero, and G. Evan, "Intrinsic tumour suppression," *Nature*, vol. 432, no. 7015, pp. 307–315, Nov. 2004, doi: 10.1038/nature03098.

[72] D. W. Scott and R. D. Gascoyne, "The tumour microenvironment in B cell lymphomas," *Nature Reviews Cancer*, vol. 14, no. 8. Nature Publishing Group, pp. 517–534, Aug. 10, 2014, doi: 10.1038/nrc3774.

[73] D. Hanahan and L. M. Coussens, "Accessories to the Crime: Functions of Cells Recruited to the Tumor Microenvironment," *Cancer Cell*, vol. 21, no. 3. Cancer Cell, pp. 309–322, Mar. 20, 2012, doi: 10.1016/j.ccr.2012.02.022.

[74] D. F. Quail and J. A. Joyce, "Microenvironmental regulation of tumor progression and metastasis," *Nature Medicine*, vol. 19, no. 11. Nature Publishing Group, pp. 1423–1437, Nov. 07, 2013, doi: 10.1038/nm.3394.

[75] A. Armulik, A. Abramsson, and C. Betsholtz, "Endothelial/pericyte interactions," *Circulation Research*, vol. 97, no. 6. Circ Res, pp. 512–523, Sep. 16, 2005, doi: 10.1161/01.RES.0000182903.16652.d7.

[76] A. Alitalo and M. Detmar, "Interaction of tumor cells and lymphatic vessels in cancer progression," *Oncogene*, vol. 31, no. 42. Oncogene, pp. 4499–4508, Oct. 18, 2012, doi: 10.1038/onc.2011.602.

[77] W. Zhu *et al.*, "Mesenchymal stem cells derived from bone marrow favor tumor cell growth in vivo," *Exp. Mol. Pathol.*, vol. 80, no. 3, pp. 267–274, Jun. 2006, doi: 10.1016/j.yexmp.2005.07.004.

[78] S. F. Schoppmann *et al.*, "Tumor-associated macrophages express lymphatic endothelial growth factors and are related to peritumoral lymphangiogenesis," *Am. J. Pathol.*, vol. 161, no. 3, pp. 947–956, 2002, doi: 10.1016/S0002-9440(10)64255-1.

[79] A. F. Olumi, G. D. Grossfeld, S. W. Hayward, P. R. Carroll, T. D. Tlsty, and G. R. Cunha, "Carcinoma-associated Fibroblasts Direct Tumor Progression of Initiated Human Prostatic Epithelium," *Cancer Res.*, vol. 59, no. 19, pp. 5002 LP – 5011, Oct. 1999, [Online]. Available: http://cancerres.aacrjournals.org/content/59/19/5002.abstract.

[80] R. Kalluri and M. Zeisberg, "Fibroblasts in cancer," *Nature Reviews Cancer*, vol. 6, no. 5. Nat Rev Cancer, pp. 392–401, May 2006, doi: 10.1038/nrc1877.

[81] T. Marsh, K. Pietras, and S. S. McAllister, "Fibroblasts as architects of cancer pathogenesis," *Biochimica et Biophysica Acta - Molecular Basis of Disease*, vol. 1832, no. 7. Elsevier, pp. 1070–1078, 2013, doi: 10.1016/j.bbadis.2012.10.013.

[82] D. Fukumura *et al.*, "Tumor induction of VEGF promoter activity in stromal cells," *Cell*, vol. 94, no. 6, pp. 715–725, Sep. 1998, doi: 10.1016/S0092-8674(00)81731-6.

[83] Y. I. Rattigan *et al.*, "Lactate is a mediator of metabolic cooperation between stromal carcinoma associated fibroblasts and glycolytic tumor cells in the tumor microenvironment," *Exp. Cell Res.*, vol. 318, no. 4, pp. 326–335, Feb. 2012, doi: 10.1016/j.yexcr.2011.11.014.

[84] D. Lindau, P. Gielen, M. Kroesen, P. Wesseling, and G. J. Adema, "The immunosuppressive tumour network: Myeloid-derived suppressor cells, regulatory T cells and natural killer T cells," *Immunology*, vol. 138, no. 2. Immunology, pp. 105–115, Feb. 2013, doi: 10.1111/imm.12036.

[85] E. Y. Lin *et al.*, "Vascular endothelial growth factor restores delayed tumor progression in tumors depleted of macrophages," *Mol. Oncol.*, vol. 1, no. 3, pp. 288–302, 2007, doi: 10.1016/j.molonc.2007.10.003.

[86] F. Balkwill, K. A. Charles, and A. Mantovani, "Smoldering and polarized inflammation in the initiation and promotion of malignant disease," *Cancer Cell*, vol. 7, no. 3. Cell Press, pp. 211–217, 2005, doi: 10.1016/j.ccr.2005.02.013.

[87] Q. Chen, X. H. F. Zhang, and J. Massagué, "Macrophage Binding to Receptor VCAM-1 Transmits Survival Signals in Breast Cancer Cells that Invade the Lungs," *Cancer Cell*, vol. 20, no. 4, pp. 538–549, Oct. 2011, doi: 10.1016/j.ccr.2011.08.025.

[88] P. Lu, K. Takai, V. M. Weaver, and Z. Werb, "Extracellular Matrix degradation and remodeling in development and disease," *Cold Spring Harb. Perspect. Biol.*, vol. 3, no. 12, Dec. 2011, doi: 10.1101/cshperspect.a005058.

[89] G. Giannelli, J. Falk-Marzillier, O. Schiraldi, W. G. Stetler-Stevenson, and V. Quaranta, "Induction of cell migration by matrix metalloprotease-2 cleavage of laminin-5," *Science (80-.).*, vol. 277, no. 5323, pp. 225–228, Jul. 1997, doi: 10.1126/science.277.5323.225.

[90] J. E. Talmadge and D. I. Gabrilovich, "History of myeloid-derived suppressor cells," *Nature Reviews Cancer*, vol. 13, no. 10. Nat Rev Cancer, pp. 739–752, Oct. 2013, doi: 10.1038/nrc3581.

[91] G. T. Motz and G. Coukos, "Deciphering and Reversing Tumor Immune Suppression," *Immunity*, vol. 39, no. 1. Immunity, pp. 61–73, Jul. 25, 2013, doi: 10.1016/j.immuni.2013.07.005.

[92] S. A. Riemersma *et al.*, "Extensive genetic alterations of the HLA region, including homozygous deletions of HLA class II genes in B-cell lymphomas arising in immune-privileged sites.," *Blood*, vol. 96, no. 10, pp. 3569–3577, Nov. 2000.

[93] Z.-Z. Yang, A. J. Novak, S. C. Ziesmer, T. E. Witzig, and S. M. Ansell, "Malignant B Cells Skew the Balance of Regulatory T Cells and TH17 Cells in B-Cell Non-Hodgkin{\textquoteright}s Lymphoma," *Cancer Res.*, vol. 69, no. 13, pp. 5522–5530, 2009, doi: 10.1158/0008-5472.CAN-09-0266.

[94] L. Bento *et al.*, "New prognosis score including absolute lymphocyte/monocyte ratio, red blood cell distribution width and beta-2 microglobulin in patients with diffuse large B-cell lymphoma treated with R-CHOP: Spanish Lymphoma Group Experience (GELTAMO)," *Br. J. Haematol.*, vol. 188, no. 6, pp. 888–897, Mar. 2020, doi: 10.1111/bjh.16263.

[95] Y. Herishanu *et al.*, "Absolute Monocyte Count Trichotomizes Chronic Lymphocytic Leukemia Into High Risk Patients With Immune Dysregulation, Disease Progression and Poor Survival," *Blood*, vol. 122, no. 21, pp. 4724–4724, Nov. 2013, doi: 10.1182/blood.V122.21.4724.4724.

[96] C. P. Pallasch *et al.*, "Sensitizing protective tumor microenvironments to antibody-mediated therapy," *Cell*, vol. 156, no. 3, pp. 590–602, Jan. 2014, doi: 10.1016/j.cell.2013.12.041.

[97] Y. Lavin, A. Mortha, A. Rahman, and M. Merad, "Regulation of macrophage development and function in peripheral tissues," *Nature Reviews Immunology*, vol. 15, no. 12. pp. 731–744, 2015, doi: 10.1038/nri3920.

[98] Kenneth Murphy; Casey Weaver, *Janeway Immunologie*, 9.Auflage. Springer Spektrum, 2018.

[99] Y. Lavin *et al.*, "Tissue-resident macrophage enhancer landscapes are shaped by the local microenvironment," *Cell*, vol. 159, no. 6, pp. 1312–1326, Dec. 2014, doi: 10.1016/j.cell.2014.11.018.

[100] S. Gordon and P. R. Taylor, "Monocyte and macrophage heterogeneity," *Nature Reviews Immunology*, vol. 5, no. 12. Nature Publishing Group, pp. 953–964, Dec. 2005, doi: 10.1038/nri1733.

[101] H. Borges Da Silva, R. Fonseca, R. M. Pereira, A. A. Cassado, J. M. Álvarez, and M. R. D'Império Lima, "Splenic macrophage subsets and their function during blood-borne infections," *Frontiers in Immunology*, vol. 6, no. SEP. Frontiers Media S.A., p. 480, Sep. 22, 2015, doi: 10.3389/fimmu.2015.00480.

[102] S. Gordon and L. Martinez-Pomares, "Physiological roles of macrophages," *Pflugers Archiv European Journal of Physiology*, vol. 469, no. 3–4. Springer Verlag, pp. 365–374, Apr. 01, 2017, doi: 10.1007/s00424-017-1945-7.

[103] T. Ganz, "Macrophages and systemic iron homeostasis," *Journal of Innate Immunity*, vol. 4, no. 5–6. J Innate Immun, pp. 446–453, Aug. 2012, doi: 10.1159/000336423.

[104] M. Casanova-Acebes *et al.*, "Rhythmic modulation of the hematopoietic niche through neutrophil clearance," *Cell*, vol. 153, no. 5, p. 1025, May 2013, doi: 10.1016/j.cell.2013.04.040.

[105] A. Chow *et al.*, "Bone marrow CD169+ macrophages promote the retention of hematopoietic stem and progenitor cells in the mesenchymal stem cell niche," *J. Exp. Med.*, vol. 208, no. 2, pp. 761–771, Feb. 2011, doi: 10.1084/jem.20101688.

[106] F. O. Martinez and S. Gordon, "The M1 and M2 paradigm of macrophage activation: Time for reassessment," *F1000Prime Rep.*, vol. 6, 2014, doi: 10.12703/P6-13.

[107] N. Wang, H. Liang, and K. Zen, "Molecular mechanisms that influence the macrophage M1-M2 polarization balance," *Frontiers in Immunology*, vol. 5, no. NOV. Frontiers Media S.A., p. 614, Nov. 28, 2014, doi: 10.3389/fimmu.2014.00614.

[108] J. Rojas *et al.*, "Macrophage Heterogeneity and Plasticity: Impact of Macrophage Biomarkers on Atherosclerosis," *Scientifica (Cairo).*, vol. 2015, pp. 1–17, 2015, doi: 10.1155/2015/851252.

[109] A. Sica and A. Mantovani, "Macrophage plasticity and polarization: In vivo veritas," *Journal of Clinical Investigation*, vol. 122, no. 3. American Society for Clinical Investigation, pp. 787–795, Mar. 01, 2012, doi: 10.1172/JCI59643.

[110] P. J. Murray, "Macrophage Polarization," *Annu. Rev. Physiol.*, vol. 79, no. 1, pp. 541–566, Feb. 2017, doi: 10.1146/annurev-physiol-022516-034339.

[111] F. O. Martinez *et al.*, "Genetic programs expressed in resting and IL-4 alternatively activated mouse and human macrophages: similarities and differences," *Blood*, vol. 121, no. 9, pp. e57–e69, Feb. 2013, doi: 10.1182/blood-2012-06-436212.

[112] F. A. W. Verreck *et al.*, "Human IL-23-producing type 1 macrophages promote but IL-10-producing type 2 macrophages subvert immunity to (myco)bacteria," *Proc. Natl. Acad. Sci.*, vol. 101, no. 13, pp. 4560–4565, Mar. 2004, doi: 10.1073/pnas.0400983101.

[113] K. Laing, "Chemokines," *Dev. Comp. Immunol.*, vol. 28, no. 5, pp. 443–460, May 2004, doi: 10.1016/j.dci.2003.09.006.

[114] C. Nathan and M. Sporn, "Cytokines in context.," *J. Cell Biol.*, vol. 113, no. 5, pp. 981–986, Jun. 1991, doi: 10.1083/jcb.113.5.981.

[115] D. M. Mosser, "The many faces of macrophage activation," *J. Leukoc. Biol.*, vol. 73, no. 2, pp. 209–212, Feb. 2003, doi: 10.1189/jlb.0602325.

[116] Bio Rad, "Macrophage Polarization - Mini-review | Bio-Rad." https://www.bio-rad-antibodies.com/macrophage-polarization-minireview.html (accessed Feb. 07, 2021).

[117] C. E. Lewis and J. W. Pollard, "Distinct Role of Macrophages in Different Tumor Microenvironments," *Cancer Res.*, vol. 66, no. 2, pp. 605–612, Jan. 2006, doi: 10.1158/0008-5472.CAN-05-4005.

[118] J. Cook and T. Hagemann, "Tumour-associated macrophages and cancer," *Current Opinion in Pharmacology*, vol. 13, no. 4. Elsevier Ltd, pp. 595–601, Aug. 01, 2013, doi: 10.1016/j.coph.2013.05.017.

[119] A. Mantovani, S. Sozzani, M. Locati, P. Allavena, and A. Sica, "Macrophage polarization: Tumor-associated macrophages as a paradigm for polarized M2 mononuclear phagocytes," *Trends in Immunology*, vol. 23, no. 11. pp. 549–555, Nov. 01, 2002, doi: 10.1016/S1471-4906(02)02302-5.

[120] A. Sica, T. Schioppa, A. Mantovani, and P. Allavena, "Tumour-associated macrophages are a distinct M2 polarised population promoting tumour progression: Potential targets of anti-cancer therapy," *Eur. J. Cancer*, vol. 42, no. 6, pp. 717–727, Apr. 2006, doi: 10.1016/j.ejca.2006.01.003.

[121] A. Mantovani, F. Marchesi, A. Malesci, L. Laghi, and P. Allavena, "Tumour-associated macrophages as treatment targets in oncology," *Nature Reviews Clinical Oncology*, vol. 14, no. 7. Nature Publishing Group, pp. 399–416, Jul. 24, 2017, doi: 10.1038/nrclinonc.2016.217.

[122] A. Mantovani, P. Allavena, A. Sica, and F. Balkwill, "Cancer-related inflammation," *Nature*, vol. 454, no. 7203. Nature Publishing Group, pp. 436–444, Jul. 01, 2008, doi: 10.1038/nature07205.

[123] F. van Dalen, M. van Stevendaal, F. Fennemann, M. Verdoes, and O. Ilina, "Molecular Repolarisation of Tumour-Associated Macrophages," *Molecules*, vol. 24, no. 1, p. 9, Dec. 2018, doi: 10.3390/molecules24010009.

[124] A. Mantovani and P. Allavena, "The interaction of anticancer therapies with tumor-associated macrophages," *J. Exp. Med.*, vol. 212, no. 4, pp. 435–445, Apr. 2015, doi: 10.1084/jem.20150295.

[125] L. Bingle, N. J. Brown, and C. E. Lewis, "The role of tumour-associated macrophages in tumour progression: implications for new anticancer therapies," *J. Pathol.*, vol. 196, no. 3, pp. 254–265, Mar. 2002, doi: 10.1002/path.1027.

[126] T. C. Stephens, G. A. Currie, and J. H. Peacock, "Repopulation of γ-irradiated Lewis lung carcinoma by malignant cells and host macrophage progenitors," *Br. J. Cancer*, vol. 38, no. 5, pp. 573–582, Nov. 1978, doi: 10.1038/bjc.1978.252.

[127] W. H. McBride, "Phenotype and functions of intratumoral macrophages," *Biochim. Biophys. Acta - Rev. Cancer*, vol. 865, no. 1, pp. 27–41, Aug. 1986, doi: 10.1016/0304-419X(86)90011-9.

[128] I. Conti and B. J. Rollins, "CCL2 (monocyte chemoattractant protein-1) and cancer," *Semin. Cancer Biol.*, vol. 14, no. 3, pp. 149–154, Jun. 2004, doi: 10.1016/j.semcancer.2003.10.009.

[129] E. Y. Lin, A. V. Nguyen, R. G. Russell, and J. W. Pollard, "Colony-Stimulating Factor 1 Promotes Progression of Mammary Tumors to Malignancy," *J. Exp. Med.*, vol. 193, no. 6, pp. 727–740, Mar. 2001, doi: 10.1084/jem.193.6.727.

[130] B. Ruffell, N. I. Affara, and L. M. Coussens, "Differential macrophage programming in the tumor microenvironment," *Trends Immunol.*, vol. 33, no. 3, pp. 119–126, Mar. 2012, doi: 10.1016/j.it.2011.12.001.

[131] B. Pang *et al.*, "Lipid peroxidation dominates the chemistry of DNA adduct formation in a mouse model of inflammation," *Carcinogenesis*, vol. 28, no. 8, pp. 1807–1813, Aug. 2007, doi: 10.1093/carcin/bgm037.

[132] S. K. Biswas, A. Sica, and C. E. Lewis, "Plasticity of Macrophage Function during Tumor Progression: Regulation by Distinct Molecular Mechanisms," *J. Immunol.*, vol. 180, no. 4, pp. 2011–2017, Feb. 2008, doi: 10.4049/jimmunol.180.4.2011.

[133] A. Mantovani, B. Bottazzi, F. Colotta, S. Sozzani, and L. Ruco, "The origin and function of tumor-associated macrophages," *Immunol. Today*, vol. 13, no. 7, pp. 265–270, Jan. 1992, doi: 10.1016/0167-5699(92)90008-U.

[134] D. Brown, J. Trowsdale, and R. Allen, "The LILR family: modulators of innate and adaptive immune pathways in health and disease," *Tissue Antigens*, vol. 64, no. 3, pp. 215–225, Sep. 2004, doi: 10.1111/j.0001-2815.2004.00290.x.

[135] P. Allavena and A. Mantovani, "Immunology in the clinic review series; focus on cancer: tumour-associated macrophages: undisputed stars of the inflammatory tumour microenvironment," *Clin. Exp. Immunol.*, vol. 167, no. 2, pp. 195–205, Feb. 2012, doi: 10.1111/j.1365-2249.2011.04515.x.

[136] D. Tugal, X. Liao, and M. K. Jain, "Transcriptional Control of Macrophage Polarization," *Arterioscler. Thromb. Vasc. Biol.*, vol. 33, no. 6, pp. 1135–1144, Jun. 2013, doi: 10.1161/ATVBAHA.113.301453.

[137] B. K. Halak, H. C. Maguire, and E. C. Lattime, "Tumor-induced Interleukin-10 Inhibits Type 1 Immune Responses Directed at a Tumor Antigen As Well As a Non-Tumor Antigen Present at the Tumor Site," *Cancer Res.*, vol. 59, no. 4, pp. 911 LP – 917, Feb. 1999, [Online]. Available: http://cancerres.aacrjournals.org/content/59/4/911.abstract.

[138] T. J. Curiel *et al.*, "Specific recruitment of regulatory T cells in ovarian carcinoma fosters immune privilege and predicts reduced survival," *Nat. Med.*, vol. 10, no. 9, pp. 942–949, Sep. 2004, doi: 10.1038/nm1093.

[139] C.-W. Li, Y.-J. Lai, J. L. Hsu, and M.-C. Hung, "Activation of phagocytosis by immune checkpoint blockade," *Front. Med.*, vol. 12, no. 4, pp. 473–480, Aug. 2018, doi: 10.1007/s11684-018-0657-5.

[140] S. R. Gordon *et al.*, "PD-1 expression by tumour-associated macrophages inhibits phagocytosis and tumour immunity," *Nature*, vol. 545, no. 7655, pp. 495–499, May 2017, doi: 10.1038/nature22396.

[141] T. E. Peterson *et al.*, "Dual inhibition of Ang-2 and VEGF receptors normalizes tumor vasculature and prolongs survival in glioblastoma by altering macrophages," *Proc. Natl. Acad. Sci.*, vol. 113, no. 16, pp. 4470–4475, Apr. 2016, doi: 10.1073/pnas.1525349113.

[142] J. Kloepper *et al.*, "Ang-2/VEGF bispecific antibody reprograms macrophages and resident microglia to anti-tumor phenotype and prolongs glioblastoma survival," *Proc. Natl. Acad. Sci.*, vol. 113, no. 16, pp. 4476–4481, Apr. 2016, doi: 10.1073/pnas.1525360113.

[143] Y. Murata, T. Kotani, H. Ohnishi, and T. Matozaki, "The CD47-SIRP signalling system: its physiological roles and therapeutic application," *J. Biochem.*, vol. 155, no. 6, pp. 335–344, Jun. 2014, doi: 10.1093/jb/mvu017.

[144] M. P. Chao *et al.*, "Anti-CD47 Antibody Synergizes with Rituximab to Promote Phagocytosis and Eradicate Non-Hodgkin Lymphoma," *Cell*, vol. 142, no. 5, pp. 699–713, Sep. 2010, doi: 10.1016/j.cell.2010.07.044.

[145] R. Majeti *et al.*, "CD47 Is an Adverse Prognostic Factor and Therapeutic Antibody Target on Human Acute Myeloid Leukemia Stem Cells," *Cell*, vol. 138, no. 2, pp. 286–299, Jul. 2009, doi: 10.1016/j.cell.2009.05.045.

[146] M. J. Glennie, R. R. French, M. S. Cragg, and R. P. Taylor, "Mechanisms of killing by anti-CD20 monoclonal antibodies," *Mol. Immunol.*, vol. 44, no. 16, pp. 3823–3837, Sep. 2007, doi: 10.1016/j.molimm.2007.06.151.

[147] I. Malyshev and Y. Malyshev, "Current Concept and Update of the Macrophage Plasticity Concept: Intracellular Mechanisms of Reprogramming and M3 Macrophage

'Switch' Phenotype," *Biomed Res. Int.*, vol. 2015, pp. 1–22, 2015, doi: 10.1155/2015/341308.

[148] D. Zhou *et al.*, "Macrophage polarization and function with emphasis on the evolving roles of coordinated regulation of cellular signaling pathways," *Cell. Signal.*, vol. 26, no. 2, pp. 192–197, Feb. 2014, doi: 10.1016/j.cellsig.2013.11.004.

[149] P. J. Murray, "The JAK-STAT Signaling Pathway: Input and Output Integration," *J. Immunol.*, vol. 178, no. 5, pp. 2623–2629, Mar. 2007, doi: 10.4049/jimmunol.178.5.2623.

[150] C. F. Nathan, H. W. Murray, M. E. Wiebe, and B. Y. Rubin, "Identification of interferon-gamma as the lymphokine that activates human macrophage oxidative metabolism and antimicrobial activity.," *J. Exp. Med.*, vol. 158, no. 3, pp. 670–689, Sep. 1983, doi: 10.1084/jem.158.3.670.

[151] C. Park, S. Li, E. Cha, and C. Schindler, "Immune Response in Stat2 Knockout Mice," *Immunity*, vol. 13, no. 6, pp. 795–804, Dec. 2000, doi: 10.1016/S1074-7613(00)00077-7.

[152] K. Shuai *et al.*, "Polypeptide signalling to the nucleus through tyrosine phosphorylation of Jak and Stat proteins."

[153] S. V. Kotenko *et al.*, "Interaction between the Components of the Interferon γ Receptor Complex," *J. Biol. Chem.*, vol. 270, no. 36, pp. 20915–20921, Sep. 1995, doi: 10.1074/jbc.270.36.20915.

[154] L. B. Ivashkiv and L. T. Donlin, "Regulation of type I interferon responses," *Nat. Rev. Immunol.*, vol. 14, no. 1, pp. 36–49, Jan. 2014, doi: 10.1038/nri3581.

[155] J. K. Riley, K. Takeda, S. Akira, and R. D. Schreiber, "Interleukin-10 receptor signaling through the JAK-STAT pathway. Requirement for two distinct receptor-derived signals for anti-inflammatory action," *J. Biol. Chem.*, vol. 274, no. 23, pp. 16513–16521, Jun. 1999, doi: 10.1074/jbc.274.23.16513.

[156] K. Takeda *et al.*, "Essential role of Stat6 in IL-4 signalling," *Nature*, vol. 380, no. 6575, pp. 627–630, Apr. 1996, doi: 10.1038/380627a0.

[157] T. Lawrence and G. Natoli, "Transcriptional regulation of macrophage polarization: Enabling diversity with identity," *Nature Reviews Immunology*, vol. 11, no. 11. Nature Publishing Group, pp. 750–761, Nov. 25, 2011, doi: 10.1038/nri3088.

[158] A. Bhattacharjee, M. Shukla, V. P. Yakubenko, A. Mulya, S. Kundu, and M. K. Cathcart, "IL-4 and IL-13 employ discrete signaling pathways for target gene expression in alternatively activated monocytes/macrophages," *Free Radic. Biol. Med.*, vol. 54, pp. 1–

16, Jan. 2013, doi: 10.1016/j.freeradbiomed.2012.10.553.

[159] P. C. HEINRICH, I. BEHRMANN, G. MÜLLER-NEWEN, F. SCHAPER, and L. GRAEVE, "Interleukin-6-type cytokine signalling through the gp130/Jak/STAT pathway1," *Biochem. J.*, vol. 334, no. 2, pp. 297–314, Sep. 1998, doi: 10.1042/bj3340297.

[160] N. Stahl *et al.*, "Association and activation of Jak-Tyk kinases by CNTF-LIF-OSM-IL-6 beta receptor components," *Science (80-.).*, vol. 263, no. 5143, pp. 92–95, Jan. 1994, doi: 10.1126/science.8272873.

[161] T. Hirano, K. Ishihara, and M. Hibi, "Roles of STAT3 in mediating the cell growth, differentiation and survival signals relayed through the IL-6 family of cytokine receptors," *Oncogene*, vol. 19, no. 21, pp. 2548–2556, May 2000, doi: 10.1038/sj.onc.1203551.

[162] B. A. Croker, H. Kiu, and S. E. Nicholson, "SOCS regulation of the JAK/STAT signalling pathway," *Seminars in Cell and Developmental Biology*, vol. 19, no. 4. Elsevier Ltd, pp. 414–422, Aug. 01, 2008, doi: 10.1016/j.semcdb.2008.07.010.

[163] Y. Shi *et al.*, "Trastuzumab Triggers Phagocytic Killing of High HER2 Cancer Cells In Vitro and In Vivo by Interaction with Fcγ Receptors on Macrophages," *J. Immunol.*, vol. 194, no. 9, pp. 4379–4386, May 2015, doi: 10.4049/jimmunol.1402891.

[164] M. B. Overdijk *et al.*, "Antibody-mediated phagocytosis contributes to the anti-tumor activity of the therapeutic antibody daratumumab in lymphoma and multiple myeloma," *MAbs*, vol. 7, no. 2, pp. 311–320, Mar. 2015, doi: 10.1080/19420862.2015.1007813.

[165] L. Kamen *et al.*, "A novel method for determining antibody-dependent cellular phagocytosis," *J. Immunol. Methods*, vol. 468, pp. 55–60, May 2019, doi: 10.1016/j.jim.2019.03.001.

[166] F. Nimmerjahn, S. Gordan, and A. Lux, "FcγR dependent mechanisms of cytotoxic, agonistic, and neutralizing antibody activities," *Trends Immunol.*, vol. 36, no. 6, pp. 325–336, Jun. 2015, doi: 10.1016/j.it.2015.04.005.

[167] N. Gül and M. van Egmond, "Antibody-Dependent Phagocytosis of Tumor Cells by Macrophages: A Potent Effector Mechanism of Monoclonal Antibody Therapy of Cancer," *Cancer Res.*, vol. 75, no. 23, pp. 5008–5013, Dec. 2015, doi: 10.1158/0008-5472.CAN-15-1330.

[168] K. Weiskopf and I. L. Weissman, "Macrophages are critical effectors of antibody therapies for cancer," *mAbs*, vol. 7, no. 2. Landes Bioscience, pp. 303–310, Mar. 13, 2015, doi: 10.1080/19420862.2015.1011450.

[169] N. Isakov, "Immunoreceptor tyrosine-based activation motif (ITAM), a unique module linking antigen and Fc receptors to their signaling cascades," *Journal of Leukocyte Biology*, vol. 61, no. 1. Federation of American Societies for Experimental Biology, pp. 6–16, 1997, doi: 10.1002/jlb.61.1.6.

[170] E. García-García and C. Rosales, "Signal transduction during Fc receptor-mediated phagocytosis.," *J. Leukoc. Biol.*, vol. 72, no. 6, pp. 1092–108, Dec. 2002, doi: 10.1189/jlb.72.6.1092.

[171] Z. Korade-Mirnics and S. J. Corey, "Src kinase-mediated signaling in leukocytes.," *J. Leukoc. Biol.*, vol. 68, no. 5, pp. 603–13, Nov. 2000, doi: 10.1189/jlb.68.5.603.

[172] M. Majeed, E. Caveggion, C. A. Lowell, and G. Berton, "Role of Src kinases and Syk in Fcgamma receptor-mediated phagocytosis and phagosome-lysosome fusion.," *J. Leukoc. Biol.*, vol. 70, no. 5, pp. 801–811, Nov. 2001.

[173] J. A. McNew *et al.*, "Compartmental specificity of cellular membrane fusion encoded in SNARE proteins," *Nature*, vol. 407, no. 6801, pp. 153–159, Sep. 2000, doi: 10.1038/35025000.

[174] T. E. Tjelle, T. Løvdal, and T. Berg, "Phagosome dynamics and function," *BioEssays*, vol. 22, no. 3, pp. 255–263, Feb. 2000, doi: 10.1002/(SICI)1521-1878(200003)22:3<255::AID-BIES7>3.0.CO;2-R.

[175] E. Cocucci and J. Meldolesi, "Ectosomes and exosomes: shedding the confusion between extracellular vesicles," *Trends Cell Biol.*, vol. 25, no. 6, pp. 364–372, Jun. 2015, doi: 10.1016/j.tcb.2015.01.004.

[176] F. Haderk *et al.*, "Extracellular vesicles in chronic lymphocytic leukemia," *Leuk. Lymphoma*, vol. 54, no. 8, pp. 1826–1830, Aug. 2013, doi: 10.3109/10428194.2013.796052.

[177] P. Subedi *et al.*, "Comparison of methods to isolate proteins from extracellular vesicles for mass spectrometry-based proteomic analyses," *Anal. Biochem.*, vol. 584, p. 113390, Nov. 2019, doi: 10.1016/j.ab.2019.113390.

[178] E. Gargiulo, P. E. Morande, A. Largeot, E. Moussay, and J. Paggetti, "Diagnostic and Therapeutic Potential of Extracellular Vesicles in B-Cell Malignancies," *Front. Oncol.*, vol. 10, Sep. 2020, doi: 10.3389/fonc.2020.580874.

[179] C. Théry *et al.*, "Minimal information for studies of extracellular vesicles 2018 (MISEV2018): a position statement of the International Society for Extracellular Vesicles and update of the MISEV2014 guidelines," *J. Extracell. Vesicles*, vol. 7, no. 1, p. 1535750, Dec. 2018, doi: 10.1080/20013078.2018.1535750.

[180] L.-R. Li, L. Wang, Y.-Z. He, and K. H. Young, "Current perspectives on the treatment of double hit lymphoma," *Expert Rev. Hematol.*, vol. 12, no. 7, pp. 507–514, Jul. 2019, doi: 10.1080/17474086.2019.1623020.

[181] S. Islam *et al.*, "Drug-induced aneuploidy and polyploidy is a mechanism of disease relapse in MYC/BCL2-addicted diffuse large B-cell lymphoma," *Oncotarget*, vol. 9, no. 89, pp. 35875–35890, Nov. 2018, doi: 10.18632/oncotarget.26251.

[182] S. Richards, M. Clarke, K. Wheatley, and R. Peto, "Chemotherapeutic Options in Chronic Lymphocytic Leukemia: a Meta-analysis of the Randomized Trials," *J. Natl. Cancer Inst.*, vol. 91, no. 10, pp. 861–868, May 1999, doi: 10.1093/jnci/91.10.861.

[183] E. J. Anaissie, "Infections in Patients with Chronic Lymphocytic Leukemia Treated with Fludarabine," *Ann. Intern. Med.*, vol. 129, no. 7, p. 559, Oct. 1998, doi: 10.7326/0003-4819-129-7-199810010-00010.

[184] C. Sauter, N. Lamanna, and M. A. Weiss, "Pentostatin in chronic lymphocytic leukemia," *Expert Opin. Drug Metab. Toxicol.*, vol. 4, no. 9, pp. 1217–1222, Sep. 2008, doi: 10.1517/17425255.4.9.1217.

[185] T. Robak, "Cladribine in the Treatment of Chronic Lymphocytic Leukemia," *Leuk. Lymphoma*, vol. 40, no. 5–6, pp. 551–564, Jan. 2001, doi: 10.3109/10428190109097654.

[186] V. Gandhi and J. A. Burger, "Bendamustine in B-Cell Malignancies: The New 46-Year-Old Kid on the Block," *Clin. Cancer Res.*, vol. 15, no. 24, pp. 7456–7461, Dec. 2009, doi: 10.1158/1078-0432.CCR-08-3041.

[187] J. L. Teeling *et al.*, "The Biological Activity of Human CD20 Monoclonal Antibodies Is Linked to Unique Epitopes on CD20," *J. Immunol.*, vol. 177, no. 1, pp. 362–371, Jul. 2006, doi: 10.4049/jimmunol.177.1.362.

[188] M. Patz *et al.*, "Comparison of the in vitro effects of the anti-CD20 antibodies rituximab and GA101 on chronic lymphocytic leukaemia cells," *Br. J. Haematol.*, vol. 152, no. 3, pp. 295–306, Feb. 2011, doi: 10.1111/j.1365-2141.2010.08428.x.

[189] F. Hagemeister, "Rituximab for the Treatment of Non-Hodgkin's Lymphoma and Chronic Lymphocytic Leukaemia," *Drugs*, vol. 70, no. 3, pp. 261–272, Feb. 2010, doi: 10.2165/11532180-000000000-00000.

[190] W. G. Wierda *et al.*, "Ofatumumab As Single-Agent CD20 Immunotherapy in Fludarabine-Refractory Chronic Lymphocytic Leukemia," *J. Clin. Oncol.*, vol. 28, no. 10, pp. 1749–1755, Apr. 2010, doi: 10.1200/JCO.2009.25.3187.

[191] M. S. Cragg, C. A. Walshe, A. O. Ivanov, and M. J. Glennie, "The Biology of CD20 and Its Potential as a Target for mAb Therapy," in *B Cell Trophic Factors and B Cell*

Antagonism in Autoimmune Disease, vol. 8, Basel: KARGER, 2004, pp. 140–174.

[192] S. Kheirallah *et al.*, "Rituximab inhibits B-cell receptor signaling," *Blood*, vol. 115, no. 5, pp. 985–994, Feb. 2010, doi: 10.1182/blood-2009-08-237537.

[193] M. Hallek *et al.*, "Addition of rituximab to fludarabine and cyclophosphamide in patients with chronic lymphocytic leukaemia: a randomised, open-label, phase 3 trial," *Lancet*, vol. 376, no. 9747, pp. 1164–1174, Oct. 2010, doi: 10.1016/S0140-6736(10)61381-5.

[194] C. S. Tam *et al.*, "Long-term results of the fludarabine, cyclophosphamide, and rituximab regimen as initial therapy of chronic lymphocytic leukemia," *Blood*, vol. 112, no. 4, pp. 975–980, Aug. 2008, doi: 10.1182/blood-2008-02-140582.

[195] B. Chapuy *et al.*, "Molecular subtypes of diffuse large B cell lymphoma are associated with distinct pathogenic mechanisms and outcomes," *Nat. Med.*, vol. 24, no. 5, pp. 679–690, May 2018, doi: 10.1038/s41591-018-0016-8.

[196] Cancer Genome Atlas Research Network, "Genomic and Epigenomic Landscapes of Adult De Novo Acute Myeloid Leukemia," *N. Engl. J. Med.*, vol. 368, no. 22, pp. 2059–2074, May 2013, doi: 10.1056/NEJMoa1301689.

[197] A. Osterborg *et al.*, "Phase II multicenter study of human CD52 antibody in previously treated chronic lymphocytic leukemia. European Study Group of CAMPATH-1H Treatment in Chronic Lymphocytic Leukemia.," *J. Clin. Oncol.*, vol. 15, no. 4, pp. 1567–1574, Apr. 1997, doi: 10.1200/JCO.1997.15.4.1567.

[198] K. R. Rai *et al.*, "Alemtuzumab in Previously Treated Chronic Lymphocytic Leukemia Patients Who Also Had Received Fludarabine," *J. Clin. Oncol.*, vol. 20, no. 18, pp. 3891–3897, Sep. 2002, doi: 10.1200/JCO.2002.06.119.

[199] M. J. Keating *et al.*, "Therapeutic role of alemtuzumab (Campath-1H) in patients who have failed fludarabine: results of a large international study," *Blood*, vol. 99, no. 10, pp. 3554–3561, May 2002, doi: 10.1182/blood.V99.10.3554.

[200] G. Hale, "The CD52 antigen and development of the CAMPATH antibodies," *Cytotherapy*, vol. 3, no. 3. Elsevier Inc., pp. 137–143, May 01, 2001, doi: 10.1080/146532401753174098.

[201] S. Stilgenbauer and H. Döhner, "Campath-1H–Induced Complete Remission of Chronic Lymphocytic Leukemia despite p53 Gene Mutation and Resistance to Chemotherapy," *N. Engl. J. Med.*, vol. 347, no. 6, pp. 452–453, Aug. 2002, doi: 10.1056/NEJM200208083470619.

[202] G. Lozanski *et al.*, "Alemtuzumab is an effective therapy for chronic lymphocytic leukemia with p53 mutations and deletions," *Blood*, vol. 103, no. 9, pp. 3278–3281, May

2004, doi: 10.1182/blood-2003-10-3729.

[203] B. Kennedy *et al.*, "Campath-1H and fludarabine in combination are highly active in refractory chronic lymphocytic leukemia," *Blood*, vol. 99, no. 6, pp. 2245–2247, Mar. 2002, doi: 10.1182/blood.V99.6.2245.

[204] S. Lepretre *et al.*, "Excess mortality after treatment with fludarabine and cyclophosphamide in combination with alemtuzumab in previously untreated patients with chronic lymphocytic leukemia in a randomized phase 3 trial," *Blood*, vol. 119, no. 22, pp. 5104–5110, Jun. 2012, doi: 10.1182/blood-2011-07-365437.

[205] L. A. Honigberg *et al.*, "The Bruton tyrosine kinase inhibitor PCI-32765 blocks B-cell activation and is efficacious in models of autoimmune disease and B-cell malignancy," *Proc. Natl. Acad. Sci.*, vol. 107, no. 29, pp. 13075–13080, Jul. 2010, doi: 10.1073/pnas.1004594107.

[206] J. C. Byrd *et al.*, "Targeting BTK with Ibrutinib in Relapsed Chronic Lymphocytic Leukemia," *N. Engl. J. Med.*, vol. 369, no. 1, pp. 32–42, Jul. 2013, doi: 10.1056/NEJMoa1215637.

[207] S. E. M. Herman *et al.*, "Bruton tyrosine kinase represents a promising therapeutic target for treatment of chronic lymphocytic leukemia and is effectively targeted by PCI-32765," *Blood*, vol. 117, no. 23, pp. 6287–6296, Jun. 2011, doi: 10.1182/blood-2011-01-328484.

[208] J. A. Woyach *et al.*, "Resistance Mechanisms for the Bruton's Tyrosine Kinase Inhibitor Ibrutinib," *N. Engl. J. Med.*, vol. 370, no. 24, pp. 2286–2294, Jun. 2014, doi: 10.1056/nejmoa1400029.

[209] K. J. Maddocks *et al.*, "Etiology of Ibrutinib Therapy Discontinuation and Outcomes in Patients With Chronic Lymphocytic Leukemia," *JAMA Oncol.*, vol. 1, no. 1, p. 80, Apr. 2015, doi: 10.1001/jamaoncol.2014.218.

[210] J. Ní Gabhann *et al.*, "Btk Regulates Macrophage Polarization in Response to Lipopolysaccharide," *PLoS One*, vol. 9, no. 1, p. e85834, Jan. 2014, doi: 10.1371/journal.pone.0085834.

[211] T. D. Shanafelt *et al.*, "Ibrutinib-Rituximab or Chemoimmunotherapy for Chronic Lymphocytic Leukemia.," *N. Engl. J. Med.*, vol. 381, no. 5, pp. 432–443, 2019, doi: 10.1056/NEJMoa1817073.

[212] J. A. Woyach *et al.*, "Ibrutinib Regimens versus Chemoimmunotherapy in Older Patients with Untreated CLL," *N. Engl. J. Med.*, vol. 379, no. 26, pp. 2517–2528, Dec. 2018, doi: 10.1056/NEJMoa1812836.

[213] A. Chanan-Khan *et al.*, "Ibrutinib combined with bendamustine and rituximab compared with placebo, bendamustine, and rituximab for previously treated chronic lymphocytic leukaemia or small lymphocytic lymphoma (HELIOS): a randomised, double-blind, phase 3 study," *Lancet Oncol.*, vol. 17, no. 2, pp. 200–211, Feb. 2016, doi: 10.1016/S1470-2045(15)00465-9.

[214] S. M. Jaglowski *et al.*, "Safety and activity of BTK inhibitor ibrutinib combined with ofatumumab in chronic lymphocytic leukemia: a phase 1b/2 study," *Blood*, vol. 126, no. 7, pp. 842–850, Aug. 2015, doi: 10.1182/blood-2014-12-617522.

[215] J. C. Byrd *et al.*, "Acalabrutinib (ACP-196) in Relapsed Chronic Lymphocytic Leukemia," *N. Engl. J. Med.*, vol. 374, no. 4, pp. 323–332, Jan. 2016, doi: 10.1056/NEJMoa1509981.

[216] J. R. Brown *et al.*, "Idelalisib, an inhibitor of phosphatidylinositol 3-kinase p110δ, for relapsed/refractory chronic lymphocytic leukemia," *Blood*, vol. 123, no. 22, pp. 3390–3397, May 2014, doi: 10.1182/blood-2013-11-535047.

[217] B. L. Ebert and J. Krönke, "Inhibition of Casein Kinase 1 Alpha in Acute Myeloid Leukemia," *N. Engl. J. Med.*, vol. 379, no. 19, pp. 1873–1874, Nov. 2018, doi: 10.1056/NEJMcibr1811318.

[218] S. Haldar, N. Jena, and C. M. Croce, "Inactivation of Bcl-2 by phosphorylation.," *Proc. Natl. Acad. Sci.*, vol. 92, no. 10, pp. 4507–4511, May 1995, doi: 10.1073/pnas.92.10.4507.

[219] A. W. Roberts *et al.*, "Targeting BCL2 with Venetoclax in Relapsed Chronic Lymphocytic Leukemia," *N. Engl. J. Med.*, vol. 374, no. 4, pp. 311–322, Jan. 2016, doi: 10.1056/NEJMoa1513257.

[220] P. Hillmen *et al.*, "Ibrutinib Plus Venetoclax in Relapsed/Refractory Chronic Lymphocytic Leukemia: The CLARITY Study," *J. Clin. Oncol.*, vol. 37, no. 30, pp. 2722–2729, Oct. 2019, doi: 10.1200/JCO.19.00894.

[221] N. Jain *et al.*, "Ibrutinib and Venetoclax for First-Line Treatment of CLL," *N. Engl. J. Med.*, vol. 380, no. 22, pp. 2095–2103, May 2019, doi: 10.1056/NEJMoa1900574.

[222] W. Ding *et al.*, "Pembrolizumab in patients with CLL and Richter transformation or with relapsed CLL," *Blood*, vol. 129, no. 26, pp. 3419–3427, Jun. 2017, doi: 10.1182/blood-2017-02-765685.

[223] D. L. Porter, B. L. Levine, M. Kalos, A. Bagg, and C. H. June, "Chimeric Antigen Receptor–Modified T Cells in Chronic Lymphoid Leukemia," *N. Engl. J. Med.*, vol. 365, no. 8, pp. 725–733, Aug. 2011, doi: 10.1056/NEJMoa1103849.

[224] A. R. Mato, M. C. Thompson, C. Nabhan, J. Svoboda, and S. J. Schuster, "Chimeric Antigen Receptor T-Cell Therapy for Chronic Lymphocytic Leukemia: A Narrative Review," *Clin. Lymphoma Myeloma Leuk.*, vol. 17, no. 12, pp. 852–856, Dec. 2017, doi: 10.1016/j.clml.2017.07.007.

[225] V. Barbarino *et al.*, "Macrophage-mediated antibody dependent effector function in aggressive B-cell lymphoma treatment is enhanced by ibrutinib *via* inhibition of JAK2," *Cancers (Basel).*, vol. 12, no. 8, pp. 1–25, 2020, doi: 10.3390/cancers12082303.

[226] I. Leskov *et al.*, "Rapid generation of human B-cell lymphomas *via* combined expression of Myc and Bcl2 and their use as a preclinical model for biological therapies," *Oncogene*, vol. 32, no. 8, 2013, doi: 10.1038/onc.2012.117.

[227] A. D. Köprülü *et al.*, "The Tyrosine Kinase Btk Regulates the Macrophage Response to Listeria monocytogenes Infection," *PLoS One*, vol. 8, no. 3, p. e60476, Mar. 2013, doi: 10.1371/journal.pone.0060476.

[228] W. N. Khan *et al.*, "Defective B cell development and function in Btk-deficient mice," *Immunity*, vol. 3, no. 3, pp. 283–299, 1995, doi: 10.1016/1074-7613(95)90114-0.

[229] C. D. Herling *et al.*, "Clonal dynamics towards the development of venetoclax resistance in chronic lymphocytic leukemia," *Nat. Commun.*, vol. 9, no. 1, p. 727, Dec. 2018, doi: 10.1038/s41467-018-03170-7.

[230] J. G. Doench and D. . Root, "Optimized sgRNA design to maximize activity and minimize off-target effects of CRISPR-Cas9 Synthesis of an arrayed sgRNA library targeting the human genome," *Nat. Biotechnol.*, vol. 34, no. 2, pp. 184–191, 2016, doi: 10.1038/nbt.3437.Optimized.

[231] E. Izquierdo *et al.*, "Loss of TP53 mediates suppression of Macrophage Effector Function *via* Extracellular Vesicles and PDL1 towards Resistance against Chemoimmunotherapy in B-cell malignancies," *bioRxiv*, 2020, doi: 10.1101/2020.06.11.145268.

[232] J. De Jong *et al.*, "The effect of food on the pharmacokinetics of oral ibrutinib in healthy participants and patients with chronic lymphocytic leukemia," *Cancer Chemother. Pharmacol.*, vol. 75, no. 5, pp. 907–916, 2015, doi: 10.1007/s00280-015-2708-9.

[233] A. Berglöf *et al.*, "Targets for Ibrutinib Beyond B Cell Malignancies," *Scandinavian Journal of Immunology*. 2015, doi: 10.1111/sji.12333.

[234] C. Lossos *et al.*, "Mechanisms of Lymphoma Clearance Induced by High-Dose Alkylating Agents," *Cancer Discov.*, vol. 9, no. 7, pp. 944–961, Jul. 2019, doi: 10.1158/2159-8290.CD-18-1393.

[235] A. Roghanian *et al.*, "Cyclophosphamide Enhances Cancer Antibody Immunotherapy in the Resistant Bone Marrow Niche by Modulating Macrophage FcγR Expression," *Cancer Immunol. Res.*, vol. 7, no. 11, pp. 1876–1890, Nov. 2019, doi: 10.1158/2326-6066.CIR-18-0835.

[236] Vorholt Daniela, "Functional Implications and Interaction of Macrophages in the Leukemic Microenvironment upon Genotoxic Stress," -Naturwissenschaftliche Fakultät, Institut für Genetik, 2016. [Online]. Available: https://kups.ub.uni-koeln.de/7644/.

[237] M. Catalano and L. O'Driscoll, "Inhibiting extracellular vesicles formation and release: a review of EV inhibitors," *J. Extracell. Vesicles*, vol. 9, no. 1, p. 1703244, Sep. 2020, doi: 10.1080/20013078.2019.1703244.

[238] T. Robak *et al.*, "Single-agent ibrutinib versus chemoimmunotherapy regimens for treatment-naïve patients with chronic lymphocytic leukemia: A cross-trial comparison of phase 3 studies," *Am. J. Hematol.*, vol. 93, no. 11, pp. 1402–1410, Nov. 2018, doi: 10.1002/ajh.25259.

[239] J. A. Burger *et al.*, "Ibrutinib as Initial Therapy for Patients with Chronic Lymphocytic Leukemia," *N. Engl. J. Med.*, vol. 373, no. 25, pp. 2425–2437, Dec. 2015, doi: 10.1056/nejmoa1509388.

[240] J. C. Byrd *et al.*, "Ibrutinib versus Ofatumumab in Previously Treated Chronic Lymphoid Leukemia," *N. Engl. J. Med.*, vol. 371, no. 3, pp. 213–223, Jul. 2014, doi: 10.1056/NEJMoa1400376.

[241] R. H. Advani *et al.*, "Bruton Tyrosine Kinase Inhibitor Ibrutinib (PCI-32765) Has Significant Activity in Patients With Relapsed/Refractory B-Cell Malignancies," *J. Clin. Oncol.*, vol. 31, no. 1, pp. 88–94, Jan. 2013, doi: 10.1200/JCO.2012.42.7906.

[242] J. A. Burger *et al.*, "Long-term efficacy and safety of first-line ibrutinib treatment for patients with CLL/SLL: 5 years of follow-up from the phase 3 RESONATE-2 study," *Leukemia*, vol. 34, no. 3, pp. 787–798, Mar. 2020, doi: 10.1038/s41375-019-0602-x.

[243] I. E. Ahn *et al.*, "Depth and durability of response to ibrutinib in CLL: 5-year follow-up of a phase 2 study," *Blood*, vol. 131, no. 21, pp. 2357–2366, May 2018, doi: 10.1182/blood-2017-12-820910.

[244] S. M. O'Brien *et al.*, "Outcomes with ibrutinib by line of therapy and post-ibrutinib discontinuation in patients with chronic lymphocytic leukemia: Phase 3 analysis," *Am. J. Hematol.*, vol. 94, no. 5, pp. 554–562, May 2019, doi: 10.1002/ajh.25436.

[245] P. M. Barr *et al.*, "Sustained efficacy and detailed clinical follow-up of first-line ibrutinib treatment in older patients with chronic lymphocytic leukemia: extended phase 3 results

from RESONATE-2," *Haematologica*, vol. 103, no. 9, pp. 1502–1510, Sep. 2018, doi: 10.3324/haematol.2018.192328.

[246] P. Langerbeins *et al.*, "IBRUTINIB VERSUS PLACEBO IN PATIENTS WITH ASYMPTOMATIC, TREATMENT-NAÏVE EARLY STAGE CLL: PRIMARY ENDPOINT RESULTS OF THE PHASE 3 DOUBLE-BLIND RANDOMIZED CLL12 TRIAL," *Hematol. Oncol.*, vol. 37, pp. 38–40, Jun. 2019, doi: 10.1002/hon.7_2629.

[247] A. Younes *et al.*, "Randomized Phase III Trial of Ibrutinib and Rituximab Plus Cyclophosphamide, Doxorubicin, Vincristine, and Prednisone in Non–Germinal Center B-Cell Diffuse Large B-Cell Lymphoma," *J. Clin. Oncol.*, vol. 37, no. 15, pp. 1285–1295, May 2019, doi: 10.1200/JCO.18.02403.

[248] M. A. Dimopoulos *et al.*, "Phase 3 Trial of Ibrutinib plus Rituximab in Waldenström's Macroglobulinemia," *N. Engl. J. Med.*, vol. 378, no. 25, pp. 2399–2410, Jun. 2018, doi: 10.1056/NEJMoa1802917.

[249] J. A. Burger *et al.*, "Randomized trial of ibrutinib vs ibrutinib plus rituximab in patients with chronic lymphocytic leukemia," *Blood*, vol. 133, no. 10, pp. 1011–1019, 2019, doi: 10.1182/blood-2018-10-879429.

[250] D. Herlyn and H. Koprowski, "IgG2a monoclonal antibodies inhibit human tumor growth through interaction with effector cells.," *Proc. Natl. Acad. Sci.*, vol. 79, no. 15, pp. 4761–4765, Aug. 1982, doi: 10.1073/pnas.79.15.4761.

[251] Z. Steplewski, M. Lubeck, and H. Koprowski, "Human macrophages armed with murine immunoglobulin G2a antibodies to tumors destroy human cancer cells," *Science (80-.).*, vol. 221, no. 4613, pp. 865–867, Aug. 1983, doi: 10.1126/science.6879183.

[252] D. O. Adams, T. Hall, Z. Steplewski, and H. Koprowski, "Tumors undergoing rejection induced by monoclonal antibodies of the IgG2a isotype contain increased numbers of macrophages activated for a distinctive form of antibody-dependent cytolysis.," *Proc. Natl. Acad. Sci.*, vol. 81, no. 11, pp. 3506–3510, Jun. 1984, doi: 10.1073/pnas.81.11.3506.

[253] A. K. Church *et al.*, "Anti-CD20 monoclonal antibody-dependent phagocytosis of chronic lymphocytic leukaemia cells by autologous macrophages," *Clin. Exp. Immunol.*, vol. 183, no. 1, pp. 90–101, Jan. 2016, doi: 10.1111/cei.12697.

[254] F. Montalvao *et al.*, "The mechanism of anti-CD20–mediated B cell depletion revealed by intravital imaging," *J. Clin. Invest.*, vol. 123, no. 12, pp. 5098–5103, Dec. 2013, doi: 10.1172/JCI70972.

[255] M. P. Chao *et al.*, "Anti-CD47 Antibody Synergizes with Rituximab to Promote

Phagocytosis and Eradicate Non-Hodgkin Lymphoma," *Cell*, vol. 142, no. 5, pp. 699–713, Sep. 2010, doi: 10.1016/j.cell.2010.07.044.

[256] M.-L. Lefebvre, S. W. Krause, M. Salcedo, and A. Nardin, "Ex Vivo-activated Human Macrophages Kill Chronic Lymphocytic Leukemia Cells in the Presence of Rituximab: Mechanism of Antibody-dependent Cellular Cytotoxicity and Impact of Human Serum," *J. Immunother.*, vol. 29, no. 4, pp. 388–397, Jul. 2006, doi: 10.1097/01.cji.0000203081.43235.d7.

[257] O. Manches *et al.*, "In vitro mechanisms of action of rituximab on primary non-Hodgkin lymphomas," *Blood*, vol. 101, no. 3, pp. 949–954, Feb. 2003, doi: 10.1182/blood-2002-02-0469.

[258] L. Chaperot *et al.*, "Differentiation of antigen-presenting cells (dendritic cells and macrophages) for therapeutic application in patients with lymphoma," *Leukemia*, vol. 14, no. 9, pp. 1667–1677, Sep. 2000, doi: 10.1038/sj.leu.2401888.

[259] A. T. Kurdi *et al.*, "Antibody-Dependent Cellular Phagocytosis by Macrophages is a Novel Mechanism of Action of Elotuzumab," *Mol. Cancer Ther.*, vol. 17, no. 7, pp. 1454–1463, Jul. 2018, doi: 10.1158/1535-7163.MCT-17-0998.

[260] M. Skarzynski *et al.*, "Interactions between ibrutinib and anti-CD20 antibodies: Competing effects on the outcome of combination therapy," *Clin. Cancer Res.*, vol. 22, no. 1, pp. 86–95, Jan. 2016, doi: 10.1158/1078-0432.CCR-15-1304.

[261] A. Manna *et al.*, "Targeting CD38 enhances the antileukemic activity of ibrutinib in chronic lymphocytic leukemia," *Clin. Cancer Res.*, vol. 25, no. 13, pp. 3974–3985, 2019, doi: 10.1158/1078-0432.CCR-18-3412.

[262] M. L. Ribeiro *et al.*, "TG-1701, a novel irreversible Bruton's kinase (BTK) inhibitor, cooperates with ublituximab-driven ADCC and ADCP in in vitro and in vivo models of ibrutinib-resistant mantle cell lymphoma," in *Immunology*, Aug. 2020, pp. 2205–2205, doi: 10.1158/1538-7445.AM2020-2205.

[263] F. Da Roit *et al.*, "Ibrutinib interferes with the cell-mediated anti-tumor activities of therapeutic CD20 antibodies: Implications for combination therapy," *Haematologica*, vol. 100, no. 1, pp. 77–86, 2015, doi: 10.3324/haematol.2014.107011.

[264] M. Borge *et al.*, "Ibrutinib impairs the phagocytosis of rituximab-coated leukemic cells from chronic lymphocytic leukemia patients by human macrophages," *Haematologica*, vol. 100, no. 4. Ferrata Storti Foundation, pp. e140–e142, 2015, doi: 10.3324/haematol.2014.119669.

[265] C. Wang *et al.*, "Characterization of murine macrophages from bone marrow, spleen and

peritoneum," *BMC Immunol.*, vol. 14, no. 1, p. 6, Dec. 2013, doi: 10.1186/1471-2172-14-6.

[266] M. Feng *et al.*, "Macrophages eat cancer cells using their own calreticulin as a guide: Roles of TLR and Btk," *Proc. Natl. Acad. Sci.*, vol. 112, no. 7, pp. 2145–2150, Feb. 2015, doi: 10.1073/pnas.1424907112.

[267] J. Jongstra-Bilen, A. Puig Cano, M. Hasija, H. Xiao, C. I. E. Smith, and M. I. Cybulsky, "Dual Functions of Bruton's Tyrosine Kinase and Tec Kinase during Fcγ Receptor-Induced Signaling and Phagocytosis," *J. Immunol.*, vol. 181, no. 1, pp. 288–298, Jul. 2008, doi: 10.4049/jimmunol.181.1.288.

[268] L. D. Shultz *et al.*, "Human Lymphoid and Myeloid Cell Development in NOD/LtSz-scid IL2R γ null Mice Engrafted with Mobilized Human Hemopoietic Stem Cells," *J. Immunol.*, vol. 174, no. 10, pp. 6477–6489, May 2005, doi: 10.4049/jimmunol.174.10.6477.

[269] S. H. Lim *et al.*, "Fc gamma receptor IIb on target B cells promotes rituximab internalization and reduces clinical efficacy," *Blood*, vol. 118, no. 9, pp. 2530–2540, Sep. 2011, doi: 10.1182/blood-2011-01-330357.

[270] S. E. M. Herman *et al.*, "Ibrutinib-induced lymphocytosis in patients with chronic lymphocytic leukemia: correlative analyses from a phase II study," *Leukemia*, vol. 28, no. 11, pp. 2188–2196, Nov. 2014, doi: 10.1038/leu.2014.122.

[271] A. Russ *et al.*, "Blocking 'don't eat me' signal of CD47-SIRPα in hematological malignancies, an in-depth review," *Blood Rev.*, vol. 32, no. 6, pp. 480–489, Nov. 2018, doi: 10.1016/j.blre.2018.04.005.

[272] W. Zhang *et al.*, "Advances in Anti-Tumor Treatments Targeting the CD47/SIRPα Axis," *Front. Immunol.*, vol. 11, p. 18, Jan. 2020, doi: 10.3389/fimmu.2020.00018.

[273] J. Liu *et al.*, "Pre-Clinical Development of a Humanized Anti-CD47 Antibody with Anti-Cancer Therapeutic Potential," *PLoS One*, vol. 10, no. 9, p. e0137345, Sep. 2015, doi: 10.1371/journal.pone.0137345.

[274] M. F. Breinholt *et al.*, "High-grade B-cell lymphomas with MYC and BCL2 translocations lack tumor-associated macrophages and PD-L1 expression: A possible noninflamed subgroup," *Hematol. Oncol.*, vol. 299, no. max 300, p. hon.2839, Feb. 2021, doi: 10.1002/hon.2839.

[275] I. Sagiv-Barfi, H. E. K. Kohrt, D. K. Czerwinski, P. P. Ng, B. Y. Chang, and R. Levy, "Therapeutic antitumor immunity by checkpoint blockade is enhanced by ibrutinib, an inhibitor of both BTK and ITK," *Proc. Natl. Acad. Sci.*, vol. 112, no. 9, pp. E966–E972,

Mar. 2015, doi: 10.1073/pnas.1500712112.

[276] N. Jain *et al.*, "Nivolumab Combined with Ibrutinib for CLL and Richter Transformation: A Phase II Trial," *Blood*, vol. 128, no. 22, pp. 59–59, Dec. 2016, doi: 10.1182/blood.V128.22.59.59.

[277] B. S. Hanna *et al.*, "Combining ibrutinib and checkpoint blockade improves CD8+ T-cell function and control of chronic lymphocytic leukemia in Em-TCL1 mice," *Haematologica*, vol. 106, no. 4, p. haematol.2019.238154, Mar. 2020, doi: 10.3324/haematol.2019.238154.

[278] F. McClanahan *et al.*, "PD-L1 checkpoint blockade prevents immune dysfunction and leukemia development in a mouse model of chronic lymphocytic leukemia," *Blood*, vol. 126, no. 2, pp. 203–211, Jul. 2015, doi: 10.1182/blood-2015-01-622936.

[279] L. Zhang, T. F. Gajewski, and J. Kline, "PD-1/PD-L1 interactions inhibit antitumor immune responses in a murine acute myeloid leukemia model," *Blood*, vol. 114, no. 8, pp. 1545–1552, Aug. 2009, doi: 10.1182/blood-2009-03-206672.

[280] T. Jelinek, J. Mihalyova, M. Kascak, J. Duras, and R. Hajek, "PD-1/PD-L1 inhibitors in haematological malignancies: update 2017," *Immunology*, vol. 152, no. 3, pp. 357–371, Nov. 2017, doi: 10.1111/imm.12788.

[281] N. van Rooijen and E. Hendrikx, "Liposomes for Specific Depletion of Macrophages from Organs and Tissues," in *Methods in molecular biology (Clifton, N.J.)*, vol. 605, Methods Mol Biol, 2010, pp. 189–203.

[282] A. Bresin *et al.*, "TCL1 transgenic mouse model as a tool for the study of therapeutic targets and microenvironment in human B-cell chronic lymphocytic leukemia," *Cell Death Dis.*, vol. 7, no. 1, pp. e2071–e2071, Jan. 2016, doi: 10.1038/cddis.2015.419.

[283] D. W. Greening, S. K. Gopal, R. Xu, R. J. Simpson, and W. Chen, "Exosomes and their roles in immune regulation and cancer," *Semin. Cell Dev. Biol.*, vol. 40, pp. 72–81, Apr. 2015, doi: 10.1016/j.semcdb.2015.02.009.

[284] G. Genard, S. Lucas, and C. Michiels, "Reprogramming of Tumor-Associated Macrophages with Anticancer Therapies: Radiotherapy versus Chemo- and Immunotherapies," *Front. Immunol.*, vol. 8, no. JUL, Jul. 2017, doi: 10.3389/fimmu.2017.00828.

[285] X.-J. Yan *et al.*, "Identification of outcome-correlated cytokine clusters in chronic lymphocytic leukemia," *Blood*, vol. 118, no. 19, pp. 5201–5210, Nov. 2011, doi: 10.1182/blood-2011-03-342436.

[286] C. U. Niemann *et al.*, "Disruption of in vivo chronic lymphocytic leukemia tumor-

microenvironment interactions by ibrutinib - Findings from an investigator-initiated phase II study," *Clin. Cancer Res.*, vol. 22, no. 7, pp. 1572–1582, Apr. 2016, doi: 10.1158/1078-0432.CCR-15-1965.

[287] M. Leidi *et al.*, "M2 Macrophages Phagocytose Rituximab-Opsonized Leukemic Targets More Efficiently than M1 Cells In Vitro," *J. Immunol.*, vol. 182, no. 7, pp. 4415–4422, Apr. 2009, doi: 10.4049/jimmunol.0713732.

[288] W. Deng *et al.*, "Mesenchymal stem cells promote CD206 expression and phagocytic activity of macrophages through IL-6 in systemic lupus erythematosus," *Clin. Immunol.*, vol. 161, no. 2, pp. 209–216, Dec. 2015, doi: 10.1016/j.clim.2015.07.011.

[289] D. J. Hess, M. J. Henry-Stanley, C. M. Bendel, B. Zhang, M.-A. Johnson, and C. L. Wells, "Escherichia coli and TNF-α Modulate Macrophage Phagocytosis of Candida glabrata," *J. Surg. Res.*, vol. 155, no. 2, pp. 217–224, Aug. 2009, doi: 10.1016/j.jss.2008.07.022.

[290] J. P. Edwards and L. A. Emens, "The multikinase inhibitor Sorafenib reverses the suppression of IL-12 and enhancement of IL-10 by PGE2 in murine macrophages," *Int. Immunopharmacol.*, vol. 10, no. 10, pp. 1220–1228, Oct. 2010, doi: 10.1016/j.intimp.2010.07.002.

[291] S. F. Hussain *et al.*, "A Novel Small Molecule Inhibitor of Signal Transducers and Activators of Transcription 3 Reverses Immune Tolerance in Malignant Glioma Patients," *Cancer Res.*, vol. 67, no. 20, pp. 9630–9636, Oct. 2007, doi: 10.1158/0008-5472.CAN-07-1243.

[292] L. Sun, B. Chen, R. Jiang, J. Li, and B. Wang, "Resveratrol inhibits lung cancer growth by suppressing M2-like polarization of tumor associated macrophages," *Cell. Immunol.*, vol. 311, pp. 86–93, Jan. 2017, doi: 10.1016/j.cellimm.2016.11.002.

[293] R. Dong *et al.*, "The involvement of M2 macrophage polarization inhibition in fenretinide-mediated chemopreventive effects on colon cancer," *Cancer Lett.*, vol. 388, pp. 43–53, Mar. 2017, doi: 10.1016/j.canlet.2016.11.029.

[294] I. Meyer, W. Martinet, D. M. Schrijvers, J.-P. Timmermans, H. Bult, and G. R. Y. Meyer, "Toll-like receptor 7 stimulation by imiquimod induces macrophage autophagy and inflammation in atherosclerotic plaques," *Basic Res. Cardiol.*, vol. 107, no. 3, p. 269, May 2012, doi: 10.1007/s00395-012-0269-1.

[295] H. D. Lum *et al.*, "Tumoristic effects of anti-CD40 mAb-activated macrophages involve nitric oxide and tumour necrosis factor-alpha," *Immunology*, vol. 118, no. 2, pp. 261–270, Jun. 2006, doi: 10.1111/j.1365-2567.2006.02366.x.

[296] E. E. Johnson *et al.*, "Enhanced T-cell-independent Antitumor Effect of Cyclophosphamide Combined With Anti-CD40 mAb and CpG in Mice," *J. Immunother.*, vol. 34, no. 1, pp. 76–84, Jan. 2011, doi: 10.1097/CJI.0b013e318200b28a.

[297] J. M. Weiss *et al.*, "Macrophage-dependent nitric oxide expression regulates tumor cell detachment and metastasis after IL-2/anti-CD40 immunotherapy," *J. Exp. Med.*, vol. 207, no. 11, pp. 2455–2467, Oct. 2010, doi: 10.1084/jem.20100670.

[298] M. M. Kaneda *et al.*, "PI3Kγ is a molecular switch that controls immune suppression," *Nature*, vol. 539, no. 7629, pp. 437–442, Nov. 2016, doi: 10.1038/nature19834.

[299] G. P. Dunn, C. M. Koebel, and R. D. Schreiber, "Interferons, immunity and cancer immunoediting," *Nat. Rev. Immunol.*, vol. 6, no. 11, pp. 836–848, Nov. 2006, doi: 10.1038/nri1961.

[300] A. S. Jassar *et al.*, "Activation of Tumor-Associated Macrophages by the Vascular Disrupting Agent 5,6-Dimethylxanthenone-4-Acetic Acid Induces an Effective CD8 + T-Cell–Mediated Antitumor Immune Response in Murine Models of Lung Cancer and Mesothelioma," *Cancer Res.*, vol. 65, no. 24, pp. 11752–11761, Dec. 2005, doi: 10.1158/0008-5472.CAN-05-1658.

[301] D. Schulz, Y. Severin, V. R. T. Zanotelli, and B. Bodenmiller, "In-Depth Characterization of Monocyte-Derived Macrophages using a Mass Cytometry-Based Phagocytosis Assay," *Sci. Rep.*, vol. 9, no. 1, p. 1925, Dec. 2019, doi: 10.1038/s41598-018-38127-9.

[302] U. Jaggi *et al.*, "Increased phagocytosis in the presence of enhanced M2-like macrophage responses correlates with increased primary and latent HSV-1 infection," *PLOS Pathog.*, vol. 16, no. 10, p. e1008971, Oct. 2020, doi: 10.1371/journal.ppat.1008971.

[303] A. Colado *et al.*, "Effect of the BTK inhibitor ibrutinib on macrophage- and γδ T cell-mediated response against Mycobacterium tuberculosis," *Blood Cancer J.*, vol. 8, no. 11, p. 100, Nov. 2018, doi: 10.1038/s41408-018-0136-x.

[304] S. Fiorcari *et al.*, "Ibrutinib modifies the function of monocyte/macrophage population in chronic lymphocytic leukemia," *Oncotarget*, vol. 7, no. 40, pp. 65968–65981, Oct. 2016, doi: 10.18632/oncotarget.11782.

[305] A. J. Gunderson *et al.*, "Bruton Tyrosine Kinase–Dependent Immune Cell Cross-talk Drives Pancreas Cancer," *Cancer Discov.*, vol. 6, no. 3, pp. 270–285, Mar. 2016, doi: 10.1158/2159-8290.CD-15-0827.

[306] M. Kinder, A. R. Greenplate, W. R. Strohl, R. E. Jordan, and R. J. Brezski, "An Fc engineering approach that modulates antibody-dependent cytokine release without

altering cell-killing functions," *MAbs*, vol. 7, no. 3, pp. 494–504, May 2015, doi: 10.1080/19420862.2015.1022692.

[307] K. Bojarczuk *et al.*, "B-cell receptor pathway inhibitors affect CD20 levels and impair antitumor activity of anti-CD20 monoclonal antibodies," *Leukemia*, vol. 28, no. 5, pp. 1163–1167, May 2014, doi: 10.1038/leu.2014.12.

[308] G. Pavlasova *et al.*, "Ibrutinib inhibits CD20 upregulation on CLL B cells mediated by the CXCR4/SDF-1 axis," *Blood*, 2016, doi: 10.1182/blood-2016-04-709519.

[309] M.-A. Schwarzbich, "Targeting PD-L1/ PD-1-mediated inhibitory signaling with BTK inhibitors in Chronic Lymphocytic Leukemia (CLL) Centre for Haemato-Oncology Barts Cancer Institute," Queen Mary University of London., 2019.

[310] J. P. Sharman *et al.*, "Acalabrutinib with or without obinutuzumab versus chlorambucil and obinutuzmab for treatment-naive chronic lymphocytic leukaemia (ELEVATE TN): a randomised, controlled, phase 3 trial," *Lancet*, vol. 395, no. 10232, pp. 1278–1291, 2020, doi: 10.1016/S0140-6736(20)30262-2.

[311] J. A. Woyach *et al.*, "Acalabrutinib plus Obinutuzumab in Treatment-Naïve and Relapsed/Refractory Chronic Lymphocytic Leukemia," *Cancer Discov.*, vol. 10, no. 3, pp. 394–405, Mar. 2020, doi: 10.1158/2159-8290.CD-19-1130.

[312] F. Hassenrück *et al.*, "Sensitive detection of the natural killer cell-mediated cytotoxicity of anti-CD20 antibodies and its impairment by B-cell receptor pathway inhibitors," *Biomed Res. Int.*, 2018, doi: 10.1155/2018/1023490.

[313] L. Dittus, T. Werner, M. Muelbaier, and M. Bantscheff, "Differential Kinobeads Profiling for Target Identification of Irreversible Kinase Inhibitors," *ACS Chem. Biol.*, vol. 12, no. 10, pp. 2515–2521, Oct. 2017, doi: 10.1021/acschembio.7b00617.

[314] J. A. Dubovsky *et al.*, "Ibrutinib is an irreversible molecular inhibitor of ITK driving a Th1-selective pressure in T lymphocytes," *Blood*, vol. 122, no. 15, pp. 2539–2549, Oct. 2013, doi: 10.1182/blood-2013-06-507947.

[315] M. Long *et al.*, "Ibrutinib treatment improves T cell number and function in CLL patients," *J. Clin. Invest.*, vol. 127, no. 8, pp. 3052–3064, Jul. 2017, doi: 10.1172/JCI89756.

[316] H. Bruns *et al.*, "A novel immunoregulatory function of beta-2-microglobulin as a promoter of myeloid derived suppressor cell induction," *Leukemia*, vol. 33, no. 5, pp. 1282–1287, May 2019, doi: 10.1038/s41375-018-0345-0.

[317] D. R. Hodge, E. M. Hurt, and W. L. Farrar, "The role of IL-6 and STAT3 in inflammation and cancer," *Eur. J. Cancer*, vol. 41, no. 16, pp. 2502–2512, Nov. 2005, doi:

10.1016/j.ejca.2005.08.016.

[318] Severin *et al.*, "In Chronic Lymphocytic Leukemia the JAK2/STAT3 Pathway Is Constitutively Activated and Its Inhibition Leads to CLL Cell Death Unaffected by the Protective Bone Marrow Microenvironment," *Cancers (Basel).*, vol. 11, no. 12, p. 1939, Dec. 2019, doi: 10.3390/cancers11121939.

[319] I. Hazan-Halevy *et al.*, "STAT3 is constitutively phosphorylated on serine 727 residues, binds DNA, and activates transcription in CLL cells," *Blood*, vol. 115, no. 14, pp. 2852–2863, Apr. 2010, doi: 10.1182/blood-2009-10-230060.

[320] E. Tiacci *et al.*, "Pervasive mutations of JAK-STAT pathway genes in classical Hodgkin lymphoma," *Blood*, vol. 131, no. 22, pp. 2454–2465, May 2018, doi: 10.1182/blood-2017-11-814913.

[321] J. E. Ramis-Zaldivar *et al.*, "MAP-kinase and JAK-STAT pathways dysregulation in plasmablastic lymphoma," *Haematologica*, May 2021, doi: 10.3324/haematol.2020.271957.

[322] U. Rozovski *et al.*, "Stimulation of the B-cell receptor activates the JAK2/STAT3 signaling pathway in chronic lymphocytic leukemia cells," *Blood*, vol. 123, no. 24, pp. 3797–3802, Jun. 2014, doi: 10.1182/blood-2013-10-534073.

[323] V. Oldfield, S. Dhillon, and G. L. Plosker, "Tocilizumab," *Drugs*, vol. 69, no. 5, pp. 609–632, Sep. 2009, doi: 10.2165/00003495-200969050-00007.

[324] D. M. Schwartz, M. Bonelli, M. Gadina, and J. J. O'Shea, "Type I/II cytokines, JAKs, and new strategies for treating autoimmune diseases," *Nat. Rev. Rheumatol.*, vol. 12, no. 1, pp. 25–36, Jan. 2016, doi: 10.1038/nrrheum.2015.167.

[325] P. C. Taylor, "Clinical efficacy of launched JAK inhibitors in rheumatoid arthritis," *Rheumatology*, vol. 58, no. Supplement_1, pp. i17–i26, Feb. 2019, doi: 10.1093/rheumatology/key225.

[326] S. Dhillon, "Tofacitinib: A Review in Rheumatoid Arthritis," *Drugs*, vol. 77, no. 18, pp. 1987–2001, Dec. 2017, doi: 10.1007/s40265-017-0835-9.

[327] T. Hofland *et al.*, "Dissection of the Effects of JAK and BTK Inhibitors on the Functionality of Healthy and Malignant Lymphocytes," *J. Immunol.*, vol. 203, no. 8, pp. 2100–2109, Oct. 2019, doi: 10.4049/jimmunol.1900321.

[328] P. Jain *et al.*, "Ruxolitinib for symptom control in patients with chronic lymphocytic leukaemia: a single-group, phase 2 trial," *Lancet Haematol.*, vol. 4, no. 2, pp. e67–e74, Feb. 2017, doi: 10.1016/S2352-3026(16)30194-6.

[329] D. E. Spaner *et al.*, "Activity of the Janus kinase inhibitor ruxolitinib in chronic

lymphocytic leukemia: results of a phase II trial," *Haematologica*, vol. 101, no. 5, pp. e192–e195, May 2016, doi: 10.3324/haematol.2015.135418.

[330] Y. Aoki, G. M. Feldman, and G. Tosato, "Inhibition of STAT3 signaling induces apoptosis and decreases survivin expression in primary effusion lymphoma," *Blood*, vol. 101, no. 4, pp. 1535–1542, Feb. 2003, doi: 10.1182/blood-2002-07-2130.

[331] L. Bai *et al.*, "A Potent and Selective Small-Molecule Degrader of STAT3 Achieves Complete Tumor Regression In Vivo," *Cancer Cell*, vol. 36, no. 5, pp. 498-511.e17, Nov. 2019, doi: 10.1016/j.ccell.2019.10.002.

[332] S. Bhattacharya, R. M. Ray, and L. R. Johnson, "STAT3-mediated transcription of Bcl-2, Mcl-1 and c-IAP2 prevents apoptosis in polyamine-depleted cells," *Biochem. J.*, vol. 392, no. 2, pp. 335–344, Dec. 2005, doi: 10.1042/BJ20050465.

[333] U. Rozovski *et al.*, "At High Levels, Constitutively Activated STAT3 Induces Apoptosis of Chronic Lymphocytic Leukemia Cells," *J. Immunol.*, vol. 196, no. 10, pp. 4400–4409, May 2016, doi: 10.4049/jimmunol.1402108.

[334] P.-H. Nguyen *et al.*, "LYN Kinase in the Tumor Microenvironment Is Essential for the Progression of Chronic Lymphocytic Leukemia," *Cancer Cell*, vol. 30, no. 4, pp. 610–622, Oct. 2016, doi: 10.1016/j.ccell.2016.09.007.

[335] E. M. Samuelson, R. M. Laird, A. M. Papillion, A. H. Tatum, M. F. Princiotta, and S. M. Hayes, "Reduced B Lymphoid Kinase (Blk) Expression Enhances Proinflammatory Cytokine Production and Induces Nephrosis in C57BL/6-lpr/lpr Mice," *PLoS One*, vol. 9, no. 3, p. e92054, Mar. 2014, doi: 10.1371/journal.pone.0092054.

[336] N. Simon, A. Antignani, S. M. Hewitt, M. Gadina, C. Alewine, and D. FitzGerald, "Tofacitinib enhances delivery of antibody-based therapeutics to tumor cells through modulation of inflammatory cells," *JCI Insight*, vol. 4, no. 5, Mar. 2019, doi: 10.1172/jci.insight.123281.

[337] D. E. Spaner, L. McCaw, G. Wang, H. Tsui, and Y. Shi, "Persistent janus kinase-signaling in chronic lymphocytic leukemia patients on ibrutinib: Results of a phase I trial," *Cancer Med.*, vol. 8, no. 4, pp. 1540–1550, Apr. 2019, doi: 10.1002/cam4.2042.

[338] T. Zhou, S. Georgeon, R. Moser, D. J. Moore, A. Caflisch, and O. Hantschel, "Specificity and mechanism-of-action of the JAK2 tyrosine kinase inhibitors ruxolitinib and SAR302503 (TG101348)," *Leukemia*, vol. 28, no. 2, pp. 404–407, Feb. 2014, doi: 10.1038/leu.2013.205.

[339] M. R. Green *et al.*, "Integrative analysis reveals selective 9p24.1 amplification, increased PD-1 ligand expression, and further induction *via* JAK2 in nodular sclerosing Hodgkin

lymphoma and primary mediastinal large B-cell lymphoma," *Blood*, vol. 116, no. 17, pp. 3268–3277, Oct. 2010, doi: 10.1182/blood-2010-05-282780.

[340] S. Gupta *et al.*, "JAK2/PD-L1/PD-L2 (9p24.1) amplifications in renal cell carcinomas with sarcomatoid transformation: implications for clinical management," *Mod. Pathol.*, vol. 32, no. 9, pp. 1344–1358, Sep. 2019, doi: 10.1038/s41379-019-0269-x.

[341] D. S. Shin *et al.*, "Primary Resistance to PD-1 Blockade Mediated by JAK1/2 Mutations," *Cancer Discov.*, vol. 7, no. 2, pp. 188–201, Feb. 2017, doi: 10.1158/2159-8290.CD-16-1223.

[342] Y. Hao, B. Chapuy, S. Monti, H. H. Sun, S. J. Rodig, and M. A. Shipp, "Selective JAK2 Inhibition Specifically Decreases Hodgkin Lymphoma and Mediastinal Large B-cell Lymphoma Growth In Vitro and In Vivo," *Clin. Cancer Res.*, vol. 20, no. 10, pp. 2674–2683, May 2014, doi: 10.1158/1078-0432.CCR-13-3007.

[343] J. J. O'Shea, M. Gadina, and R. D. Schreiber, "Cytokine Signaling in 2002," *Cell*, vol. 109, no. 2, pp. S121–S131, Apr. 2002, doi: 10.1016/S0092-8674(02)00701-8.

[344] F. R. Bertani *et al.*, "Classification of M1/M2-polarized human macrophages by label-free hyperspectral reflectance confocal microscopy and multivariate analysis," *Sci. Rep.*, vol. 7, no. 1, p. 8965, Dec. 2017, doi: 10.1038/s41598-017-08121-8.

[345] M. A. Mir, "Costimulation Immunotherapy in Infectious Diseases," in *Developing Costimulatory Molecules for Immunotherapy of Diseases*, Elsevier, 2015, pp. 83–129.

[346] P. Allavena, M. Chieppa, P. Monti, and L. Piemonti, "From Pattern Recognition Receptor to Regulator of Homeostasis: The Double-Faced Macrophage Mannose Receptor," *Crit. Rev. Immunol.*, vol. 24, no. 3, pp. 179–192, 2004, doi: 10.1615/CritRevImmunol.v24.i3.20.

[347] H. Chen *et al.*, "JAK1/2 pathway inhibition suppresses M2 polarization and overcomes resistance of myeloma to lenalidomide by reducing TRIB1, MUC1, CD44, CXCL12, and CXCR4 expression," *Br. J. Haematol.*, vol. 188, no. 2, pp. 283–294, Jan. 2020, doi: 10.1111/bjh.16158.

[348] E. A. Irey *et al.*, "JAK/STAT inhibition in macrophages promotes therapeutic resistance by inducing expression of protumorigenic factors," *Proc. Natl. Acad. Sci.*, vol. 116, no. 25, pp. 12442–12451, Jun. 2019, doi: 10.1073/pnas.1816410116.

[349] E. Campo *et al.*, "TP53 aberrations in chronic lymphocytic leukemia: an overview of the clinical implications of improved diagnostics," *Haematologica*, vol. 103, no. 12, pp. 1956–1968, Dec. 2018, doi: 10.3324/haematol.2018.187583.

[350] N. Raj and L. D. Attardi, "Tumor suppression: P53 alters immune surveillance to restrain

liver cancer," *Current Biology*, vol. 23, no. 12. Cell Press, Jun. 17, 2013, doi: 10.1016/j.cub.2013.04.076.

[351] X. Yu, S. L. Harris, and A. J. Levine, "The Regulation of Exosome Secretion: a Novel Function of the p53 Protein," *Cancer Res.*, vol. 66, no. 9, pp. 4795–4801, May 2006, doi: 10.1158/0008-5472.CAN-05-4579.

[352] S. Ma *et al.*, "Gain-of-function p53 protein transferred *via* small extracellular vesicles promotes conversion of fibroblasts to a cancer-associated phenotype," *Cell Rep.*, vol. 34, no. 6, p. 108726, Feb. 2021, doi: 10.1016/j.celrep.2021.108726.

[353] E. Goulielmaki *et al.*, "Tissue-infiltrating macrophages mediate an exosome-based metabolic reprogramming upon DNA damage," *Nat. Commun.*, vol. 11, no. 1, p. 42, Dec. 2020, doi: 10.1038/s41467-019-13894-9.

[354] L. N. de S. Andrade *et al.*, "Extracellular Vesicles Shedding Promotes Melanoma Growth in Response to Chemotherapy," *Sci. Rep.*, vol. 9, no. 1, p. 14482, Dec. 2019, doi: 10.1038/s41598-019-50848-z.

[355] H. Shinohara *et al.*, "Regulated Polarization of Tumor-Associated Macrophages by miR-145 *via* Colorectal Cancer–Derived Extracellular Vesicles," *J. Immunol.*, vol. 199, no. 4, pp. 1505–1515, Aug. 2017, doi: 10.4049/jimmunol.1700167.

[356] T. Cooks *et al.*, "Mutant p53 cancers reprogram macrophages to tumor supporting macrophages *via* exosomal miR-1246," *Nat. Commun.*, vol. 9, no. 1, p. 771, Dec. 2018, doi: 10.1038/s41467-018-03224-w.

[357] G. Chen *et al.*, "Exosomal PD-L1 contributes to immunosuppression and is associated with anti-PD-1 response," *Nature*, vol. 560, no. 7718, pp. 382–386, Aug. 2018, doi: 10.1038/s41586-018-0392-8.

[358] F. Haderk *et al.*, "Tumor-derived exosomes modulate PD-L1 expression in monocytes," *Sci. Immunol.*, vol. 2, no. 13, p. eaah5509, Jul. 2017, doi: 10.1126/sciimmunol.aah5509.

[359] M. Pascual *et al.*, "PD-1/PD-L1 immune checkpoint and p53 loss facilitate tumor progression in activated B-cell diffuse large B-cell lymphomas," *Blood*, vol. 133, no. 22, pp. 2401–2412, May 2019, doi: 10.1182/blood.2018889931.

[360] M. A. Cortez *et al.*, "PDL1 Regulation by p53 *via* miR-34," *JNCI J. Natl. Cancer Inst.*, vol. 108, no. 1, Jan. 2016, doi: 10.1093/jnci/djv303.

[361] Z.-Y. Dong *et al.*, "Potential Predictive Value of TP53 and KRAS Mutation Status for Response to PD-1 Blockade Immunotherapy in Lung Adenocarcinoma," *Clin. Cancer Res.*, vol. 23, no. 12, pp. 3012–3024, Jun. 2017, doi: 10.1158/1078-0432.CCR-16-2554.

[362] S. Assoun *et al.*, "Association of TP53 mutations with response and longer survival

under immune checkpoint inhibitors in advanced non-small-cell lung cancer," *Lung Cancer*, vol. 132, pp. 65–71, Jun. 2019, doi: 10.1016/j.lungcan.2019.04.005.

[363] S. L. Topalian, C. G. Drake, and D. M. Pardoll, "Immune Checkpoint Blockade: A Common Denominator Approach to Cancer Therapy," *Cancer Cell*, vol. 27, no. 4, pp. 450–461, Apr. 2015, doi: 10.1016/j.ccell.2015.03.001.

[364] Z. Y. Xu-Monette *et al.*, "Immune Profiling and Quantitative Analysis Decipher the Clinical Role of Immune-Checkpoint Expression in the Tumor Immune Microenvironment of DLBCL," *Cancer Immunol. Res.*, vol. 7, no. 4, pp. 644–657, Apr. 2019, doi: 10.1158/2326-6066.CIR-18-0439.

[365] B. Diskin *et al.*, "PD-L1 engagement on T cells promotes self-tolerance and suppression of neighboring macrophages and effector T cells in cancer," *Nat. Immunol.*, vol. 21, no. 4, pp. 442–454, Apr. 2020, doi: 10.1038/s41590-020-0620-x.

[366] S. D. Smith *et al.*, "Pembrolizumab with R-CHOP in previously untreated diffuse large B-cell lymphoma: potential for biomarker driven therapy," *Br. J. Haematol.*, vol. 189, no. 6, pp. 1119–1126, Jun. 2020, doi: 10.1111/bjh.16494.

12 Erklärung

Hiermit versichere ich an Eides statt, dass ich die vorliegende Dissertation selbstständig und ohne die Benutzung anderer als der angegebenen Hilfsmittel und Literatur angefertigt habe. Alle Stellen, die wörtlich oder sinngemäß aus veröffentlichten und nicht veröffentlichten Werken dem Wortlaut oder dem Sinn nach entnommen wurden, sind als solche kenntlich gemacht. Ich versichere an Eides statt, dass diese Dissertation noch keiner anderen Fakultät oder Universität zur Prüfung vorgelegen hat; dass sie - abgesehen von unten angegebenen Teilpublikationen und eingebundenen Artikeln und Manuskripten - noch nicht veröffentlicht worden ist sowie, dass ich eine Veröffentlichung der Dissertation vor Abschluss der Promotion nicht ohne Genehmigung des Promotionsausschusses vornehmen werde. Die Bestimmungen dieser Ordnung sind mir bekannt. Darüber hinaus erkläre ich hiermit, dass ich die Ordnung zur Sicherung guter wissenschaftlicher Praxis und zum Umgang mit wissenschaftlichem Fehlverhalten der Universität zu Köln gelesen und sie bei der Durchführung der Dissertation zugrundeliegenden Arbeiten und der schriftlich verfassten Dissertation beachtet habe und verpflichte mich hiermit, die dort genannten Vorgaben bei allen wissenschaftlichen Tätigkeiten zu beachten und umzusetzen. Ich versichere, dass die eingereichte elektronische Fassung der eingereichten Druckfassung vollständig entspricht.

Teilpublikationen:

V. Barbarino, S. Henschke, S. J. Blakemore, E. Izquierdo, M. Michalik, N. Nickel, I. Möllenkotte, D. Vorholt, L. Müller, R. Brinker, O. Fedorchenko, N. Mikhael, T. Seeger-Nukpezah, M. Hallek, and C. P. Pallasch, "Macrophage-mediated antibody dependent effector function in aggressive B-cell lymphoma treatment is enhanced by ibrutinib *via* inhibition of JAK2," *Cancers (Basel).*, vol. 12, no. 8, pp. 1–25, 2020, doi: 10.3390/cancers12082303.

E. Izquierdo, D. Vorholt, B. Sackey, J. L. Nolte, S. J. Blakemore, J. Schmitz, V. Barbarino, N. Nickel, D. Bachurski, L. Lobastova, M. Nikolic, M. Michalik, R. Brinker, O. Merkel, R. Neuhaus, M. Koch, G. Knittel, L. Frenzel, H. C. Reinhardt, M. Peifer, R. Rebollido-Rios, H. Bruns, M. Krüger, M. Hallek, and C. P. Pallasch, "Loss of TP53 mediates suppression of Macrophage Effector Function *via* Extracellular Vesicles and PDL1 towards Resistance against Chemoimmunotherapy in B-cell malignancies," *bioRxiv*, 2020, doi: 10.1101/2020.06.11.145268.

Verena Barbarino, Köln den 21.05.21